AD-A071 262 PURDUE UNIV LAFAYETTE IND RAY W HERRICK LABS F/G 20/4
FOLD-OVER, INTERMITTENCY AND CROSSING FREQUENCY OF A PLANE JET --ETC(U)
FEB 77 C O AJAGU, V W GOLDSCHMIDT N00014-67-A-0226-0025
UNCLASSIFIED HL-76-22 NL

1 OF 3
AD A071262

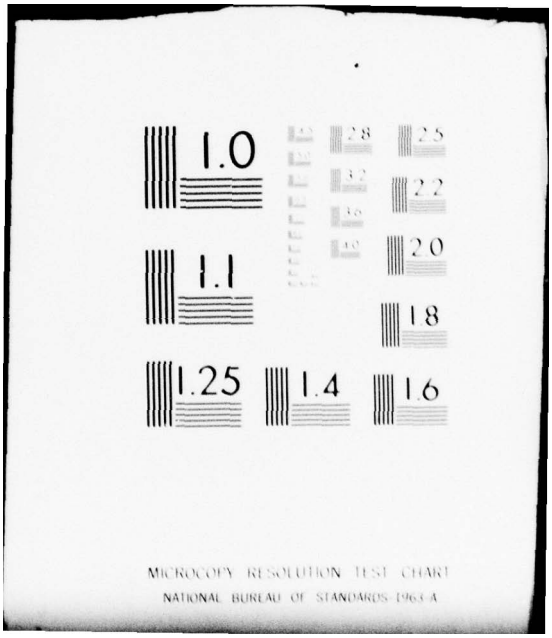
1.0
1.1
1.25
1.4
1.6
2.8
2.5
3.2
2.2
3.6
2.0
4.0
1.8
MICROCOPY RESOLUTION TEST CHART
NATIONAL BUREAU OF STANDARDS 1963-A

RAY W. HERRICK LABORATORIES

A Graduate Research Facility
of The School of Mechanical Engineering

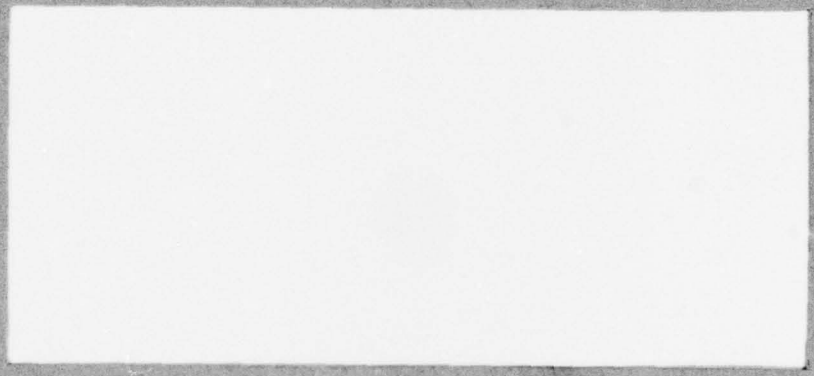

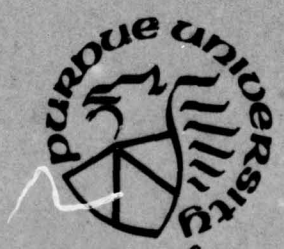

Approved for public release; distribution unlimited

Purdue University

West Lafayette, Indiana 47907

DATA SHEET

PHOTOGRAPH

THIS SHEET

II
LEVEL

I
INVENTORY

AD A071262
DDC ACCESSION NUMBER

HL 76-22
DOCUMENT IDENTIFICATION

DISTRIBUTION STATEMENT A
Approved for public release;
Distribution Unlimited
DISTRIBUTION STATEMENT

Accession For
NTIS GRA&I
DDC TAB
Unannounced
Justification
By
Distribution/
Availability Codes
Dist | Avail and/or special
A

DISTRIBUTION STAMP

DDC
RECEIVED
JUL 17 1979
D

DATE ACCESSIONED

DDC FILE COPY

790705 096
DATE RECEIVED IN DDC

PHOTOGRAPH THIS COPY

Prepared under NSF Eng 74-20078
(PRF contract 9010)
and ONR N00014-67-A-0226-0025
(PRF contract 8673)

FOLD-OVER, INTERMITTENCY AND CROSSING FREQUENCY OF A PLANE JET INTERFACE WITH AND WITHOUT AN ACOUSTIC DISTURBANCE

Sponsored by

National Science Foundation
and
Office of Naval Research

HL 76-22

Submitted by:

C.O. Ajagu, Graduate Research Assistant
Victor W. Goldschmidt, Principal Investigator
and Project Director

Approved for public release; distribution unlimited

February 1977

FOLD-OVER, INTERMITTENCY AND CROSSING FREQUENCY OF A PLANE JET INTERFACE WITH AND WITHOUT AN ACOUSTIC DISTURBANCE

Prepared Under NSF Eng 74-2078
and ONR N00014-67-A-0226-0025

HL 76-22

by

C.O. Ajagu and V.W. Goldschmidt
School of Mechanical Engineering
Purdue University

July 1976

NOTE:

This report is part of a thesis submitted by Mr. Chris Ajagu in partial fulfillment of the requirements for the degree of Master of Science in Mechanical Engineering. The thesis was dated May 1976. Professor Goldschmidt assisted in this work as thesis advisor and major professor.

Phases of this work were sponsored by an NSF Grant Eng 74-2078 and an ONR Contract N0014-67-0226-0025. The authors are indebted and grateful for both.

TABLE OF CONTENTS

LIST OF TABLES

LIST OF FIGURES

Appendix Figure — Page

NOMENCLATURE

b	Velocity half-width
c	Capacitor (equation C-1)
C	Threshold level, threshold value (Chapter III, Section 5b; not used in this work)
C^2	Threshold level (equation 3-14)
C_1	Geometric virtual origin
C_2	Kinematic virtual origin
D	Slot width (Figure 2-1)
D	Cylinder diameter (Table 5-1)
e	Fluctuating hot-wire voltage output
e_i	Input voltage to differentiator circuit (Figure C-1)
e_o	Output voltage to differentiator circuit (Figure C-1)
F	Frequency of the acoustic disturbance
F_c	Cut-off frequency; highest frequency of interest (equation A-1)
F_{ch}	Characteristic frequency (equation 3-9)
F_γ	Interface crossing frequency
$F_{\gamma m}$	Maximum interface crossing frequency
F_θ	Fold-over frequency (equation 3-19)
$F_{\theta m}$	Maximum fold-over frequency
$F(n)$	$\overline{U}/\overline{U}_m$ (equation 3-1)
h	Averaging time in discretized voltage representation (Figure A-1)

$H(t)$	Intermediate intermittency function (Figure 3-29)
$I(t)$	Intermittency function (Figure 3-29)
k_1	Widening rate of velocity field
k_2	Velocity decay rate
ℓ_c	Characteristic length (Section III-6)
L	Length scale
ℓ_k	Kolmogoroff length scale (Section II-2a)
$N(t)$	Non-turbulent part of signal S(t)
$N'(t) = n$	rms of N(t)
N	Sample size (equation A-2)
n	Number of turbulent bursts
P	C^2/S'^2 (equation 3-14)
P1, P2	Ratios of threshold and mean square for probes 1 and 2
R_{e_D}	Reynolds number based on D
$S(t)$	Detector input signal (Figure 3-29)
S', s'	rms of S(t) (equation 3-9)
S'^2	Mean square of S(t)
T	Total sampling time
TF	Transfer function for differentiator circuit (equation C-5)
T_{ch}	Characteristic time scale of turbulence (equation 3-9)
TH1, TH2	Threshold level (Figure B-3)
t	Small time (Figure A-1)
Δt	Time increment (equation A-1)
U	Velocity in the axial direction (Section III-5b)

$\overline{U}_m$	Maximum centerline average velocity (equation 3-1)
$\overline{U}_0$	Average jet exit velocity (equation 3-6)
u	Axial fluctuating velocity
u'	rms of u
U_∞	Free stream velocity
V, V1, V2	"Voltage" of S(t) (Figure B-2)
V	Instantaneous lateral velocity (Section III-5b)
$\overline{V}$	Mean lateral velocity
V_i	Velocity of the interface (equation 5-1)
V_{i1}, V_{i2}, V_{i3}	Definitions of V_i (Used by Mulej (1975))
V_j	Increment on V1, V2, V (j = 1,2, ...)
V_0	Average interface velocity (Section II-2a)
W_1, W_2	Width of a turbulent burst (Figure 3-31)
x	Axial coordinate
X_n	A set of data points (equation A-2)
y	Lateral coordinate
$\overline{Y}$	Mean position of the interface (where $\gamma = 0.5$)
$\overline{Y}_\gamma, \overline{Y}_f, \overline{Y}_\theta$	$\overline{Y}$ for γ, F_γ, and F_θ
z	Coordinate normal to x,y
Z_i, Z_f	Input and feedback impedance (Figure C-1)
δ	Boundary layer thickness (Section III-5b)
Δy	Probe separation in lateral direction
ε	Turbulence dissipation (Section II-2a)
γ	Intermittency, intermittency factor (Figure 4-1)
η	Nondimensional similarity variable $\frac{\sigma y}{x}$
σ	Constant in the similarity variable

σ	Variance (standard deviation) (Table 5-1)
σ'	Nondimensional variance (equation 4-1)
$\sigma_\gamma, \sigma_f, \sigma_\theta$	Parameters for the intermittency, crossing frequency and fold-over frequency curve fit (Table 5-1)
τ_d	Delay time (equation 3-11)
τ_H	Hold time (see Figure 3-29)
θ	Subscript for the fold-over frequency
ϕ_f	Percent fold-over (Figure 3-18)
ν	Kinematic viscosity
$(\nu^3/\varepsilon_0)^{\frac{1}{4}}$	Kolmogoroff microscale
ω	Vorticity
ω_b	Break frequency for differentiator circuit (equation C-7)
ω_{ch}	Characteristic frequency (= 2 F_{ch}) (equation 3-11)
<=>	If and only if (equation 3-16)

CHAPTER I. INTRODUCTION

One aspect of turbulent shear flows that needs empiricism to be able to predict it is the turbulent transport and spreading of these types of flows. A turbulent plane jet, for example, has a linear widening rate away from the mouth of the jet which has not been predicted from turbulent flow theories, but rather determined from measurements themselves. Various models have been proposed to try to explain the spreading rate of turbulent developing shear flows. In recent years, the recognition of some coherent structures in turbulence has led to different models and approaches that attempt to explain turbulent flows. Some of these were aptly summarized by Davies and Yule (1974)* following a conference in Southampton.

This idea of coherent structures in turbulent flows is an extension and companion to the concept of a distinct surface separating the turbulent primary flow, as for instance in a jet, from the entrained external nonturbulent flow. The existence of this interface has been well defined, and will be alluded to in future paragraphs. In the last two or three years, it has been recognized that occasionally this interface separating the turbulent from the nonturbulent flows tends to fold-over, or seemingly

*Also published in JFM (1975), Vol. 69, Part 3, pp. 513-537.

engulf the external nonturbulent flow in a "nibbling" fashion. In the presence of fold-over, a region of the turbulent fluid may have nonturbulent fluid between it and the main fully turbulent region.

The overall objective of this work was to try to gain further understanding into the structure of turbulent flows, and to observe the effects of an acoustic disturbance upon them. The specific objective of this work, to which the attention is now directed, was a measure of the fold-over of the interface between the turbulent and nonturbulent flows, and the effect of an acoustic disturbance upon it. In addition to that, the intermittency and crossing frequency of the interface were recorded. The frequency of the acoustic disturbance was purposely chosen to match that frequency at which the most interaction is expected, as exhibited by the noticeable increase in the widening rate of the acoustically disturbed jet compared with the jet without any sound applied to it. This effect of the acoustic field on the jet is discussed further in Chapter II.

The initial goal of this work was then to see if an acoustic disturbance in the form of a plane traveling wave at specific frequencies could indeed change the occurrence of fold-over in a two dimensional plane turbulent jet. These specific frequencies will be discussed further in Chapter II. Folding of the interface as discussed by

Townsend (1970), Kohan (1969), Paizis (1972), LaRue (1973), LaRue and Libby (1974), Davies and Yule (1974), Paizis and Schwarz (1974), and Mulej (1975) is defined as the process by which a region of turbulent fluid has nonturbulent fluid between it and the fully turbulent region. In an attempt to describe this folding phenomenon, some investigators have used different terms. LaRue (1973) for example, used "overhangs," Mulej (1975) used "folding" and "fold-over" interchangeably, and Paizis and Schwarz (1974) referred to it as simply "folding." This will be discussed further in Chapter III. The term "fold-over," will be used in the present work.

Mulej (1975) measured the percent fold-over, ϕ_i, in a plane turbulent jet, and found that it decreased with the lateral position, y/b, of the jet. (The description of the jet is given in Chapter III.) The present research was partly motivated by his report. A new and hopefully better method of measuring fold-over was sought. The method used by Mulej (1975) is discussed and evaluated in Chapter III. The method adopted in this research is a digital method. Analog signals were digitized and processed in a digital computer.

Fold-over measurements required detecting the turbulent-nonturbulent interface, using two hot wire probes separated by a pre-selected distance in the lateral direction of the flow. Corrsin (1943) was credited with

discovering that turbulent shear flows may exhibit flows which are intermittently turbulent or *nonturbulent*. He was exploring the flow field of a heated jet. The existence of this phenomenon was later established for all free shear flows, and Townsend (1948) proposed a measure of the degree of intermittency. This became known as the intermittency factor, γ, and is defined as the fraction of time the flow is turbulent. The intermittency function, I(t), was also due to Townsend (1949). This function is a random square wave which is equal to 1 (unity), when the flow is turbulent, and zero when it is nonturbulent.

Recognizing the difficulty involved in detecting the turbulent-nonturbulent interface, the objectives of this research were expanded and are three-fold: (1) to detect the turbulent-nonturbulent interface using both analog and digital techniques, (2) to measure fold-over using the developed detection technique, and (3) to observe the effects of a plane traveling acoustic wave of selected frequencies on fold-over, crossing frequency of the interface, and intermittency. The interface crossing frequency is defined as the rate at which the intermittency function, I(t), changes from unity to zero or vice versa.

Whereas some investigators contend that fold-over is an important part of the entrainment process, only very few attempts have been made to quantify it. In the plane turbulent jet, for example, the only reported attempt to

measure fold-over was made by Mulej (1975). Some of the questions raised by his work are: (1) Why does the detection of fold-over seem to increase as one moves towards the center-line of the jet where the flow is fully turbulent? (2) Do fold-over events actually increase as one moves towards the center-line of the jet? (3) Is measuring the percent fold-over the best way to quantify fold-over?

This work is then a natural extension of the work done by Jenkins (1974) and Mulej (1975) in plane turbulent jets without the application of an acoustic disturbance. The effects of an acoustic wave on turbulent jets have been reported for many years. None of the previous works considered the intermittent region of the jet. Simcox (1969), for example, predicted theoretically that the spreading rate of the jet is enhanced by an acoustic disturbance. It was proposed by him that this interaction of an acoustic wave with the jet may be applicable to the development of a new type of amplifier. Experiments by Kaiser (1971) and others confirmed that the widening rate of the jet was increased by the application of an acoustic wave. Research to establish the mechanism through which an applied sound interacts with a plane turbulent jet is being conducted by Chambers (1976). The location in the jet at which this interaction occurs is also being investigated by him.

It is hoped that the present research will provide more information concerning the interaction of an acoustic wave with a plane turbulent jet, as well as the structure of the turbulent-nonturbulent interface. This might lead to a better understanding of turbulence and its interaction with an acoustic disturbance.

CHAPTER II. THE TWO-DIMENSIONAL JET

1. Characteristics of the Jet

Among the simplest types of turbulent shear flows is a jet. It is an unbounded flow and is formed when a fluid moving with a velocity greater than that of the surrounding medium discharges through an orifice into the medium. (The medium considered here is air and the fluid forming the jet is also air.) The resulting diffusion pattern can be divided into three regions: the initial region, the transitional region, and the main region (see Figure 2-1).

Within the initial region of the jet, there exists a potential core bounded by two mixing layers. The velocity in this potential core remains constant. At the mouth of the jet, this velocity is equal to the discharge velocity. As the flow spreads, the axial velocity decreases. Turbulent flow results due to the gradient and corresponding exchange caused by the initial velocity discontinuity between the jet and the surrounding media. The ensuing turbulent stresses bring about a transverse exchange of momentum between the fluid and the surrounding media. The "eating up" of the jet beyond the initial area shows up both in its widening as well as in variation of the velocity along its axis (see Abramovich (1963).

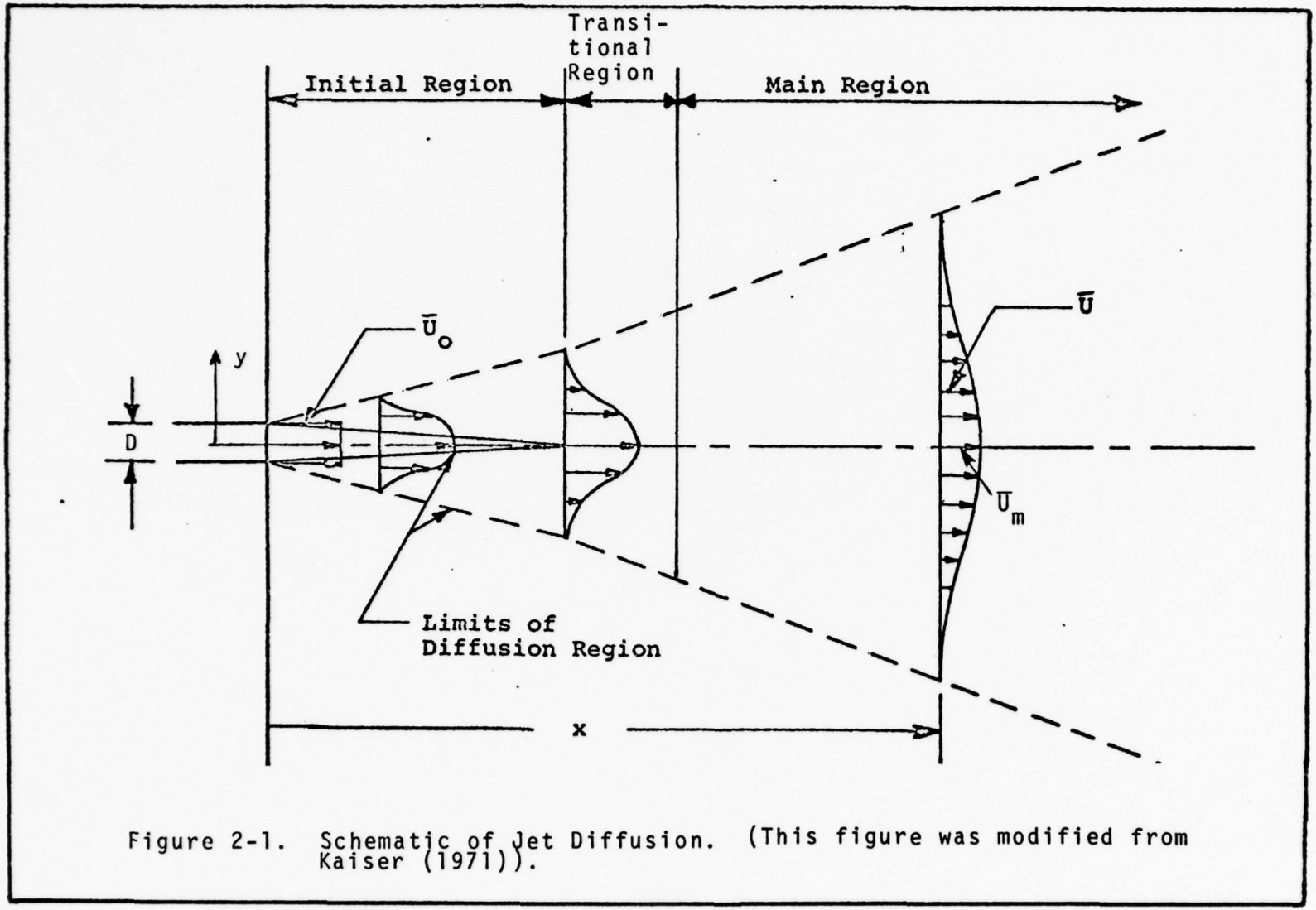

Figure 2-1. Schematic of Jet Diffusion. (This figure was modified from Kaiser (1971)).

The mean velocity profile in the transitional region will essentially be fully developed; however, a finite distance is required for the turbulence to become fully developed.

The main region begins when the turbulence becomes fully developed. It is characterized by a continuous acceleration of the surrounding fluid accompanied by a deceleration of the fluid in the central region. The measurements presented later were taken in this region of the flow field.

There exists a zone of demarcation between turbulent and nonturbulent regions of the shear flow. This zone is characterized by a sharp, randomly convoluted interface. The turbulent-nonturbulent region (see Figure 2-2) is the intermittent region with which this work is concerned.

The shape of the jet profile remains unchanged when an acoustic disturbance is applied to it. However, the spreading rate of the jet is increased and the geometric virtual origin shifted (see Figure 2-3) when the disturbance is at a specific frequency.

2. General Review of Previous Work Related to Turbulent Jets

It was observed earlier that the only reported attempt to quantify fold-over in a plane turbulent jet was that due to Mulej (1975). It was also noted that no work has been done to establish the effects of acoustic disturbances,

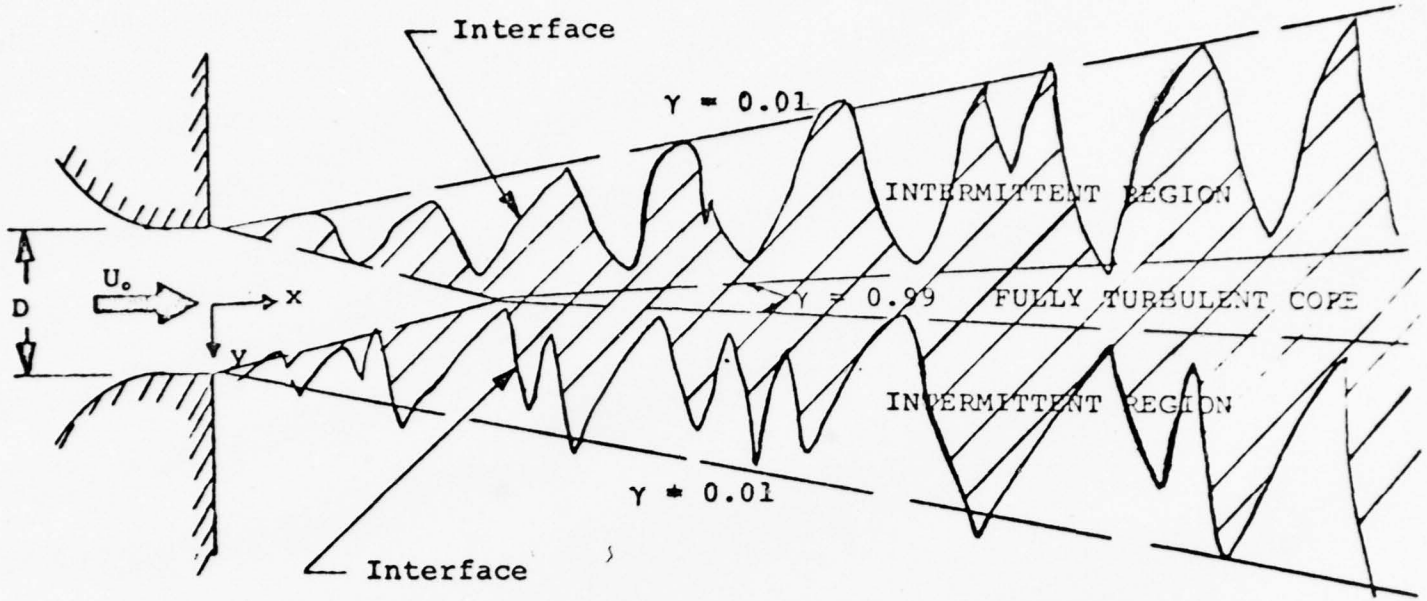

Shaded Regions are Turbulent.
The sketch does not suggest any special pattern.

Figure 2-2. The Two-dimensional Jet Showing Intermittent Region. (This figure was taken from Jenkins (1974)).

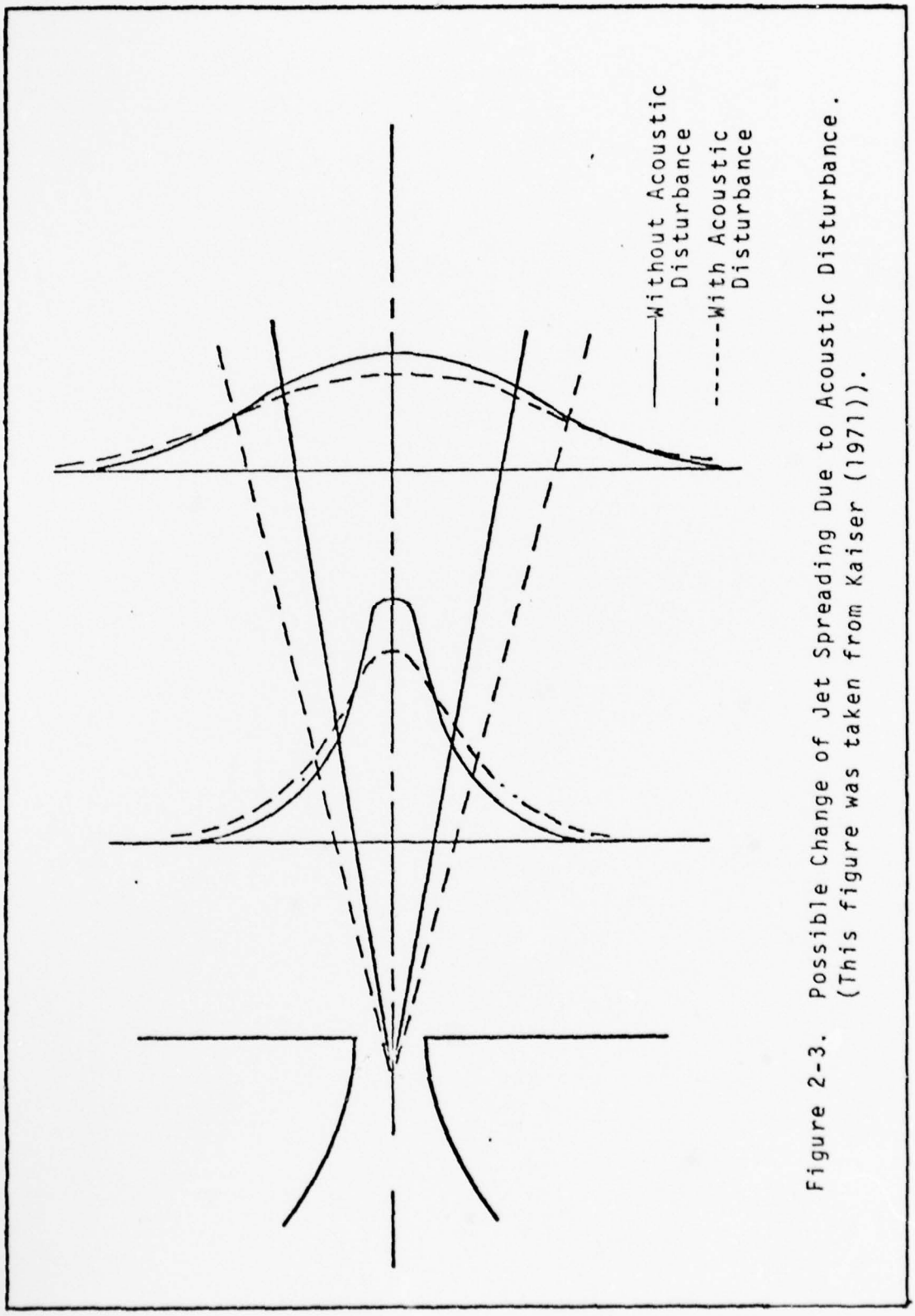

Figure 2-3. Possible Change of Jet Spreading Due to Acoustic Disturbance. (This figure was taken from Kaiser (1971)).

at specific frequencies, on the structure of the turbulent-nonturbulent interface of a two dimensional plane turbulent jet. This section therefore aims at presenting a brief review of the literature of some of the work that has been done by previous investigators studying turbulent jets. Studies in other flow fields like wakes and boundary layers will be mentioned where they help to explain concepts like intermittency and conditional sampling. A specific review of the previous techniques used by other investigators to detect the turbulent-nonturbulent interface will be given in Chapter III when the detection of the turbulent-nonturbulent interface is discussed. Also the work done in wakes and boundary layers to measure fold-over will be presented in Chapter III. Hence this review will be divided into two parts: (a) the undisturbed flow and (b) the acoustically excited flow.

a. The Undisturbed Flow

It was noted in Chapter I that the characteristically intermittent hot wire signal obtained from probes placed in the turbulent-nonturbulent region of a heated jet flow was first observed by Corrsin (1943). The existence of the phenomenon of intermittency was later established for all free shear flows, and Townsend (1948) proposed a measure of the degree of intermittency. This became known as the intermittency factor, γ, and is defined as the fraction of time the flow is turbulent. The Intermittency function,

I(t), was also due to Townsend (1949). This function is a random square wave which is equal to 1 (unity) when the probe is in turbulent flow and zero when it is in the non-turbulent flow.

Townsend (1948) first explored statistical properties of the intermittent region for the two-dimensional wake and Corrsin and Kistler (1954) investigated the boundary layer. The thickness of the interface (or superlayer, as termed by Corrsin and Kistler (1954)) was investigated by Corrsin and Kistler (1954), and was found to be proportional to the Kolmogoroff microscale $(\nu^3/\varepsilon_0)^{\frac{1}{4}}$. The existence of this interface has been well defined following measurements conducted by investigators like Kovasznay (1967), Uberoi and Freymuth (1969), LaRue (1973) and Kibens (1968). Kovasznay (1967), argued that the thickness of the turbulent-nonturbulent interface (superlayer) is of the same order as the smallest turbulent eddies and estimated this thickness to be $10\nu V_0^{-1}$ where ν is the kinematic viscosity and V_0 is the average entrainment velocity. LaRue (1973), and also LaRue and Libby (1974) argued that in a wake the order of a minimum duration of a fully turbulent "patch" of fluid was equal to twice the Kolmogoroff length transit time or approximately $2(\ell_K/U_\infty)$ where ℓ_K is Kolmogoroff length and U_∞ is the free stream velocity. Using U_∞ obtained by Uberoi and Freymuth (1969) they obtained the minimum duration to be 160 μs. Further discussion of the interface and its

thickness will be given in Chapter III.

Conventional mean measurement techniques require continuous averaging of flow properties as obtained from a stationary hot-wire probe. These techniques are inherently incapable of examining separately the detailed properties of the turbulent and nonturbulent flow, or of the transition (or interface) between the two states. Corrsin and Kistler (1954) realized the need for a new technique. The method of conditional sampling was developed primarily by Kibens and Kovasznay (1969) in answer to this need. Among the early workers in this field were Kibens (1968), Kovasznay, Kibens and Blackwelder (1970), Jenkins (1974) and others. Jenkins (1974) measured the velocity and temperature profiles with respect to the interface in a heated two-dimensional plane jet, and presented an up-to-date literature review on conditional sampling.

Phillips (1972) looked at the part played by the interface in the entrainment of the surrounding ambient fluid. A pseudo-Lagrangian description of the entrainment process was proposed by him. Paizis and Schwarz (1974) studied the shape of the interface and noted the significant amount of fold-over which occurred in the interface. They also measured the characteristic scales and convection velocity of the interface for a turbulent wall jet. More discussion on the significant amount of fold-over measured by them is made in Chapter III.

Mulej (1975) measured the lateral component of the velocity of the turbulent-nonturbulent interface. Preliminary measurements of the amount of fold-over in the interface as a function of location were also taken by him.

b. The Acoustically Excited Flow

A survey of the interaction of a transverse acoustic wave with various flows is presented here. This discussion is not limited to plane traveling waves and is not intended to be an exhaustive one. The emphasis is on turbulent jet flows.

Two types of interaction should be distinguished: (1) that interaction that promotes an earlier transition in the case of an initially laminar jet; and (2) that which causes an apparent enhancement of mixing in the fully turbulent jet. These interactions will be discussed further in this chapter.

The influence of sound on a flow field has been known and documented for many years. Chanaud and Powell (1962) claim that the first reported observation of this phenomenon was made in 1838 by LeConte, who noticed that gas lights had a tendency to flicker when in the presence of music. It was not until 1935 that Brown (1935) investigated this phenomenon. He studied sound sensitive laminar jets, and concluded that the influence of sound was basically an effect upon the laminar-turbulent transition.

Simcox (1969) first represented the vorticity fluctuations due to turbulence by a single frequency harmonic function, and superimposed to it an acoustic disturbance. He noticed that the disturbance caused an increase in the vorticity. The single frequency representation was then converted to a spectral representation using Fourier transforms which described a two-dimensional turbulent jet flow. He analyzed the interaction of a traveling acoustic wave with the turbulent flow field, and claimed that there were, in general, two types of interaction: a direct interaction (described by the single eddy theory) and a secondary interaction among the eddies due to the addition of energy by the acoustics. His analysis suggested an increase of the turbulence intensity, and no change of the Reynolds stress. He predicted an increase in the turbulent mixing, and further inferred an increased spreading rate of the jet, since the spreading was proportional to the kinetic energy of the turbulence, which in turn, is a function of the turbulence intensity. Although the theory that the spreading rate of the jet is proportional to the kinetic energy of the turbulence has not been proved experimentally, it appears to be the consensus among other investigators like Abramovich (1963) and Townsend (1956). Simcox (1969) further claimed that the change in the spreading rate of the jet can be used to produce a control on the switching or proportioning of flow in a fluidic device, and that the

interaction may be applicable to the development of a new type of amplifier. Part of the work by Simcox (1969) is published in Simcox and Hoglund (1971).

Williams (1969) considered a longitudinally resonant acoustic field in a developing turbulent pipe flow, and concluded that the input in some cases led to a decrease in the microscales and macroscales of turbulence. Although he did not consider jet flows, he noticed some structural changes in turbulence due to an acoustic signal.

In his experimental program concerning the effect of sound on a reattaching jet at low Reynolds numbers, Weinger (1965) noticed that the reattachment point moved upstream with increasing acoustic intensity at selective frequencies. He concluded that the laminar-turbulent transition shifted upstream with increasing acoustic intensity and that once the transition point reached the orifice, the reattachment point began to move downstream. This agreed with Brown's (1935) observation.

Roffman and Toda (1969), experimenting with both laminar and turbulent jets, found an increase in the jet widening rate at selective frequencies. They also found that the Strouhal number ($St = FD/U_0$) remained constant over the range of their investigation ($200 \leq R_{e_D} \leq 9000$). It was Powell (1953) who first recognized the significance of the Strouhal number and Reynolds number in analyzing the sensitivity of jets to periodic disturbances.

Glass (1968) undertook an experimental investigation concerning the acoustic feedback on supersonic jets. He placed a plate near the flow field in order to reflect the aerodynamically generated sound back into the jet. He found that this type of acoustic input destroyed the shock structure of the jet and caused an increase of spreading and decay rates. The effect appeared to be at a maximum at 10,000 Hz, although it was noticeable at other frequencies.

Rockwell (1971) collected most of the data of the investigators mentioned above and presented them in terms of two-dimensionless groups: the Strouhal number and the Reynolds number. His plot (Rockwell (1971), Figure 3) of Strouhal number versus Reynolds number on a log-log scale showed that the log of the dimensionless sensitive frequencies for two-dimensional jets varies approximately linearly with the logarithm of the Reynolds number. Hence, it is possible to determine the frequency at which a given flow is most sensitive to an acoustic disturbance.

The influence of sound on turbulent jet flows may be through an effect on transition, acoustic streaming, an induced oscillation due to aerodynamic loading or a direction interaction with the turbulent field itself. Simcox (1969) argued qualitatively, that

for subsonic air jets of moderate Reynolds number, neither acoustic streaming, nor aerodynamic loading can lead to a change in the spreading rate. Experiments conducted by Kaiser (1971) confirm Simcox's (1969) claim. Hence the noticeable effects of an acoustic input on a free jet are through an upstream shift or modulation of the laminar-turbulent transition, and/or a direct interaction with the turbulent flow itself.

To evaluate Simcox's theoretical predictions, Kaiser (1971) conducted his experiments using a two-dimensional turbulent jet. He noted that the similarity of the flow remained unaltered when an acoustic signal was introduced normal to the jet. Hence, the form ($\overline{U}/\overline{U}_m = F(\eta)$) remained unaltered. He confirms that the jet spreading rate is enhanced by an acoustic disturbance. From the plot of widening rate versus frequency, Kaiser (1971) noticed a periodic behavior which he could not explain. He noticed that as the Reynolds number of the flow was decreased, the frequency for which the maximum widening rate occurred also decreased. This agreed with Rockwell's (1971) findings. The geometric origin of the jet tends to move downstream at the frequencies where the maximum widening rate occurred. The velocity origin remained approximately zero.

Some of the issues not answered by Kaiser (1971) and other experimenters were: the cause of the periodic

behavior of the widening rate as a function of frequency, and the mechanism through which an applied sound field interacts with a plane turbulent jet. Kaiser's (1971) results are also published in Goldschmidt and Kaiser (1971).

More recent studies have been made to better understand the behavior of a disturbed jet. Chan (1974) studied spatial waves in a low speed axisymmetric turbulent free jet. His results showed that the wave-numbers of the pressure waves increased monotonically, while the phase velocities decreased with the jet Strouhal number. Further studies on phase velocities were made by Bechert and Pfizenmaier (1975). They applied axial disturbances to a free jet and reported the presence of "ultra-fast" phase velocities which exceeded the mean velocity of the jet. Hussain and Zaman (1975) studied the effect of an acoustic excitation on the turbulence structure of a circular jet operated at the Reynolds number range 11,000-113,000. The acoustic excitation was in a plenum chamber. They observed that at a Strouhal number of 1.6, the turbulent intensity in the near field of the nozzle was strongly suppressed but that at higher Strouhal numbers the effect of excitation was insignificant. Stiffler (1975) found that the signal transit velocities in a turbulent plane jet were much less than the jet center-line velocity.

Merkine and Liu (1975) studied the noise-producing large-scale wavelike eddies in a plane turbulent jet. They

found that for a given frequency parameter, different modes had different streamwise lifetimes.

It was pointed out earlier that this survey was not intended to give a historical account of all the research studies that have been done in the interaction of an acoustic wave with turbulent jets. It aimed at pointing out some of the observations that have been made. Whereas many different studies have been conducted concerning the interaction of an acoustic wave with turbulent jets, no report has been made of the effect of an acoustic disturbance on intermittency, fold-over and crossing frequency of the turbulent-nonturbulent interface.

CHAPTER III. INVESTIGATION TECHNIQUES AND EQUIPMENT

1. Introduction

It was previously stated that the conventional mean measurement techniques require continuous averaging of flow properties as obtained from a stationary hot-wire probe. Those measurement techniques were inherently incapable of examining separately the detailed properties of the turbulent and nonturbulent flows, or of the transition (or interface) between the two states. The method of conditional sampling was developed primarily by Kibens and Kovasznay (1969) in answer to this problem. Two types of conditional averages can be defined within the turbulent region of a jet. These are the "zone" averages (taken at a fixed point in space throughout the turbulent history of the flow at that point) and the "point" averages, which are taken at a point within the turbulent flow and averaged whenever the interface is crossing some other reference point. The former ("zone" averages) were employed in this work. The continuous signals originating from two hot-wire probes placed in the intermittent zone of the free turbulent jet were classified into "turbulent" or "nonturbulent" by digital methods and processed in a computer. Before the details of this method are presented, a brief discussion

of the experimental setup and the flow field will be given.

2. Experimental Setup

a. The Flow Field

The two dimensional plane jet used for this research was essentially the same as that used by Jenkins (1974) and Mulej (1975) (see Figure 3-1). It was powered by a 0.56 kW (0.75 hp) blower. A 4 kW mesh wire heating element located in a 56 x 51 cm plenum chamber was capable of heating the flow. This heating capability used by Jenkins (1974) was not used for this work. The flow was directed from the plenum chamber via a gradual contraction to a smaller 5.98 in x 11.97 in. (15.2 x 30.4 cm) plenum chamber having flow straightening elements. It was then discharged through a vertical slot 0.5 in. x 11.97 in. (1.27 x 30.4 cm) on a 35.98 in. x 11.97 in. (91.4 x 30.4 cm) wall. Two confining horizontal walls 35.98 in. x 47.64 in. (91.4 x 121.0 cm) were built to maintain the two dimensionality of the flow. The Reynolds number (based on the jet slot width) was held constant at 1.78×10^4.

A two-dimensional traversing mechanism was used to move the probe appratus (see Figure 3-1). The range of the traversing device was 60 slot-widths longitudinally (x-direction) and 44 slot-widths laterally (y-direction) with an accuracy better than $\pm$0.02 in. ($\pm$0.04 cm). An L.C. Smith actuator that permitted independent movement of one of the sampling probes was mounted on the probe actuator mount

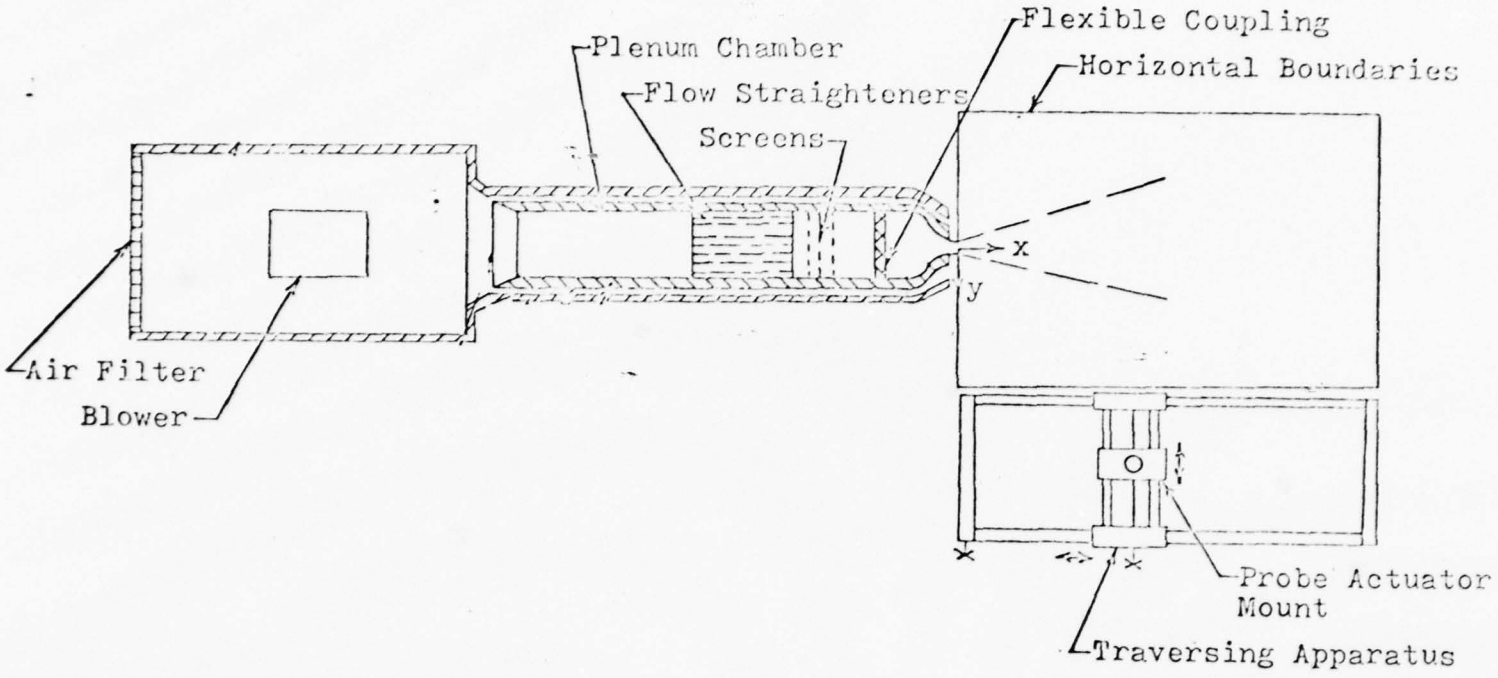

Figure 3-1. Schematic of Plane Jet and Traversing Mechanism. (This figure was modified from Mulej (1975)).

(Figure 3-1). The other sampling probe was mounted to, and was moved manually, with the mount. The actuator provided electrical, remote controlled, traversing of one of the sampling probes. A DC voltage across a 10-turn potentiometer provided a remote voltage proportional to the lateral traverse. The total available traverse was approximately 30 slot-widths relative to the actuator mount with an accuracy of $\pm$0.01 in. ($\pm$0.02 cm). The use of the actuator was later abandoned since the calibration curve (voltage versus the lateral traverse) varied appreciably before and after a run. The probe separation (in the lateral direction) was now achieved manually and this was as accurate as reading the scales on a ruler. Only the top probe was moved manually (Figure 3-2). The probes could be moved up to a separation of 8 slot-widths, or 4 in. (10.16 cm). Most measurements were taken at a probe separation of 0.125 in. (0.3175 cm). Figure 3-2 shows the two hot wire probes. The hot wire probes, part of the traversing mechanism and the confining horizontal walls of the jet can be seen in Figure 3-3.

The block diagrams of the experimental setup used to take the various measurements and to digitize the recorded analog signals are shown in Figures 3-4 and 3-5, respectively. Figure 3-6 shows part of the instrumentation. The outputs of the hot wire probes, which were located at preselected stations in the flow field, were recorded

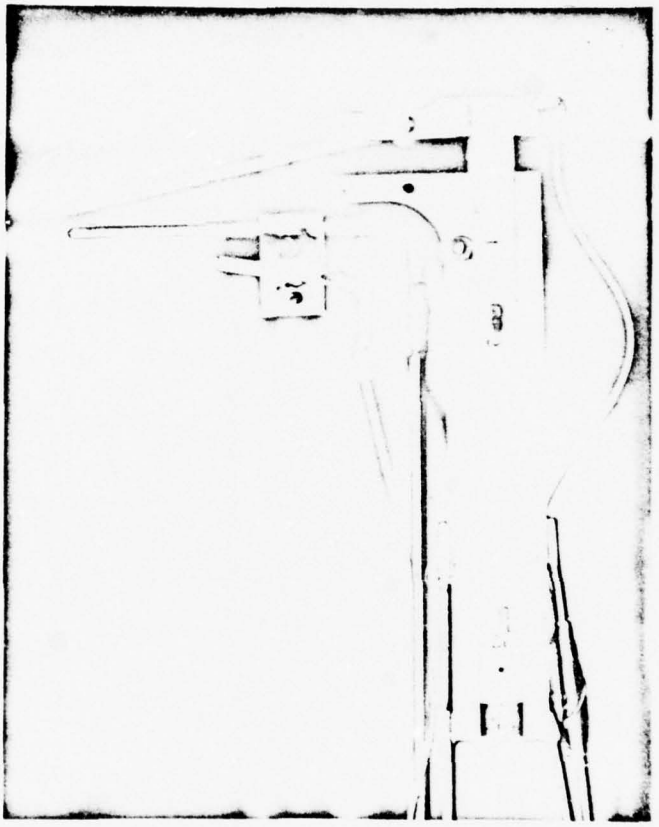

Figure 3-2. Hot Wire Probes.

Figure 3-3. Hot Wire Probes with Part of the Traversing Mechanism and Confining Horizontal Walls.

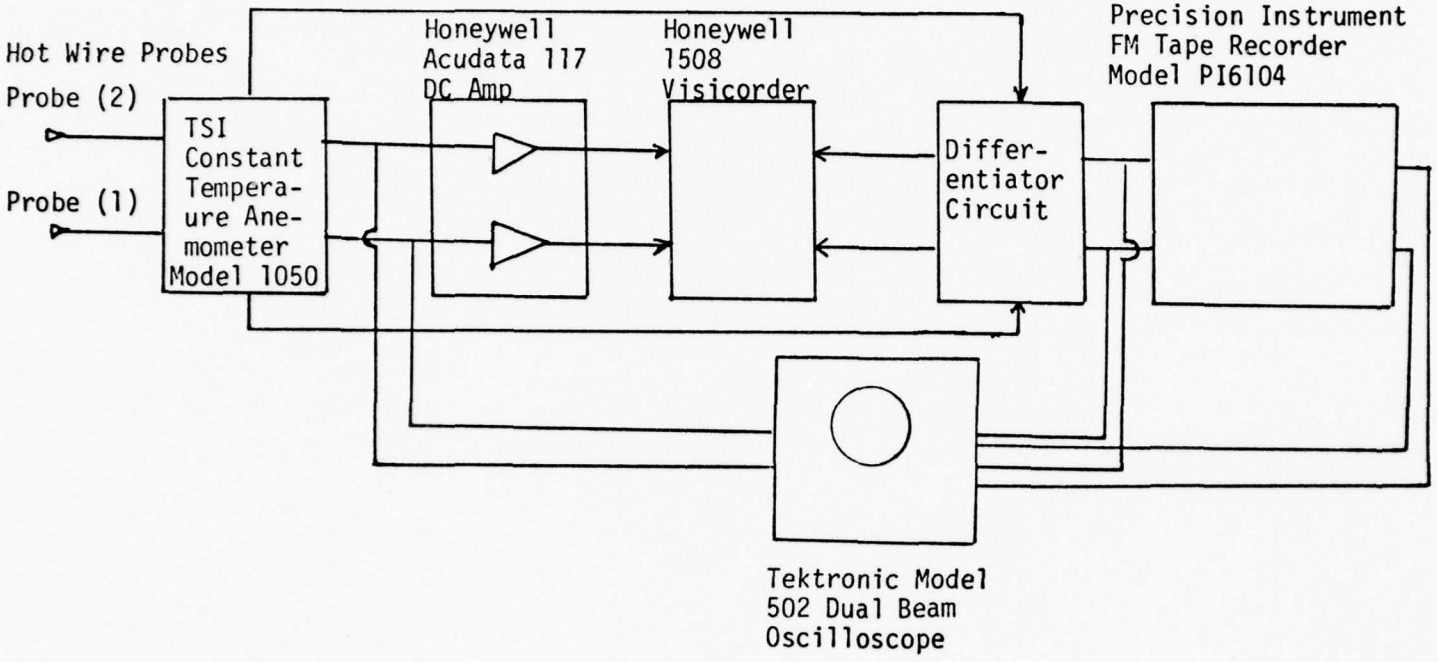

Figure 3-4. Schematic of Data Acquisition Process.

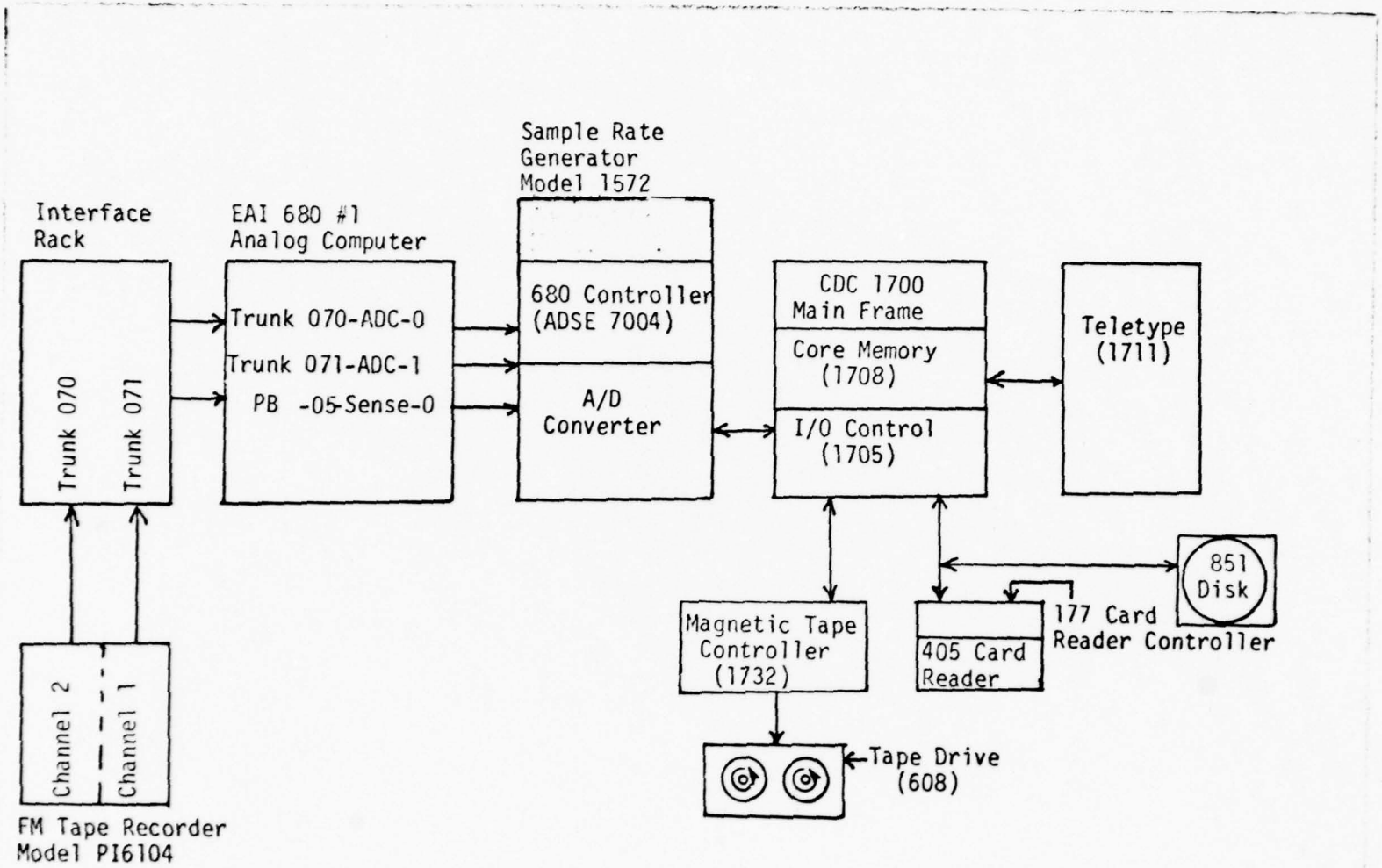

Figure 3-5. Schematic of Digitization Process

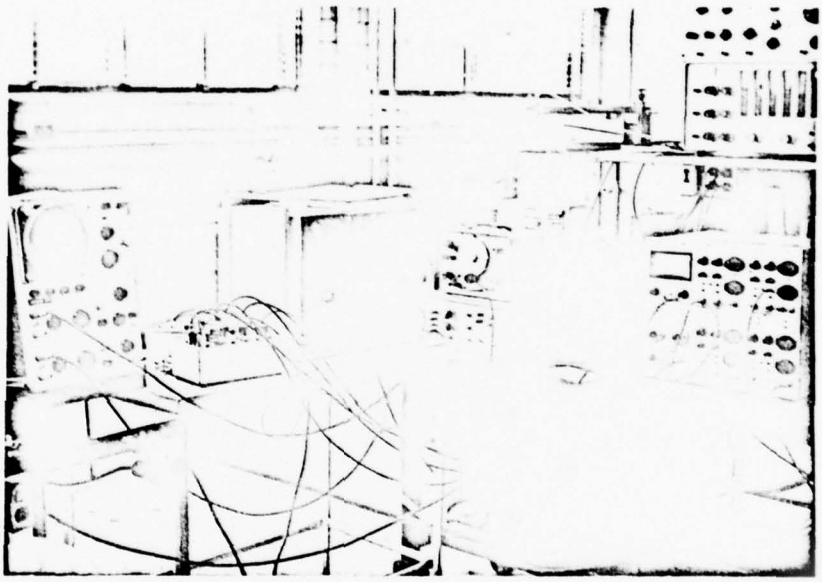

Figure 3-6. Part of Instrumentation for Data Acquisition.

simultaneously. Figure 3-7 shows a typical record from the visicorder. The time derivatives of the hot wire voltages were recorded with an FM tape recorder. Figure 3-8 shows a typical visicorder output of the derivative signals. Comparing this figure with Figure 3-7, it can be seen that the derivative signals discriminate between the turbulent-nonturbulent zones much better than the voltage signals. The choice of the discrimination signal will be discussed in detail in a later section. The procedure used to digitize the time derivatives of the hot wire voltages is presented in Appendix A.

b. Acoustic Excitation

The acoustic disturbance was generated by an Altec 290E acoustic driver, connected to a rectangular section exponential horn, designed with a low frequency cutoff of 166 Hz (see Figure 3-9). The exponential horn was designed by Chambers (1975). The horn was 28 in.(71.12 cm) long and had a mouth 7.25 in.(18.415 cm) by 19 in.(48.26 cm). The input to the driver was supplied by a Brüel and Kjaer Beat Frequency Oscillator type 1022 coupled to a Marantz Model 9 Amplifier. A Systron-Donner Model 114 Counter measured the frequency of the signal.

It was noted in Chapter II that there is a frequency at which a given jet is most sensitive to an acoustic disturbance. It was also noted there that Rockwell (1971) collected data from different investigators and presented

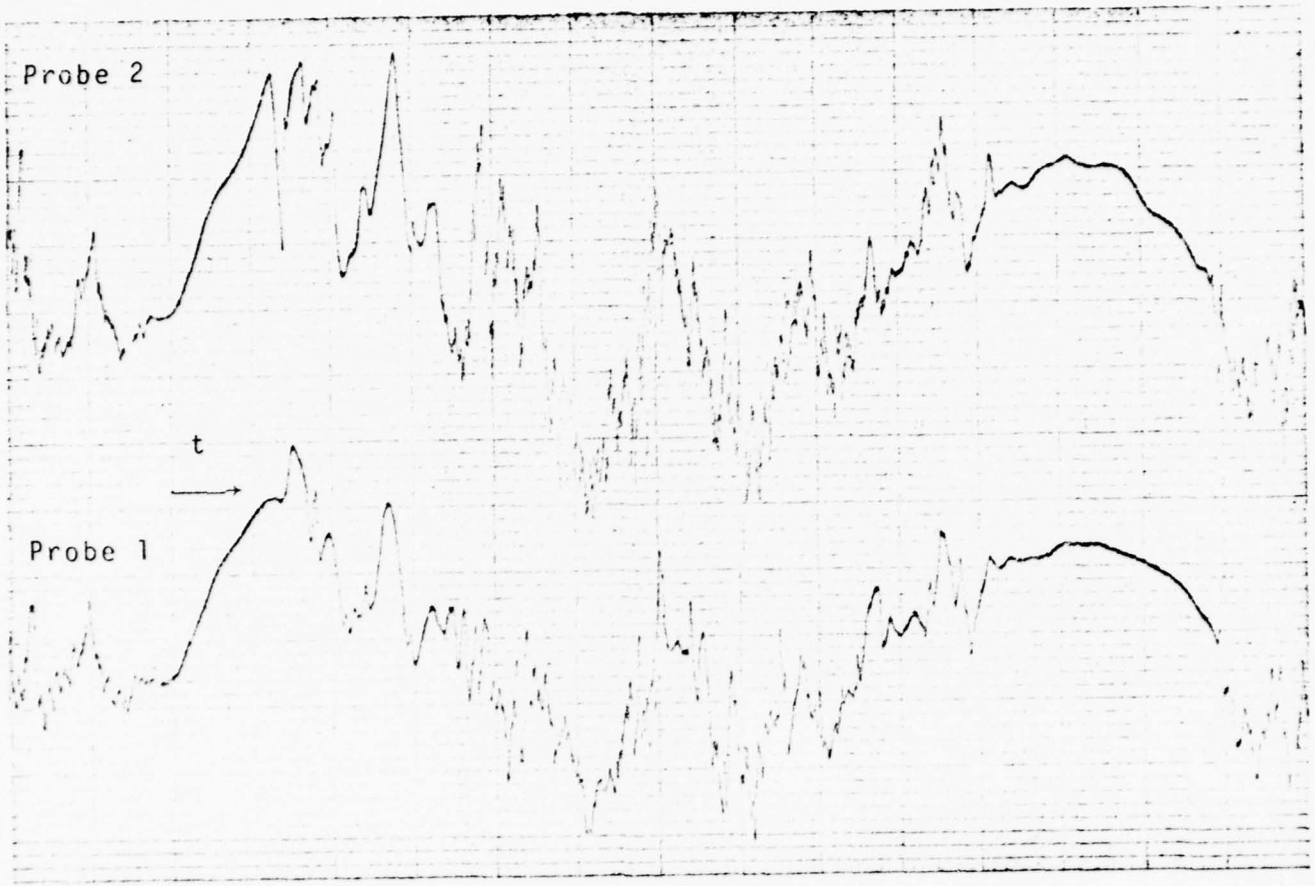

x/D = 45; y/b = 1.19; Δy = 0.125 in. (0.3175 cm)

Figure 3-7. Typical Visicorder Output of Hot Wire Voltages.

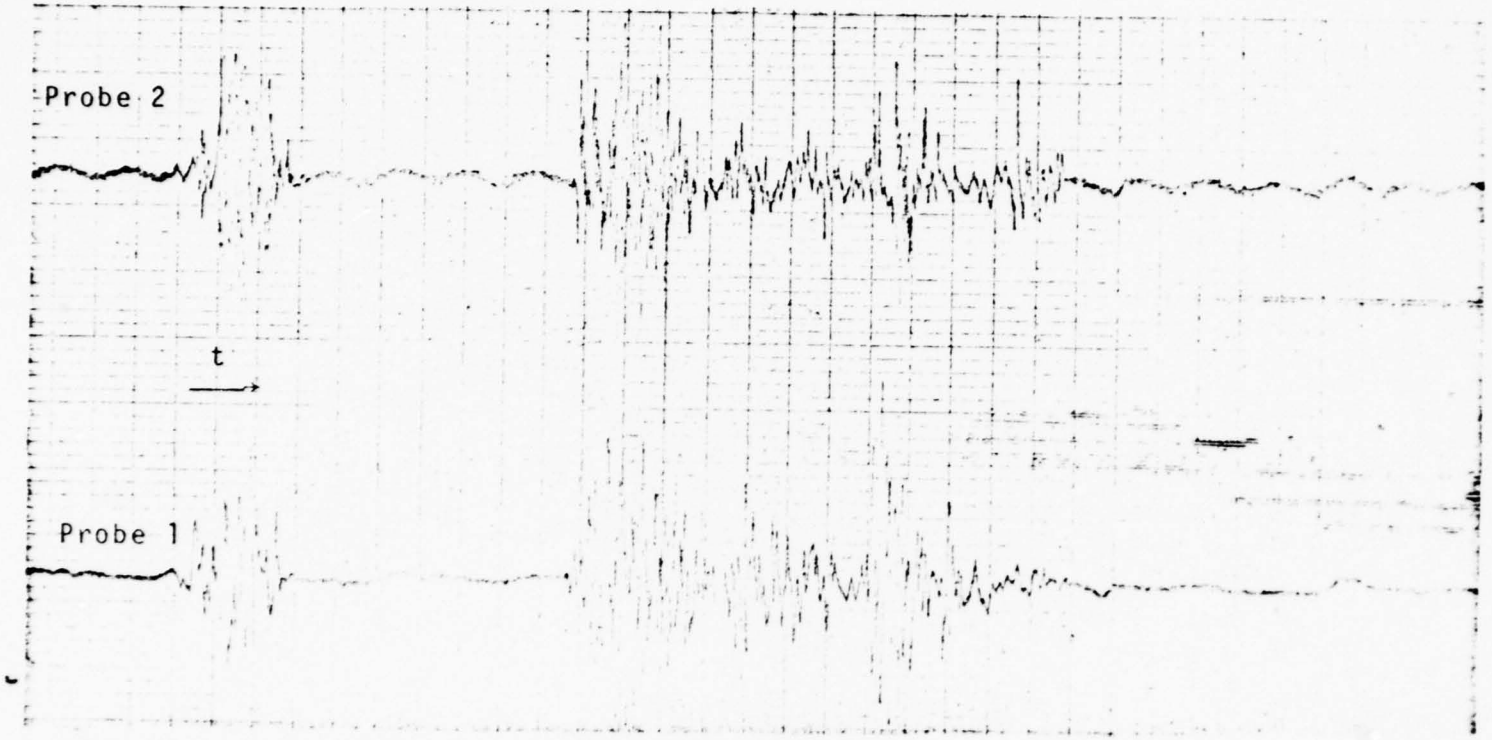

x/D = 45; y/b = 1.66; Δy = 0.125 in.(0.3175 cm)

Figure 3-8. Typical Visicorder Output of Derivatives of Hot Wire Voltages.

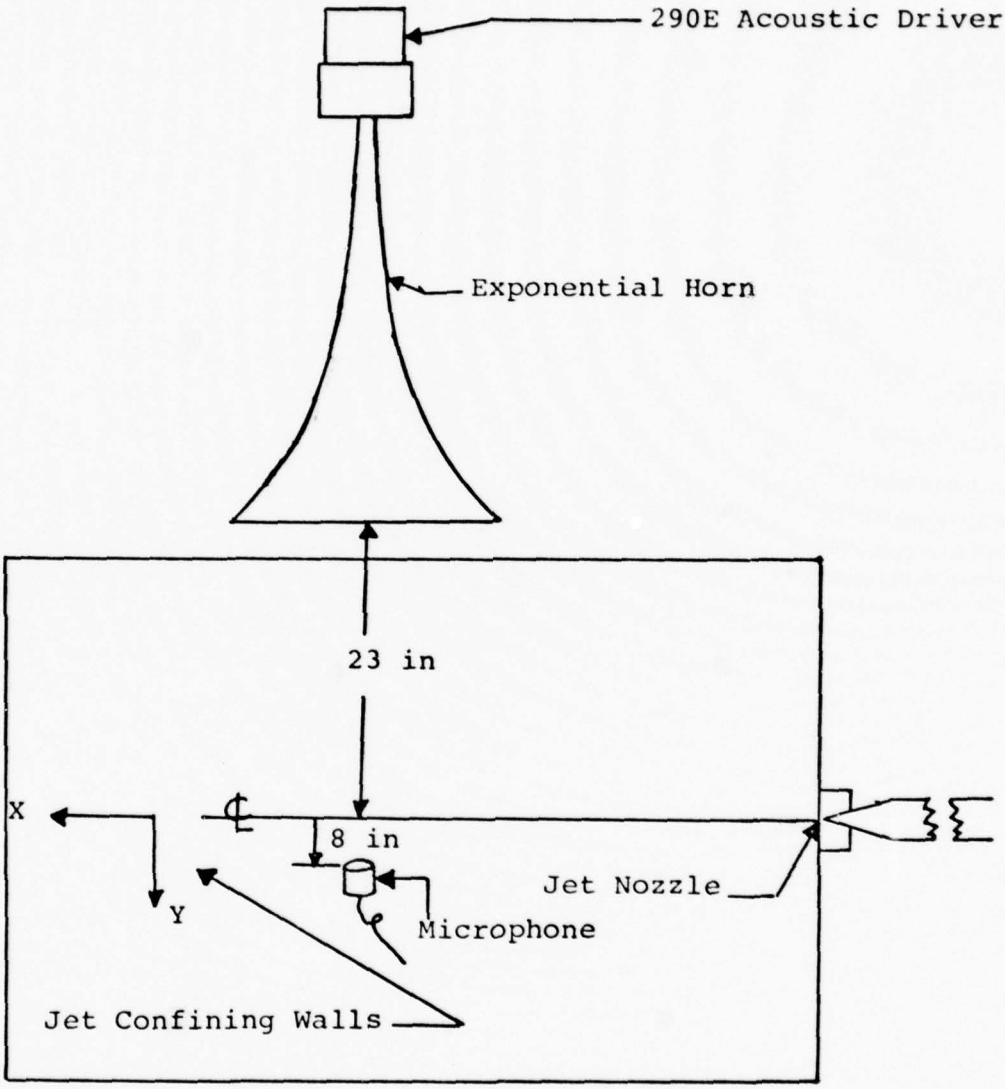

Figure 3-9. Schematic of Horn and Microphone Arrangement for Acoustic Excitation.

them in terms of two dimensionless groups: the Strouhal number and the Reynolds number. He plotted the log of the Strouhal number versus the log of the Reynolds number. This curve was approximately a straight line. From this curve, it is possible to determine the frequency at which a given flow will be most sensitive to an acoustic disturbance. Based on that curve, the Strouhal number at which the jet should be most sensitive to the acoustic disturbance was computed. From this, the first frequency of measurable sensitivity was calculated to be 1143.64 Hz. To verify this, the pitot static tube was placed at the center-line of the jet and the Beat Frequency Oscillator was traversed up to a frequency of 3500 Hz. The sound pressure level was maintained at 105 dB re 20 $\mu N/m^2$. This was measured with a Brüel and Kjaer 1/2 inch (1.27 cm) microphone placed at x/D = 45, y = 8 in. (20.32 cm) and z = 8.25 in. (20.955 cm). The microphone was connected to a B & K 2107 Frequency Analyzer operating in the linear, non-filtering mode (Figure 3-9). By traversing the Beat Frequency oscillator, the first measurable frequency at which the jet was most sensitive was found to be 1149 Hz. This was determined by watching the pressure fluctuation in a micro-manometer as the oscillator settings were changed. This value agreed with that calculated using Rockwell's (1971) curve.

The sound measurements were taken at three x/D stations varying the lateral locations. In all the cases, the sound pressure level was maintained at 105 dB, and the frequency of the acoustic disturbance was held at 1149 Hz. A block diagram of the equipment used to take the sound measurements is shown in Figure 3-10.

3. Preliminary Measurements

To determine how well the jet agreed with published results of previous investigators, a series of preliminary measurements were taken. Specifically, the mean velocity profiles for the undisturbed and acoustically excited cases were measured at three x/D stations and are shown in Figures 3-11 and 3-12 respectively. It appears that Goertler's (1942) equation is the most applicable to the two dimensional jet. This equation takes the form

$$\frac{U}{U_m} = 1 - \tanh^2 \eta \qquad (3\text{-}1)$$

where $\eta = (\sigma\, y)/x$ and σ is a characteristic of the jet. Equation (3-1) can be written as:

$$\frac{U}{U_m} = 1 - \tanh^2 [\sigma\, y/x]$$

$$\frac{U}{U_m} = 1 - \tanh^2 \left[\frac{\sigma}{x/D}(b/D)(y/b)\right] \qquad (3\text{-}2)$$

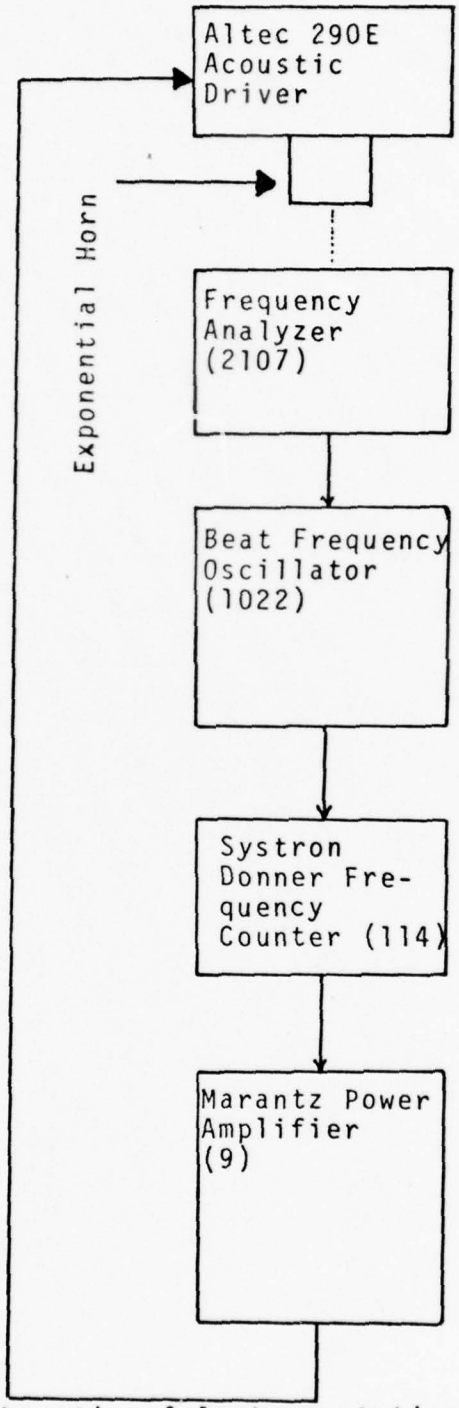

Figure 3-10. Schematic of Instrumentation for Acoustic Excitation.

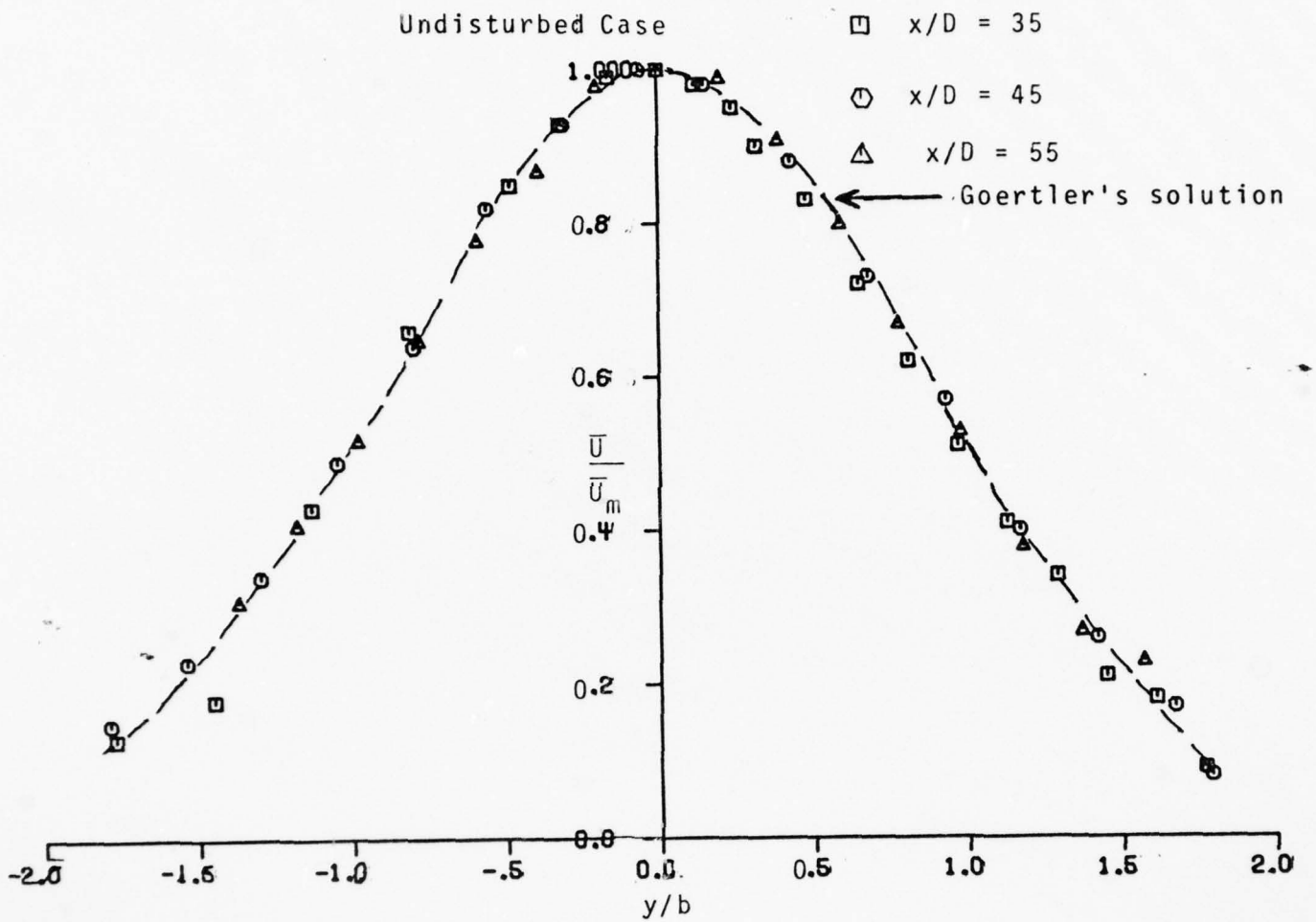

Figure 3-11. Mean Velocity vs. y/b: Undisturbed.

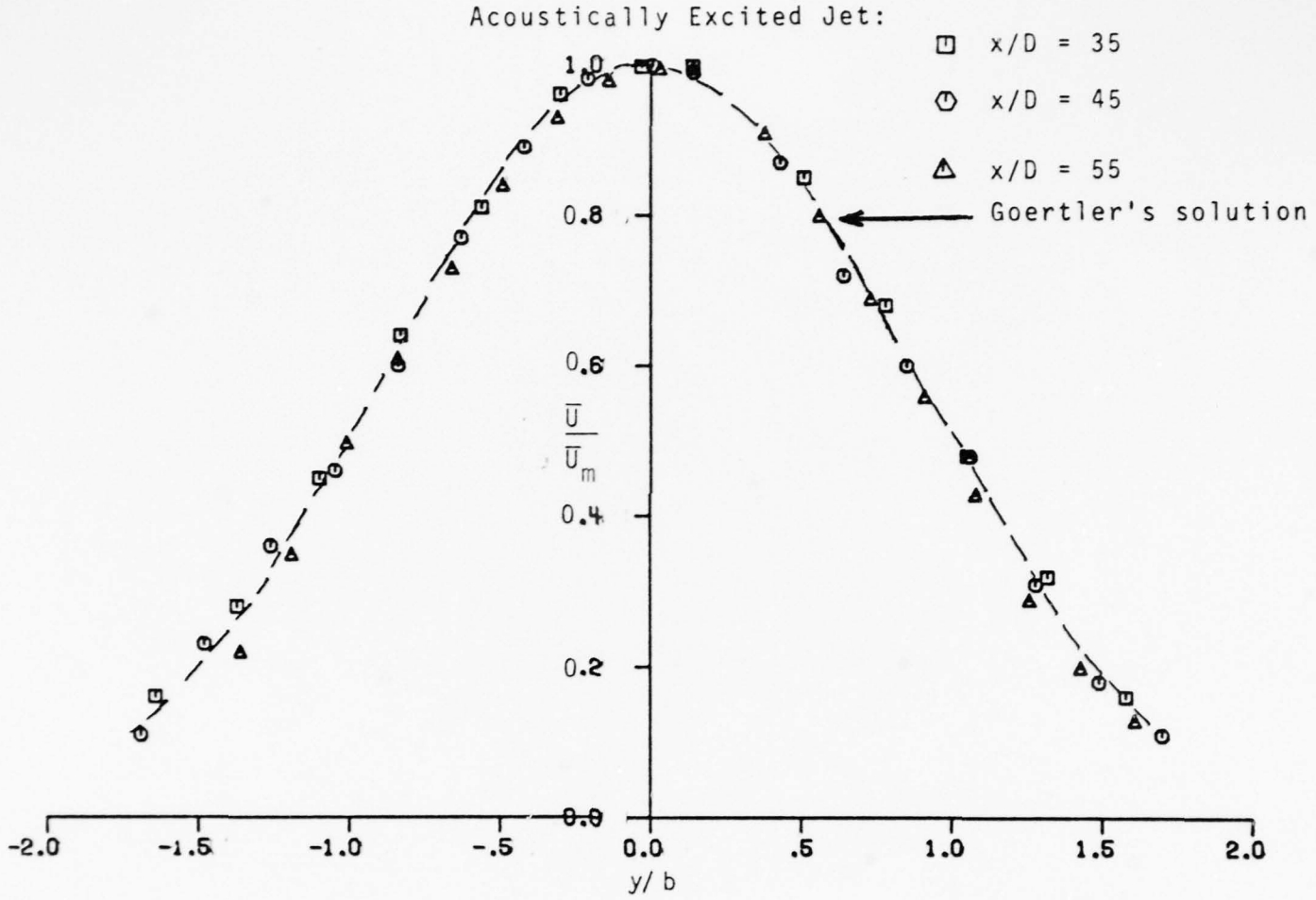

Figure 3-12. Mean Velocity vs. y/b: Excited.

The value for σ can be computed at any x/D station. The velocity half width, b, is defined as the location where the mean velocity is equal to one half the center-line velocity at that x/D station. Hence, at y = b, $\bar{U}/\bar{U}_m = 0.5$. Solving equation (3-2) for x/D = 35 and y/b = 1, the value of σ (for the undisturbed case) was found to be 9.40, and at x/D = 55 and y/b = 1 the value of σ was found to be 9.46. Hence, σ remained essentially constant at all x/D stations in the similarity region. For the acoustically excited case, σ was found to be 8.28 at x/D = 35 and this value also remained constant at all other x/D stations in the similarity region.

Measurements to assure that the jet obeyed the principles of similarity and self preservation as discussed by Lin (1959), Abramovich (1963), Schlichting (1968), Hinze (1959) and Tennekes and Lumley (1972), were taken. One such principle states that the velocity half width is directly proportional to the distance downstream of the jet exit. Stated mathematically, this principle will take the form:

$$\frac{b}{D} = k_1(x/D - C_1) \qquad (3\text{-}3)$$

where k_1 is the widening rate of the velocity field and C_1 is the geometric virtual origin of the jet. Measurements reported by investigators like Van der Hegge Zijnen (1957), Miller and Commings (1957), Heskestad (1965), Bradbury (1965), Jenkins (1974) and Mulej (1975) confirm the linear

relationship given in equation (3-2). The jet used by the author was the same as that used by Jenkins (1974 and Mulej (1975). Since the jet was built by Jenkins (1974), it was necessary for him to take several points to confirm that the principles of similarity and self preservation were obeyed by his jet. To check if the slope and intercept of this straight line agree with those reported by Jenkins (1974) and Mulej (1975), the author merely used three points to construct the straight line. More points, however, would offer less experimental scatter. The three points used were found to be sufficient (Figure 3-13). The values for k_1 and C_1 were found to agree with those reported. The resulting equations for the jet are:

(a) Undisturbed Case (see Figure 3-13)

$$\frac{b}{D} = 0.092\ (x/D + 0.7) \tag{3.4}$$

(b) Acoustically Excited Case (see Figure 3-14)

$$\frac{b}{D} = 0.1\ (x/D + 2.25) \tag{3.5}$$

The other test for similarity involves the decay of the center-line velocity. It states that the square of the center-line velocity is inversely proportional to the distance downstream of the jet exit plane. This can be represented by the equation:

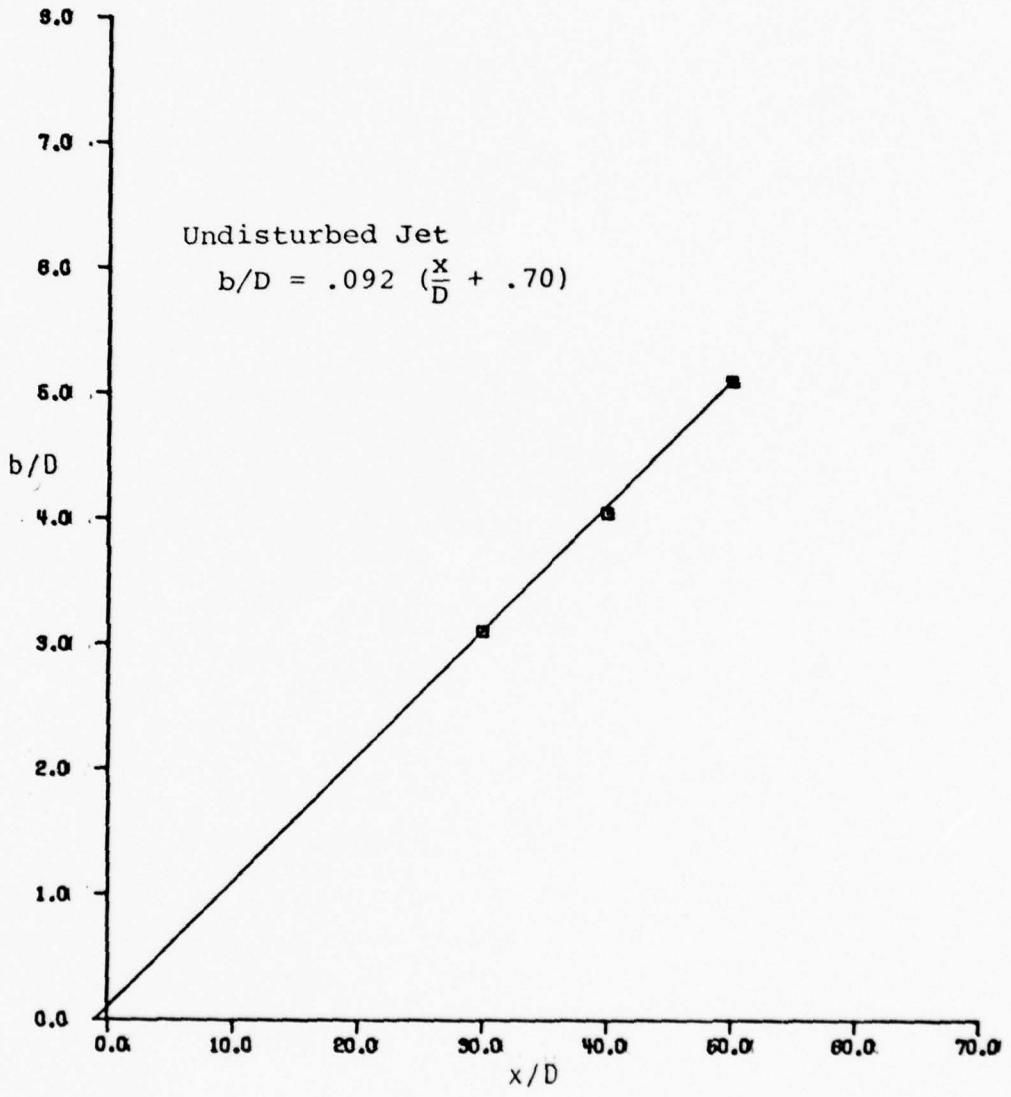

Figure 3-13. Jet Widening Rate: Undisturbed.

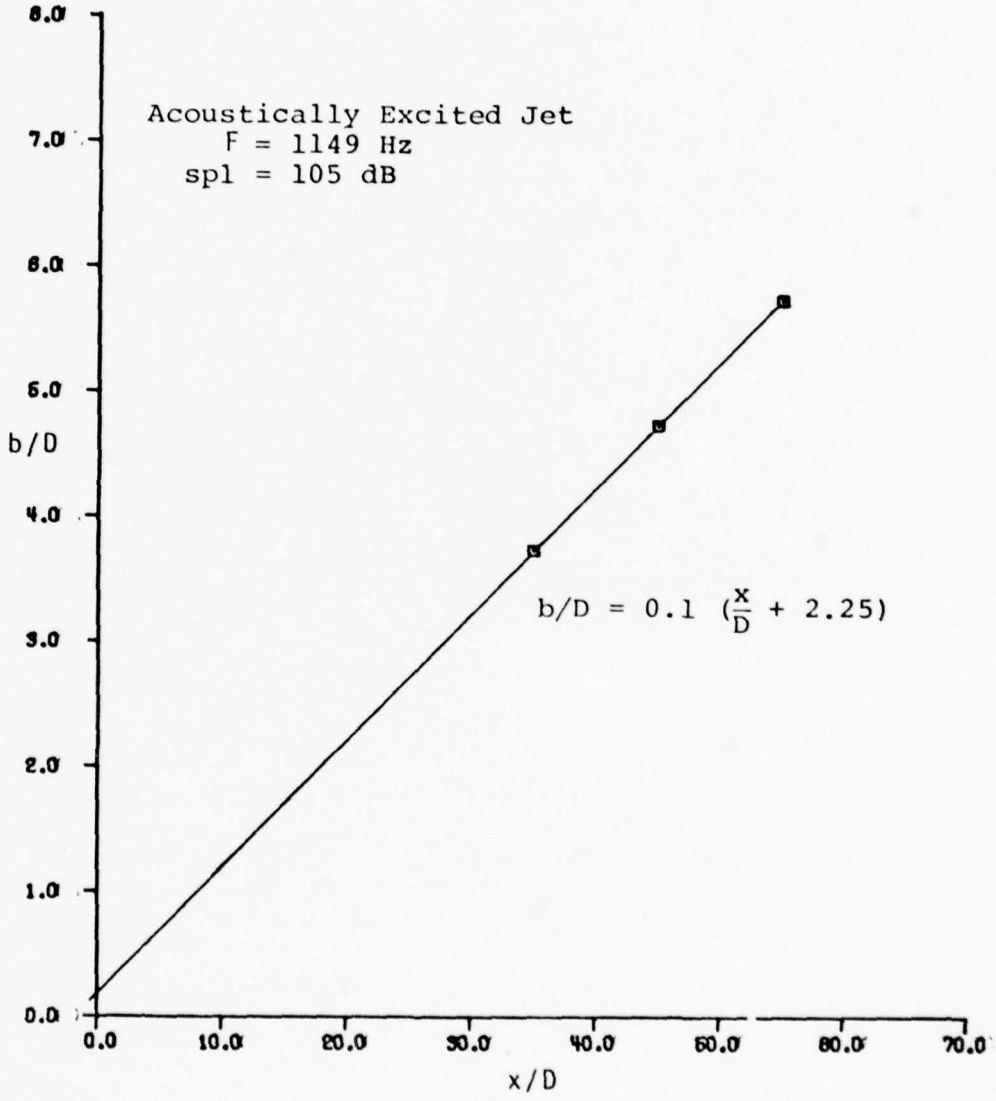

Figure 3-14. Jet Widening Rate : Excited.

$$\left(\frac{U_m}{U_0}\right)^{-2} = k_2 \, (x/D - C_2) \qquad (3\text{-}6)$$

where k_2 is the decay rate of the center-line velocity and C_2 is the kinematic virtual origin of the jet. Flora and Goldschmidt (1969) noted that there was no reason to expect any relationship between the two virtual origins. The undisturbed and disturbed cases are shown in Figures 3-15 and 3-16, respectively. The resulting equations are:

(a) Undisturbed Case (Figure 3-15)

$$\left(\frac{U_m}{U_0}\right)^{-2} = 0.182 \, (x/D - 3.30) \qquad (3\text{-}7)$$

(b) Acoustically Excited Case (Figure 3-16)

$$\left(\frac{U_m}{U_0}\right)^{-2} = 0.185 \, (x/D - 2.97) \qquad (3\text{-}8)$$

4. Comparison with other Shear Flows

The mean velocity profiles (see Figures 3-11 and 3-12) agree with the theoretical results of Goertler (1942) (see also equation(3-1)). The principles of similarity and self preservation are satisfied and the empirical constants obtained from experiments compare adequately with those of previous investigators. The values are tabulated in Table 3-1. For the range of Reynolds number ($0.45 \times 10^4 \leq R_{e_D} \leq 8.0 \times 10^4$) considered by the investigators, the widening

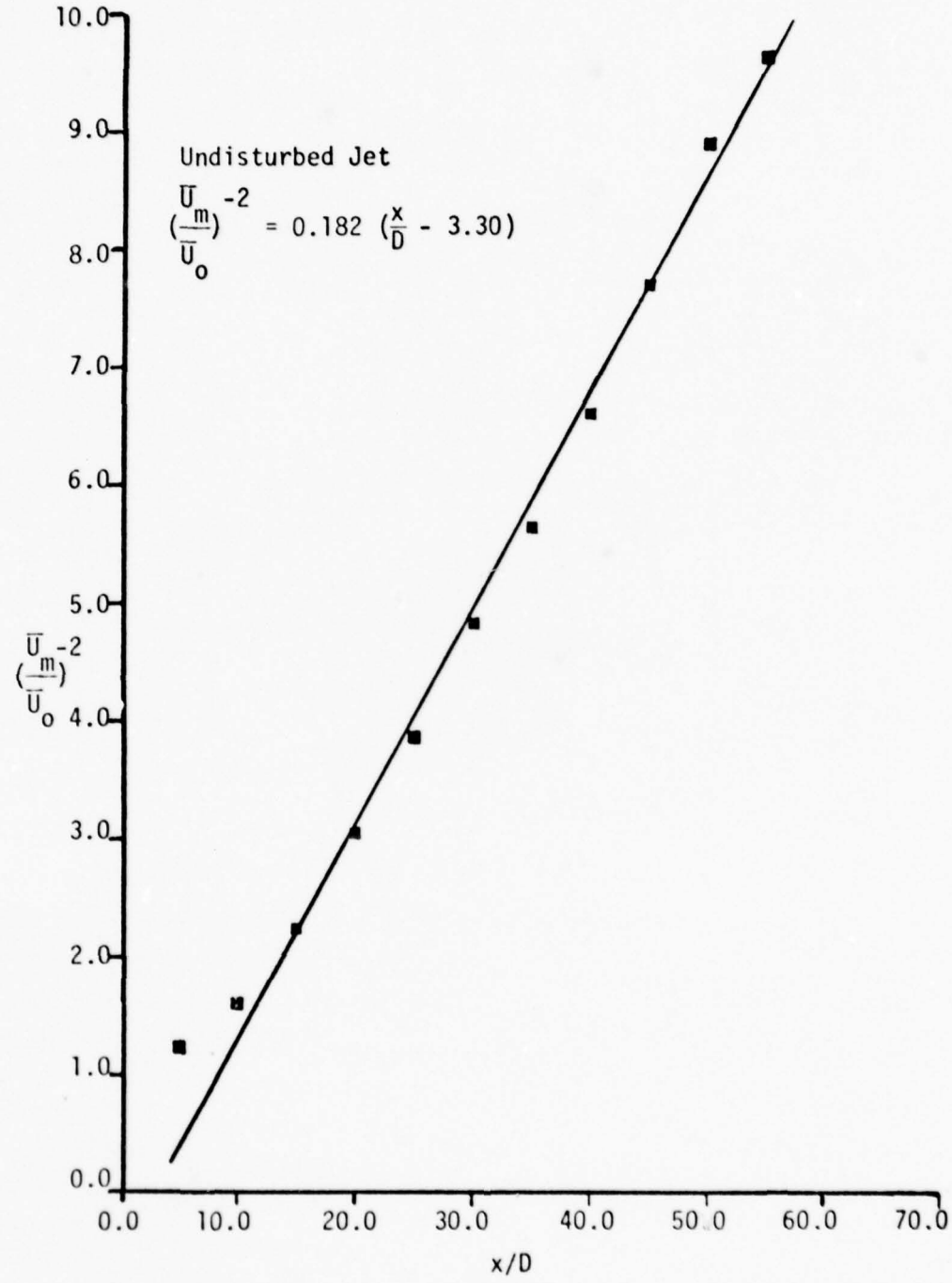

Figure 3-15. Center-line Velocity Decay Rate: Undisturbed.

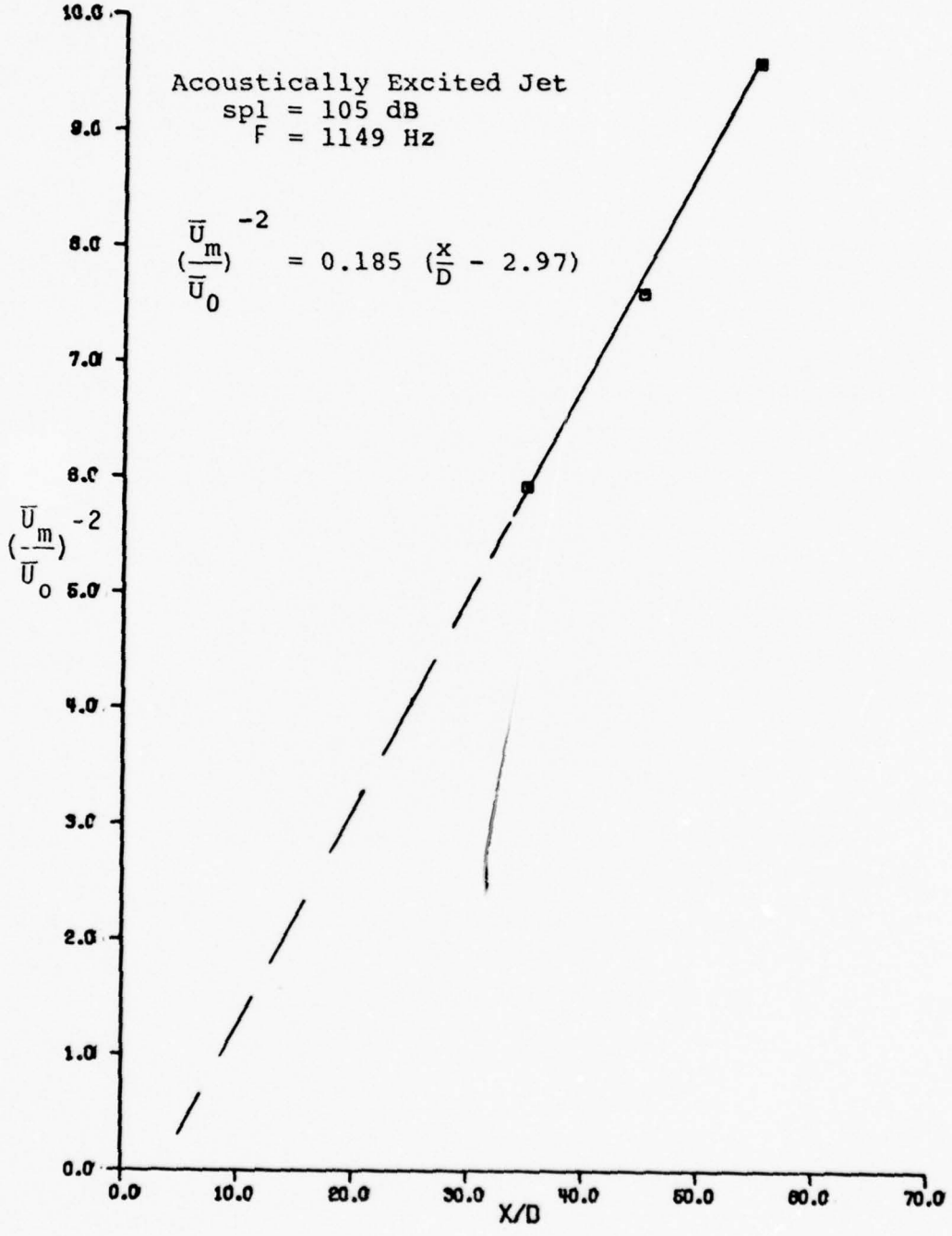

Figure 3-16. Center-line Velocity Decay Rate: Excited.

Table 3-1. Characteristic Parameters of Plane Jets Compared.

Investigator	R_{e_D}	k_1	k_2	C_1	C_2
Miller & Commings (1957)	1.78×10^4	0.0983	0.227	-1.572	-1.572
Van der Hegge Zijnen (1957)	1.33×10^4	0.100	0.205	0.0	-1.70
Foss (1965)	5.5×10^4	0.085	0.2565	-2.0	6.50
Heskestad (1965)*	2.5×10^4	0.110	0.364	5.3	5.3
Householder (1968)	$4.-8. \times 10^4$	0.0908	0.1927	-1.46	6.98
Flora (1969)	$2.-3. \times 10^4$	0.109-0.318	0.158-0.227	-15.0	2.0
Kaiser (1971)**	0.45×10^4	0.128	0.240	1.2	0.0
Kaiser (1971)	$0.45\text{-}0.60 \times 10^4$	0.101	0.208	-2.6	0.0
Kaiser (1971)**	0.60×10^4	0.117	0.209	-2.4	0.0
Ott (1972)	1.0×10^4	0.0968	0.228	-3.0	7.0
Young (1973)	1.0×10^4	0.0875	0.150	-8.75	-1.25
Jenkins (1974)***	1.45×10^4	0.091	0.160	-3.0	4.0
Mulej (1975)	1.6×10^4	0.095	0.185	-0.789	13.2
Present Work	1.78×10^4	0.092	0.182	-0.70	3.30
Present Work**	1.78×10^4	0.10	0.185	-2.25	2.97

*mixing at the jet exit
**acoustically excited jet
***heated 20.7° above ambient

rate varied from 0.085 to 0.110 and the decay rate of the center-line velocity varied from 0.150 to 0.364. The rather high value, 0.364, was for the case of mixing at the jet exit. The two dimensionality of the jet used by the author had been established by Jenkins (1974) and was not repeated here.

The jet widening rate at a Reynolds number of 1.78×10^4 increased by 8% when an acoustic disturbance was applied. This percent increase was compared with those obtained by Kaiser (1971). He reported a 21.1% increase for a Reynolds number of 0.45×10^4 and a 13.7% increase for a Reynolds number of 0.60×10^4. These values confirm Rockwell's (1971) claim that the Reynolds number is an important parameter in determining the maximum sensitivity of jets to an applied disturbance.

The objective of taking these preliminary measurements was to check if the flow field is indeed a plane turbulent jet. These measurements confirm the validity of the jet and hence, it can be used as a valid flow field to proceed with the proposed objectives of measuring intermittency, fold-over and crossing frequency of the turbulent-nonturbulent interface.

5. Detection of the Turbulent Nonturbulent Interface

a. Introduction

The original objective of this research was to see if a traveling acoustic wave could change the occurrence of fold-over of the interface of a plane turbulent jet. It was realized that in order to achieve this goal a more definite method than that used by Mulej (1975) needed to be developed. Mulej (1975) examined visually a continuous visicorder record of two hot wire voltages. As will be discussed later, the ability to measure fold-over credibly depends on how well the turbulent-nonturbulent interface is detected for each of the two hot wire voltages. Since the hot wire probes used by Mulej (1975) were positioned at approximately 0.10 in.(0.254 cm) apart, the difficulty of visually detecting, at all times, which of the two probes first becomes turbulent or nonturbulent cannot be overemphasized (see Figure 3-7). Hence the objective of this research expanded to include detecting the turbulent-nonturbulent interface by a digital analysis. This makes it possible to process a larger amount of data and hence to get a more meaningful average.

Before presenting the details of the actual method used, a brief review of some of the techniques used by previous investigators will now be given. The purpose of this review is to show how arbitrary the interface detection techniques are.

b. Review of Some Previous Techniques

Several different methods have been used to separate a continuous signal originating from an intermittently turbulent flow into "turbulent" and "nonturbulent" zones. These methods can be grouped into two. The first method is to examine a continuous record of the signal, either visually, or by computer analysis (Kaplan and Laufer (1968), LaRue (1973), Hedley and Keffer (1974), Spencer (1970), etc.) when the length of record available for inspection is considerably larger than the length of a typical "turbulent burst." The second, the analog approach, is characterized by a built-in decision time and a detection delay. This detection delay time is set between the actual event and the time at which the decision is made. This decision is made on the basis of the past history of the signal without the benefit of knowing the future. Kaplan and Laufer (1968) and Kibens and Kovasznay (1970) independently came to the conclusion that an important requirement for good detection is a knowledge of the future of the signal. This knowledge can easily be achieved through a digital computer method since digitized signals can be stored. The analog method requires some time to generate the detector function (the intermittency function, I(t)) and consequently, the signal from other wires has to be delayed to account for this time delay.

Both the digital and the analog methods have been proved credible. The choice between these two methods

depends on the cost of laboratory time versus computer time. As observed by Kibens and Kovasznay (1970) and other researchers, a certain amount of arbitrariness in forming the intermittency function, I(T), is inevitable. The difficulty in defining the location of the turbulent-nonturbulent interface has been compared with that of the shoreline of the sea (see Kibens and Kovasznay (1970)). The location is dependent on the magnification, or coarseness of the method of detection. Depending on the size of details taken into account, the shoreline of the sea could on one hand be considered relatively smooth and on the other hand, full of inlets and islands.

The choice of an input signal referred to by Kaplan and Laufer (1968) as the criterion function, is an important step in the discrimination process. This signal must offer the best contrast between the turbulent and nonturbulent regions. In general, the criterion function should be small in the nonturbulent regions, and appreciably large in the turbulent regions.

Townsend (1949), investigating the turbulent wake of a circular cylinder, used the velocity time derivative as the input signal. Corrsin and Kistler (1954) also used the velocity time derivative for their work in the boundary layer, but suggested that an improved detection would result if I(t) were formed from a signal proportional to the instantaneous vorticity level in the flow. Fiedler

and Head (1966) modified the circuit used by Corrsin and Kistler (1954) by phase-shifting the rectified signal by a time which was small compared to the period between successive turbulent bursts, and adding it to the non-shifted rectified signal.

Kaplan and Laufer (1968) used the short-time variance of the time derivative of the hot wire voltage as the criterion function. The variance was computed over a relatively short time interval which varied from 2.5 to 8 msec. The computed variance was compared to a threshold level derived by taking a fraction of the local maxima of the criterion function. If the variance exceeded the threshold level, the intermittency function, I(t), was given the value of unity, otherwise zero.

Kibens and Kovasznay (1970) used the time derivative of a component of the vorticity. Jenkins (1974) also used the same input signal. LaRue (1973) claimed that the temperature signal of the wake of a heated rod offered a good contrast between the turbulent and nonturbulent zones. Antonia (1972), in the boundary layer, used the time derivative of the Reynolds shear stress while in the mixing layer. Wygnanski and Fiedler (1970) used the sum of the squares of the first and second time derivatives of the longitudinal velocity.

Most investigators agree that the best criterion function is that based on the local vorticity, which is

zero in the nonturbulent regions, and appreciably large in the turbulent zones. However, the vorticity is rather difficult to measure since, the measurement of even one component of the vorticity vector would require four precisely positioned, and nearly identical, hot-wire probes. Because of this difficulty, most experimenters use other physical variables, or a combination of them, as their input signal even though those signals offer less contrast between the turbulent and nonturbulent zones. In the plane jet, for example, Heskestad (1965) used the band passed velocity squared, while Thomas (1973) used the sum of the square of the band passed velocity and its derivative in the plane turbulent wake.

When an adequate input signal is chosen, the next important steps involve the choice of the detection criteria, which consist of two adjustable parameters: the threshold level, and the hold time, τ_H. The threshold level, or the gate level, can be defined as that level to which the input signal, S(t), is compared to determine whether the intermittency function, I(t), would be set to unity or zero. In general, therefore, the intermittency function is set equal to unity when the input signal is equal to or greater than the threshold level. Otherwise the intermittency function is set equal to zero.

The other parameter, the hold time, τ_H, is the length of time intervals over which the threshold criterion is

applied. This implies that the intermittency function, I(t), is allowed to change only when the input signal crosses the threshold level for a sufficiently long time, τ_H.

Selection of nominal values for those parameters, threshold level and hold time, is again rather arbitrary. Each investigator selects the nominal values best suited to his flow field.

Kaplan and Laufer (1968) selected their threshold level by choosing a fraction of the local maxima of the criterion function over a time interval they considered reasonable. The short time variance which constituted their criterion function had no "zero-crossings." No hold time was imposed on their criterion function to determine the intermittency function. However, by taking the short time variance of the time derivative of the hot wire voltage, they were in effect smoothing the derivative signal. This smoothing was tantamount to applying a hold time, τ_H, to the square of the derivative of the hot wire voltage.

Kibens and Kovasznay (1970) chose the nominal value of the threshold level by examining how the intermittency factor, γ, and the crossing frequency, F_γ, varied with different threshold levels. Their threshold was a fixed constant determined by the threshold circuitry, but the threshold level (gain), which they defined as the

ratio of the rms of the turbulent part of the input signal S(t), to the fixed threshold value, varied. They found that between certain threshold levels, the intermittency factor, and the crossing frequency approaches some asymptotic value. Within this range of threshold levels, therefore, both the intermittency factor, and the crossing frequency varied very slightly. Their final choice of a threshold level for a given location was arbitrarily made within the range of acceptable threshold levels.

Kibens and Kovasznay (1970) chose their hold time differently from the way they chose the threshold level. The hold time was related to a characteristic time, T_{ch}, or a characteristic frequency, F_{ch}. These were defined by:

$$\dot{S}' = 2\pi F_{ch} S' = \frac{2\pi}{T_{ch}} S' \qquad (3\text{-}9)$$

where $\dot{S} = \frac{\partial S(t)}{\partial t}$ (3-10)

$\dot{S}$ is the time derivative of the input signal, S(t); S' and $\dot{S}'$ are the rms values of S(t) and $\dot{S}(t)$, respectively. They noted that the choice of the nominal value of the hold time, τ_H, should be proportional to T_{ch}. Their criterion for choosing τ_H was that $\tau_H/T_{ch} \geq 1$. Specifically, they chose the ratio to be 4/3. They noted that in the boundary layer in which they were measuring, the characteristic frequency was 330 Hz at $y/\delta = 0.26$. The characteristic

time was computed from $T_{ch} = \frac{1}{F_{ch}} = 3$ msec. Consequently, they chose the hold time, τ_H, to be 4 msec. This value was held constant for the rest of their measurements.

LaRue (1973) selected his threshold level in a manner similar to Kibens and Kovasznay (1970). However, his hold time was selected differently. He noted that the order of the minimum duration of a fully turbulent "patch" should be twice the Kolmogoroff length transit time, $2(\ell_k/U_\infty)$, where U_∞ is the free stream velocity. He contended that in order to detect the smallest turbulent "patches," the hold time should be chosen to be near this value. Since he analyzed his data digitally, with a time step between digital samples of 239 μs, he chose a nominal hold time of 240 μs, or $3(\ell_k/U_\infty)$. Both the threshold level and the hold time were subsequently held constant for the rest of his experiment. This method of choosing the hold time was also used by Hedley and Keffer (1974). Their input signal, however, was a double-component function which involved the derivatives of U and V separately.

Jenkins (1974) followed a procedure similar to Kibens and Kovasznay (1970) in selecting his detection criteria. The detector circuitry and choice of input signal were similar, although the flow was not. While Kibens and Kovasznay (1970) were concerned with the boundary layers, Jenkins (1974) considered a plane turbulent jet. He selected a threshold level by a method almost similar to Kibens and

Kovasznay (1970). Both Kibens and Kovasznay (1970) as well as LaRue (1973) report that both the crossing frequency, F_γ, and the hold time, τ_H, should be relatively insensitive to the threshold level selected to be credible in the discrimination process. Jenkins (1974) obtained a range of threshold level over which the crossing frequency, F_γ, was relatively flat. Within this range, the intermittency factor, γ, varied almost linearly. It seems, therefore, that he based his choice of a threshold level only on the crossing frequency. He noted, however, that at his nominal threshold level, the intermittency factor reduced in slope (see Jenkins (1974) Figure 3-7).

A typical characteristic frequency, F_{ch} measured by Jenkins (1974) at a relatively small x/D station and close to the center-line was in the order of 615 Hz. He defined the delay time, τ_d, which was equal to the hold time, τ_H, by the relation:

$$\tau_d = \left(\frac{2\pi}{\omega_{ch}}\right) \ell n\ 2 = \frac{\ell n 2}{F_{ch}} \qquad (3\text{-}11)$$

Substituting 615 Hz for F_{ch}, he obtained a delay or hold time equal to 1.13 msec. Sweeping through the remainder of the flow field and finding corresponding characteristic frequencies, he varied the nominal value of the hold time from 3.60 to 7.5 msec, depending on the position in the flow.

While the investigation techniques used by the various experimenters reviewed were considerably different, their

intermittency and crossing frequency distribution functions as measured seemed to obey the same expressions. Corrsin and Kistler (1954) established that the probability density function of the interface position Y, was very nearly Gaussian and that the distribution of Y could be expressed using the error function. Specifically, the intermittency profile is approximated by the expression:

$$\gamma(y) = \frac{1}{2}\left[1 - \text{erf}\left(\frac{y - \overline{Y}}{\sqrt{2}\,\sigma}\right)\right] \qquad (3\text{-}12)$$

where $\overline{Y}$ is the mean position of the interface and σ is its standard deviation. $\overline{Y}$ is defined as the location where $\gamma = .5$. The crossing frequency distribution is approximated by the expression:

$$F_{\gamma}(y) = F_{\gamma m} \exp[-(y - \overline{Y})^2/(2\sigma^2)] \qquad (3\text{-}13)$$

where $F_{\gamma m}$ is the maximum crossing frequency and occurs at $\overline{Y}$.

c. Method Used

It was pointed out in the last section that the original objective of this research was expanded to include detecting the turbulent-nonturbulent interface by digital analysis. The review of some of the previous techniques used by other experimenters shows the degree of arbitrariness in discriminating between turbulent and nonturbulent zones. The method used here involves selecting: (i) the input signal,

(ii) the threshold level, and (iii) the hold time. Each of these will be discussed fully here to establish the credibility of the discrimination process.

(i) The Input Signal, S(t)

The square of the time derivative of the hot wire voltage was used as the criterion function (input signal). This is comparable to the variance signal used by Kaplan and Laufer (1968), the velocity time derivative used by Townsend (1949), Corrsin and Kistler (1955), and the square of the time derivative used by Fiedler and Head (1966). The voltages from two hot wire probes placed 0.125 in. (0.3175 cm) apart were passed through a differentiator circuit (see Appendix C). The resulting time derivatives of these voltages were recorded on an analog tape recorder at a speed of 37.5 in/sec (95.25 cm/sec). During the play back, at the same speed, the signals were digitized simultaneously on a CDC 1700 Hybrid computer, using the appropriate software (assembly language). The sampling rate was 4000 samples/sec since the highest frequency of interest was 2KHz. Further explanation for this choice of sampling rate is given in Appendix A. The data were processed on the Purdue University CDC 6400-6500 dual MACE digital computer. 10.74 sec of data (42960 samples) were analyzed. This was true for all cases except those in which the hold time and total time of sampling were varied purposely. Details of the digitization process are given in Appendix A.

Computer programs to check the validity of the digitized samples are presented and explained in Appendix B. A comparison of Figures 3-7 and 3-8 justifies the use of the time derivatives of the hot wire voltages rather than the direct voltages in attempting to discriminate between the turbulent and the nonturbulent zones.

(ii) The Threshold Level

The threshold level used in this work is defined by the relation:

$$C^2 = PS'^2 \qquad (3\text{-}14)$$

where C^2 is the threshold level which varies with the gain, P; S'^2 is the mean square of the input signal, S(t). Curves similar to Figure 3-17 were plotted to see how the intermittency and crossing frequency varied with different threshold levels at the selected hold time, τ_H^*, of 10 msec. As can be seen from the figure, a range of threshold level ($P \geq 0.6$) exists that makes F_γ relatively flat. It can also be seen that at $P = 0.6$, the intermittency has changed slope drastically, and has started to converge to an asymptotic value. Of course, both curves will eventually go to zero as $P \to \infty$. The selected value of P in this case was 0.65. Hence the threshold level for this particular location was $C^2 = 0.65\ S'^2$.

The different values of P used to plot Figure 3-17 were obtained from the computer program. For example:

*The hold time, τ_H, is discussed in the next section.

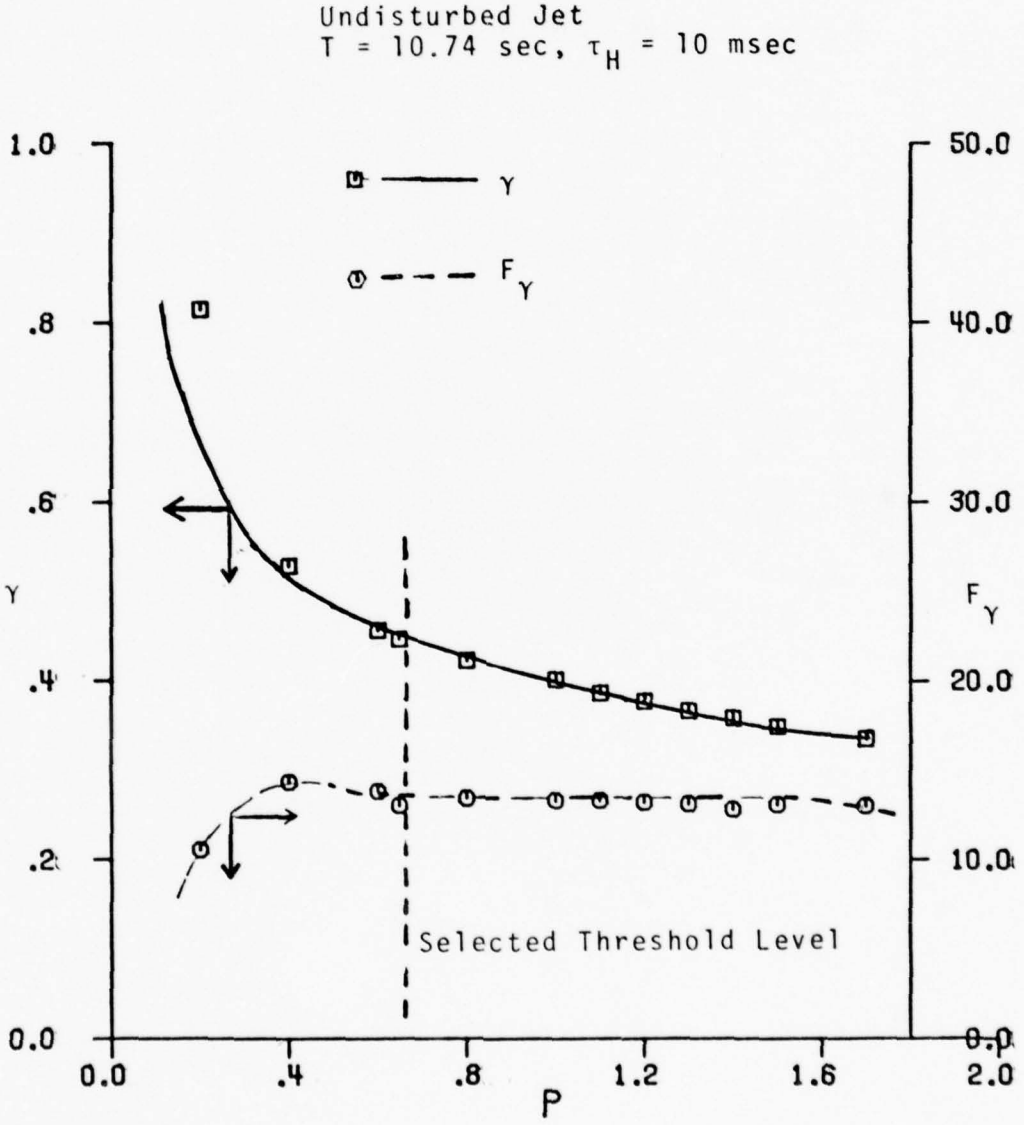

Figure 3-17. γ and F_γ vs. P at x/D = 45, y/b = 1.66.

P could be initialized to 0.0 and a "DO LOOP" command imposed on the program. This would cause P to take values of 0.2, 0.4 etc. up to say, 1.4, if the increment chosen was 0.2. For each value of P, values of γ and F_γ could be computed. Curves (γ and F_γ versus P) similar to Figure 3-17 could then be plotted to see if either F_γ or γ had exhibited an asymptotic behavior. By examining the curves, P* and hence the threshold level, C^2, could be selected.

The procedure explained above was repeated for each location in the flow field examined. The selected value of P and hence the threshold level varied with location. The variation of the selected values of P with y/b can be seen in Figures 3-18, 3-19 and 3-20 for x/D = 35, 45 and 55 respectively and the hold time, τ_H, = 10 msec. The same procedure was also used for the cases of the acoustically excited jet. Here again the selected values of P varied with location as can also be seen in Figures 3-18, 3-19 and 3-20 for x/D = 35, 45 and 55 and τ_H = 10 msec. The curves reveal that the threshold level increases nonlinearly with lateral location.

Notice that for each selected threshold level, values of γ and F_γ were computed. In Figure 3-17, for example, the selected value of P at x/D = 45, y/b = 1.66 is 0.65. At this value of P, the corresponding values of γ and F_γ are 0.446 and 13.04 Hz respectively. At other locations

*P was selected to give the correct γ.

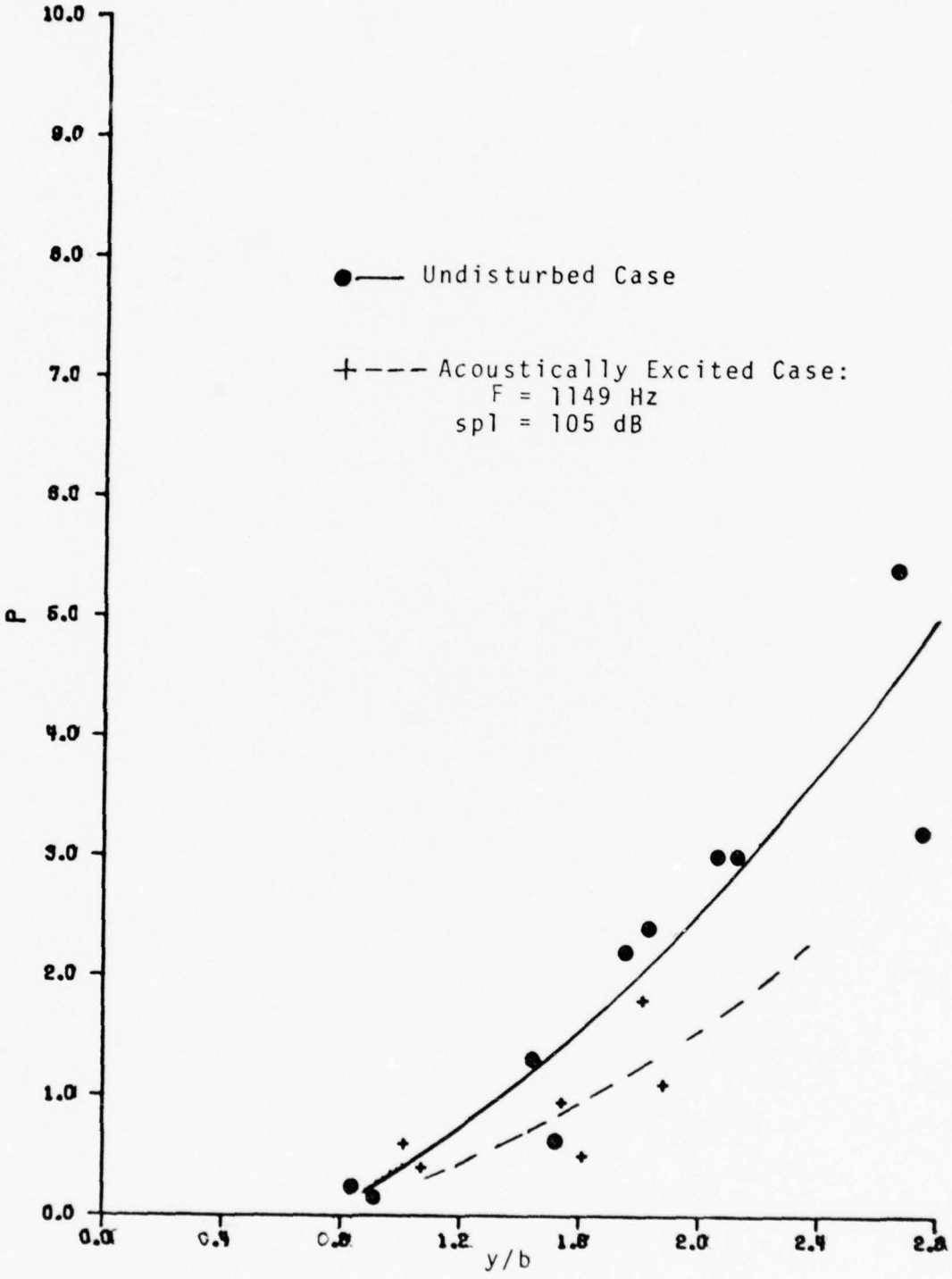

Figure 3-18. P vs. y/b at x/D = 35.

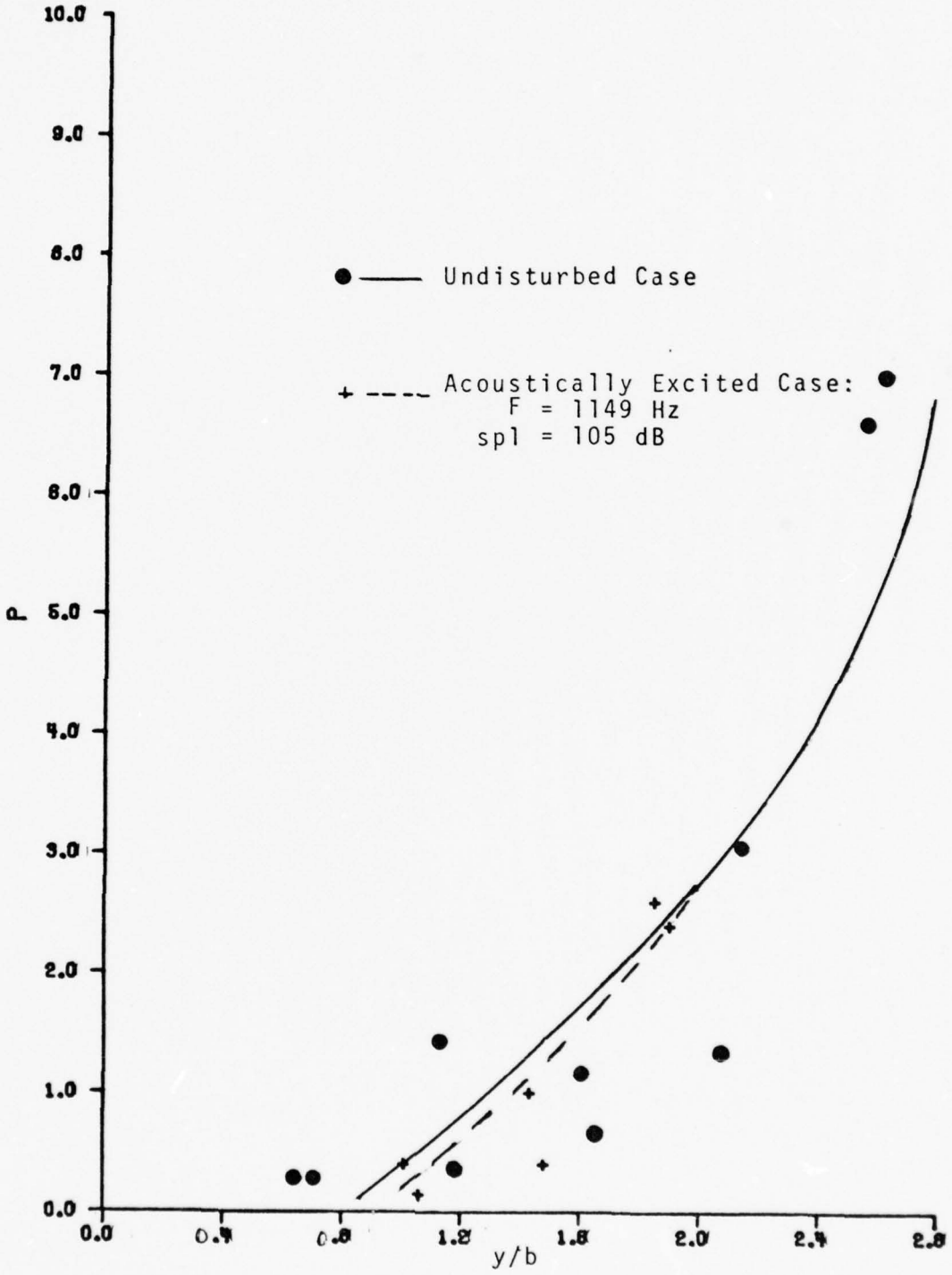

Figure 3-19. P vs y/b at x/D = 45.

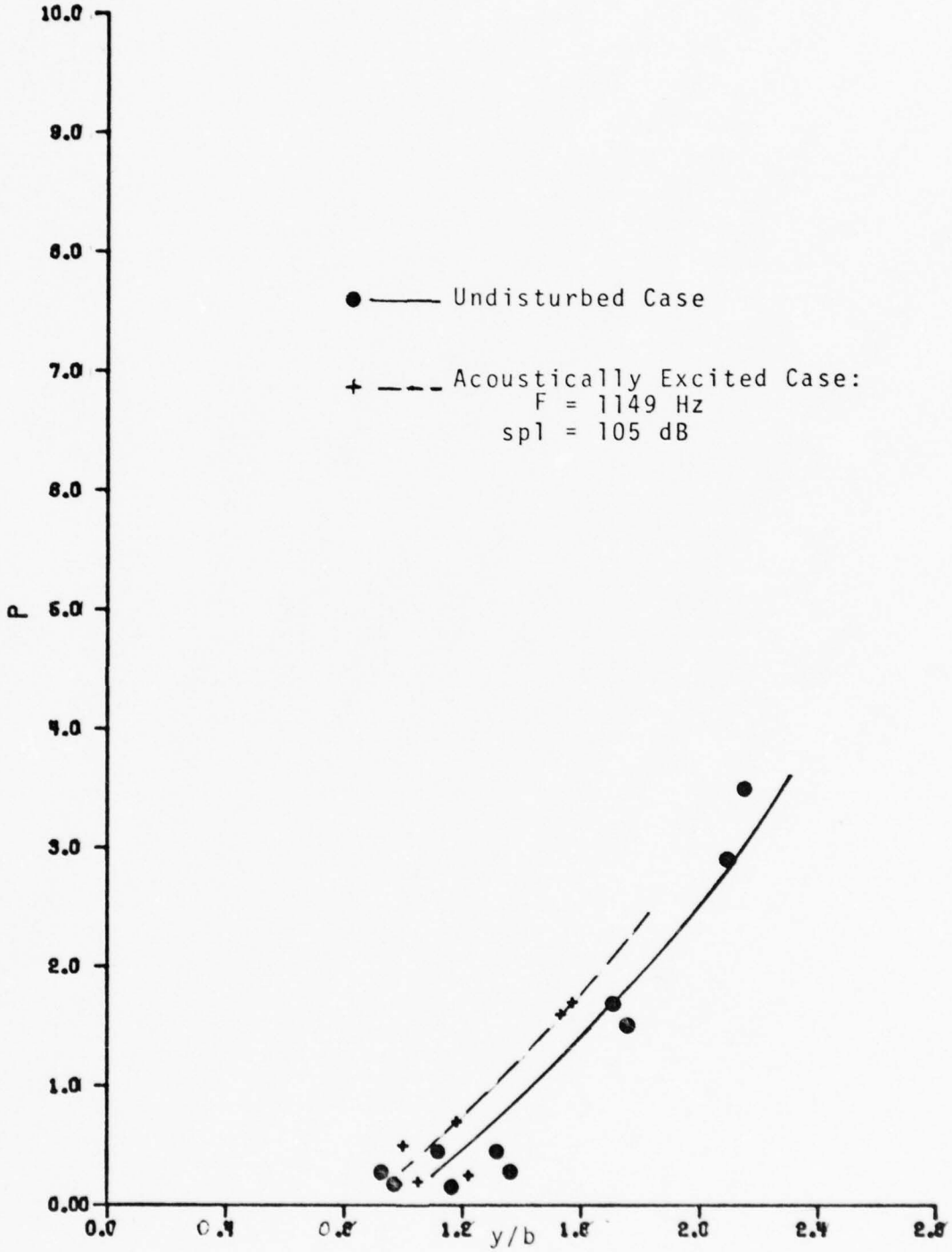

Figure 3-20. P vs. y/b at x/D = 55.

different values of γ and F_γ were similarly obtained. Figure 3-21 shows a curve of the selected values of P versus the corresponding values of γ at x/D = 35 and τ_H = 10 msec.

(iii) The Hold Time

Whereas the threshold level was varied from location to location (as explained in the last section), the hold time was held constant at 10 msec for all cases. This method of varying the threshold level but maintaining a fixed hold time is comparable to that used by Kibens and Kovasznay (1970), Kaplan and Laufer (1968), Antonia (1972), and Hedley and Keffer (1974). However, the actual hold time used by those investigators varied. For example Kaplan and Laufer (1968) used τ_H = 0 sec; Kibens and Kovasznay (1970) used 4 msec and Antonia (1972) used 0.67 msec. LaRue (1973) fixed both the threshold level and the hold time. He chose τ_H = 240 μs and the threshold level was constant. Jenkins (1974) chose a fixed threshold level, and varied the hold time from 3.6 msec to 7.5 msec.

LaRue (1973) stated that an analog circuit was necessary to study the effect of hold time on γ and F_γ. He noted that it was not possible to program into the computer a hold time other than the time between digital samples. Based on his argument a hold time of 250 μs was first chosen in the initial phases of this work. Figure 3-22 shows a typical curve (similar to Figure 3-17) obtained using this value of τ_H (250 μs). It appears that F_γ

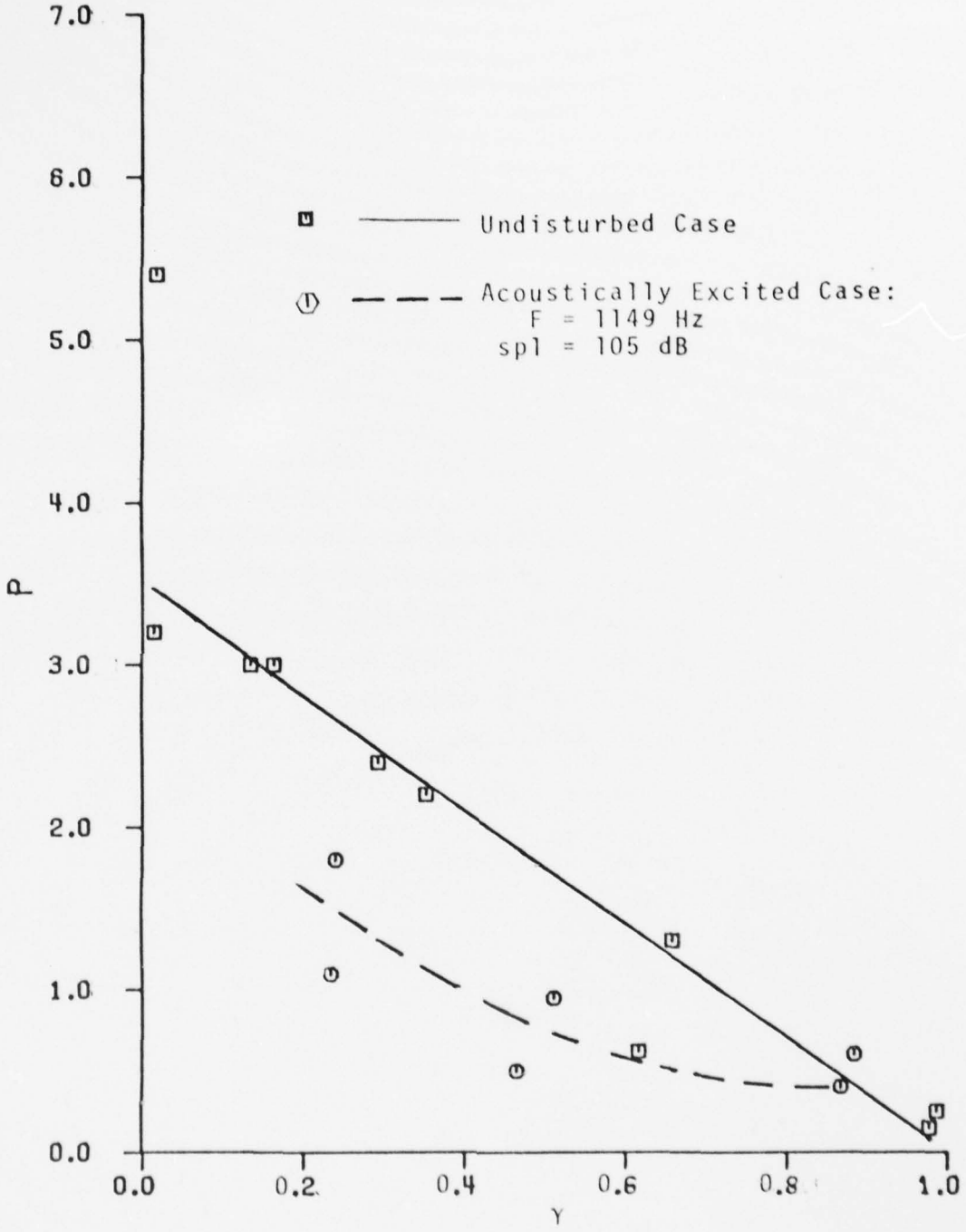

Figure 3-21. P vs. γ at x/D = 35.

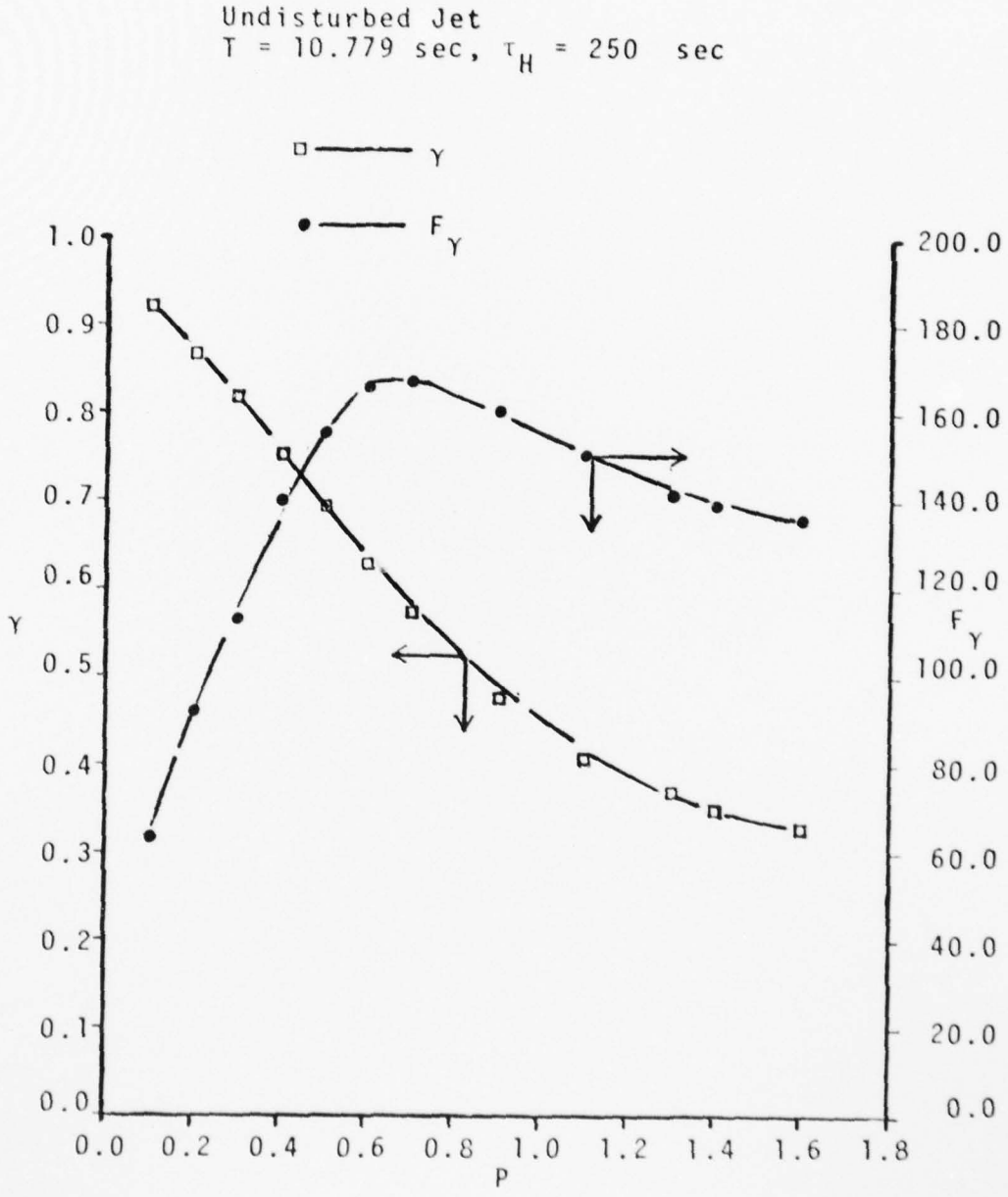

Figure 3-22. γ and F_γ vs. P at x/D = 45, y/b = 1.66; T = 10.779.

starts approaching an asymptotic value at P = 1.6. The corresponding crossing frequency, F_γ, is approximately equal to 135 Hz. This value is considered to be high for a plane turbulent jet based on the work of Jenkins (1974) and Mulej (1975). Jenkins (1974) reported a value of about 28 Hz. Furthermore, the corresponding intermittency factor, γ, at this point approximately equals 0.325 (see Figure 3-22). However, the value obtained by other investigators is approximately 0.45. This meant that either the hold time was incorrectly chosen or that somehow the samples were not properly averaged. It was first thought that the total sampling time (10.779 sec) was too short; it was hence increased to 16.1685 sec (64674 data points) to check if indeed the sampling time was too short. Figure 3-23 shows the results for a longer sampling time. There is no significant difference between it and that with a shorter sampling time (Figure 3-22). It became obvious then that the sampling time was indeed sufficiently long but that some method had to be employed to vary the hold time and hence select the "correct" value.

To that purpose, data were taken at the center-line of the jet where the flow should be fully turbulent. Using this hold time (250 μsec), the values of γ obtained were: $\gamma = 0.877$ for P = 0.4 and $\gamma = 0.238$ for P = 4.0. The "correct" hold time should give $\gamma \cong 0.99$ for a reasonable range of P. This range should be chosen such that

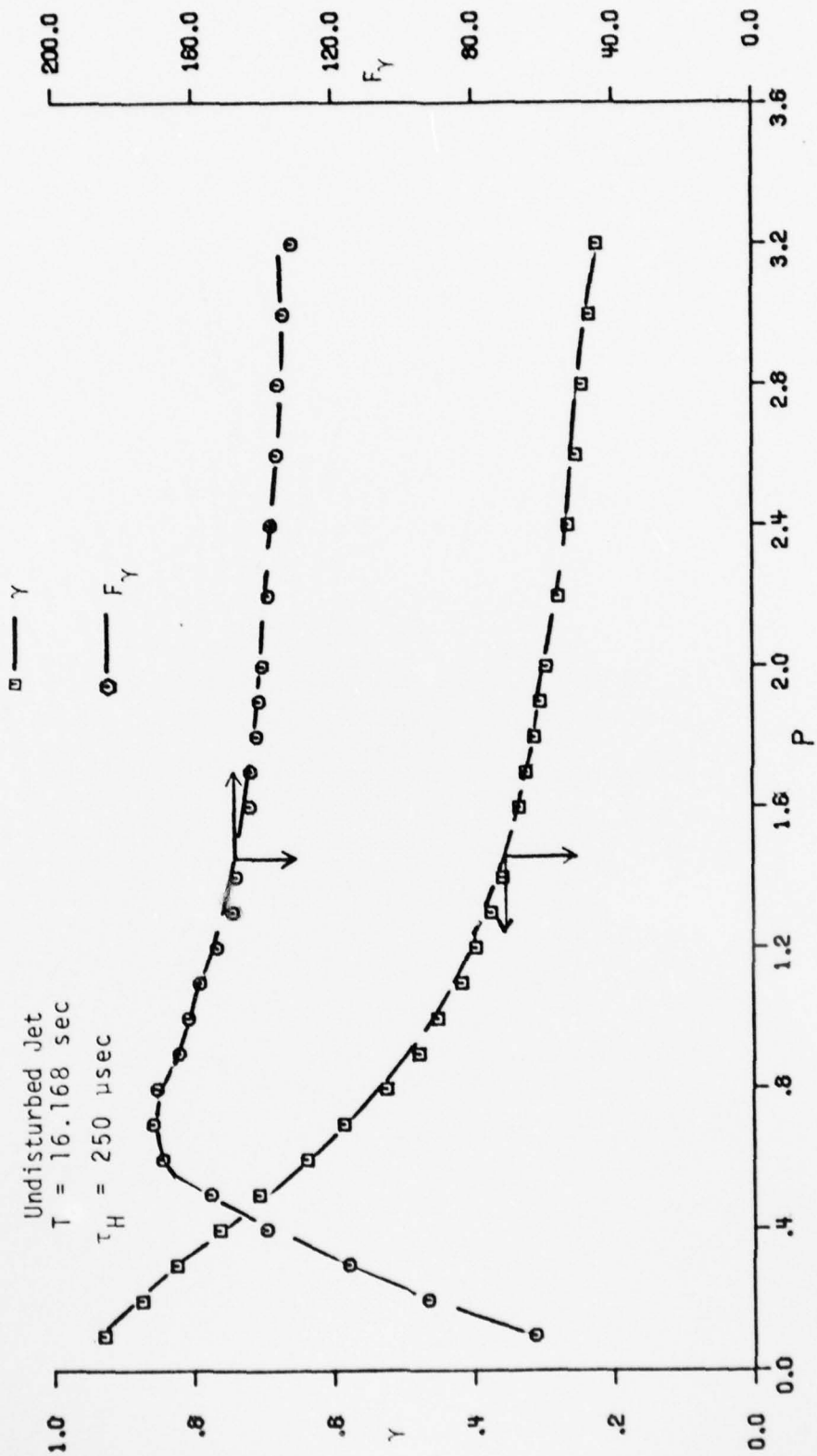

Figure 3-23. γ and F_γ vs. P at x/D = 45, y/b = 1.66 ; T = 16.168.

$C^2 \leq V_{max}$ where V_{max} is the square of the maximum voltage of the samples. This is further explained later. A computer program (see Appendix B) to vary the hold time, τ_H, was developed. In this program, the hold time was varied from 4 msec to 12 msec. At each hold time, the threshold level, C^2, was varied and the corresponding values of γ and F_γ computed. Curves of γ versus P for the various values of hold time are shown in Figure 3-24. From these curves, the nominal hold time was chosen to be 10 msec. This was at one x/D station (x/D = 45). It was assumed that this hold time would apply at all x/D stations. To further check this value of hold time, the procedure explained above was repeated at x/D = 45 and y/b = 1.61. At this lateral location, the value of γ should be approximately 0.5. This value was obtained by referring to the intermittency curve of Jenkins (1974) who had compared his curve to those obtained by other investigators like Heskestad (1965) and Bradbury (1965). Those investigators used similar flow fields as Jenkins (1974) and the author. Curves for τ_H = 4, 5, 7 and 10 msec are shown in Figures 3-25, 3-26, 3-27 and 3-28, respectively. It can be seen from these figures that the only hold time, τ_H, that gives the "correct" intermittency is τ_H = 10 msec. This correct intermittency factor is γ = 0.5. This confirms that

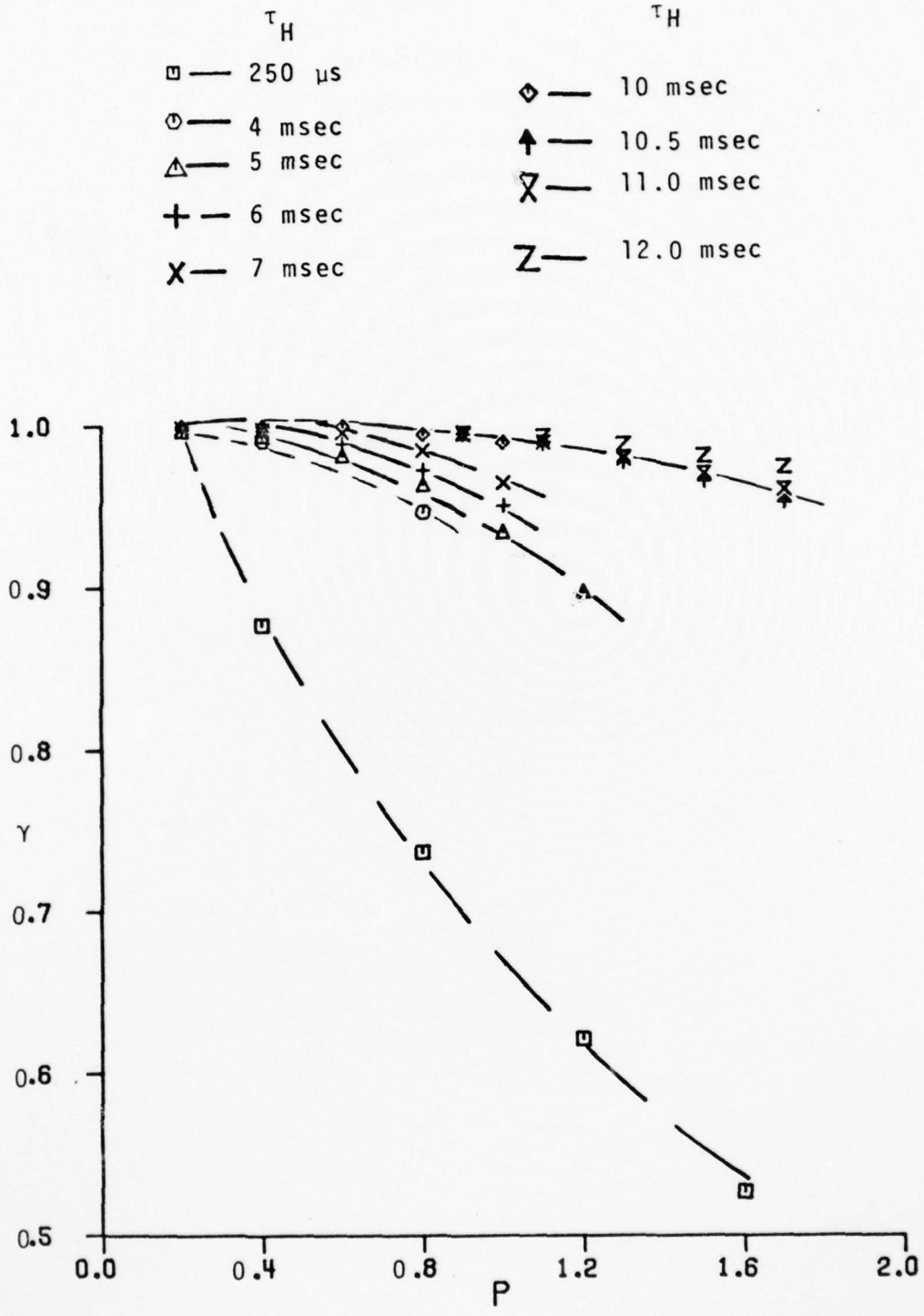

Figure 3-24. γ vs. P at x/D = 45, y/b = 0.

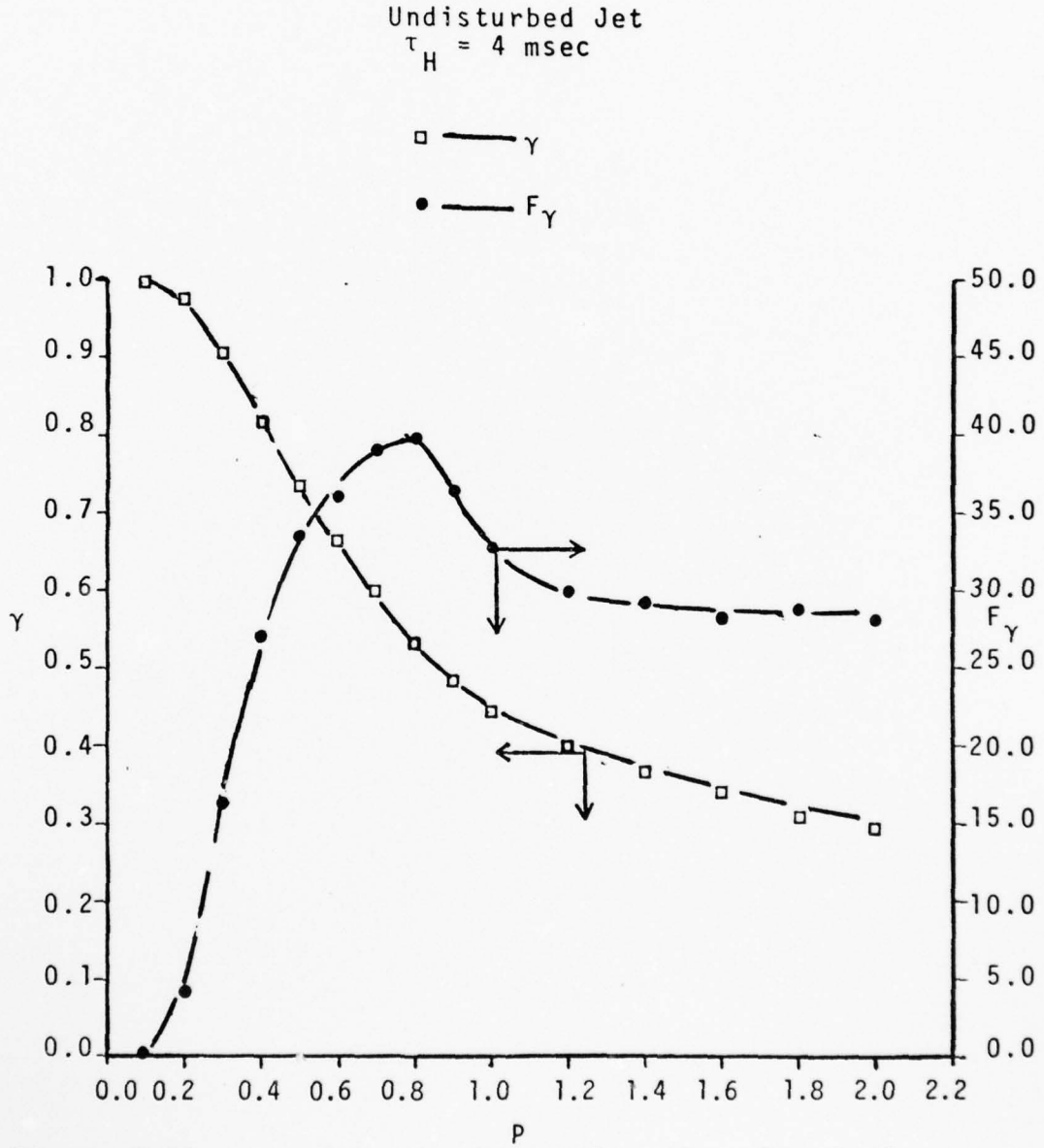

Figure 3-25. γ and F_γ vs. P at x/D = 45, y/b = 1.61, τ_H = 4 msec.

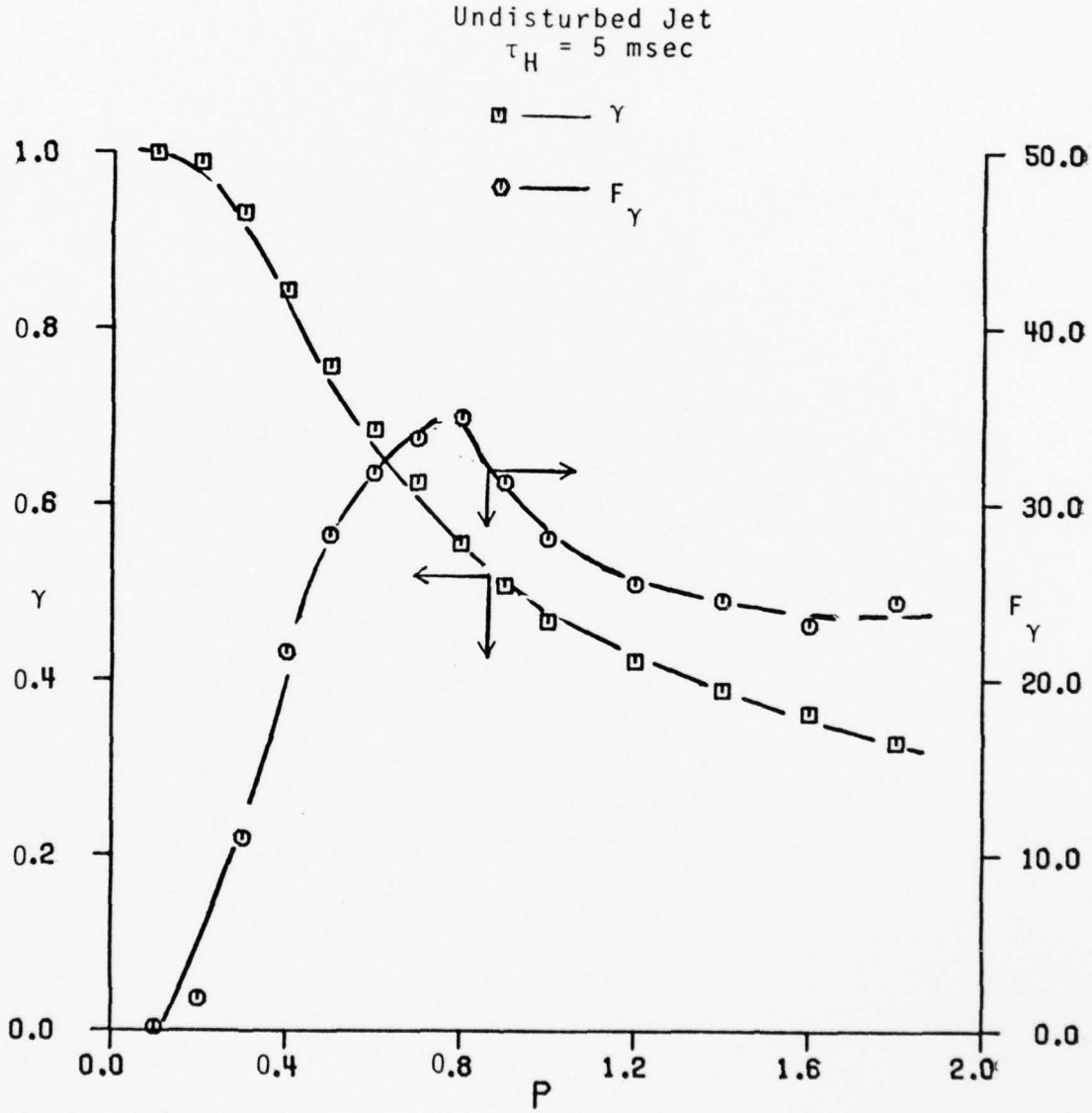

Figure 3-26. γ and F_γ vs. P at x/D = 45, y/b = 1.61, τ_H = 5 msec.

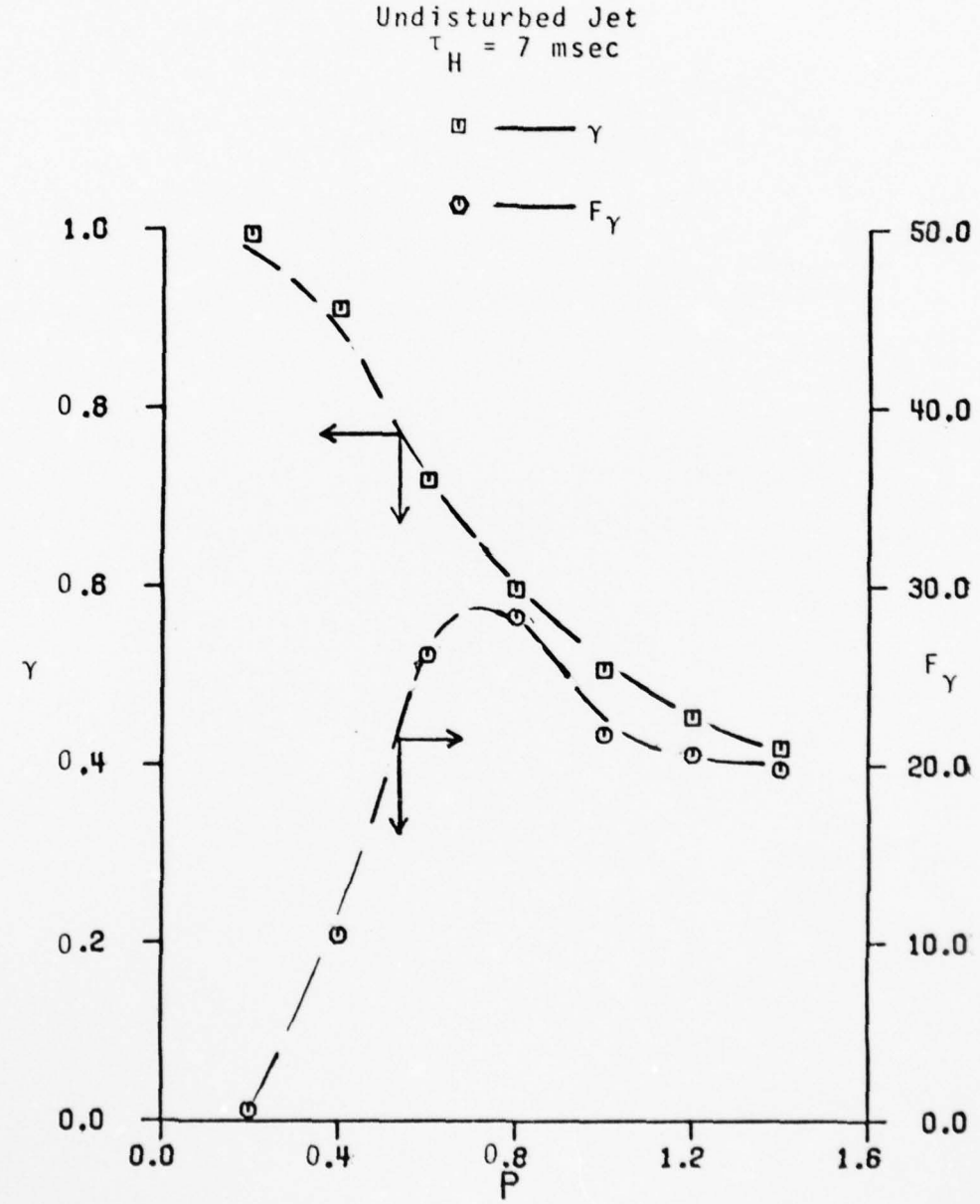

Figure 3-27. γ and F_γ vs. P at x/D = 45, y/b = 1.61, τ_H = 7 msec.

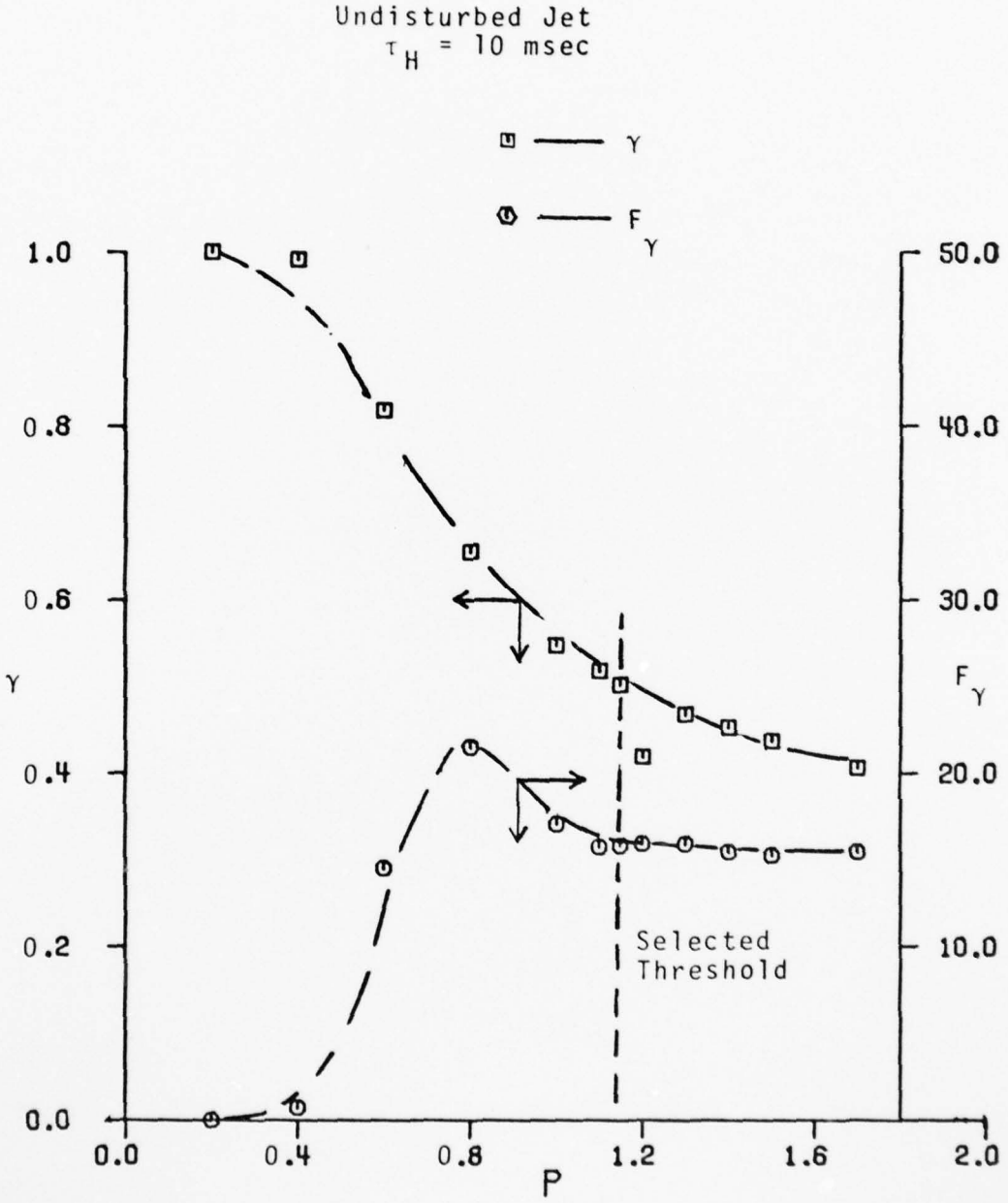

Figure 3-28. γ and F_γ vs. P at x/D = 45, y/b = 1.61, τ_H = 10 msec.

τ_H = 10 msec is the "correct" hold time. If hold times less or greater than 10 msec are chosen, "false"(*) values of the crossing frequency will be obtained. This second test was applied at two other x/D stations (x/D = 35, 55) using four other hold time values (τ_H = 5, 7.5, 9 and 10 msec). Again it was found that the intermittency factor was equal to 0.5 only at τ_H = 10 msec.

It was observed from these experiments that the necessary and sufficient test for selecting the "correct" hold time is to examine what values of γ are obtained for all values of C^2 at the center-line of the jet (y/b = 0). It is obvious that if P gets very large, C^2 will also get very large (see equation 3-14). If, for example, C^2 gets larger than the maximum value of the samples being analyzed, the intermittency factor, γ, will be zero for all times. The criterion for deciding what range of values of P is reasonable is discussed shortly.

As explained in Appendix B, a program which compares the magnitude of each sample and selects the maximum value, V_{max}, of these samples is used. The mean square S'^2 is also computed. The ratio of V_{max} to S'^2 is calculated. This ratio helps decide on the range of reasonable values for P. A value of P greater than 20 percent of this is possibly unreasonably high.

Figure 3-29 shows sketches of the steps taken to construct the intermittency function, I(t). The top sketch Figure 3-29(a) represents the hot wire voltage; 3-29(b) is

---

(*) This may be due to program used.

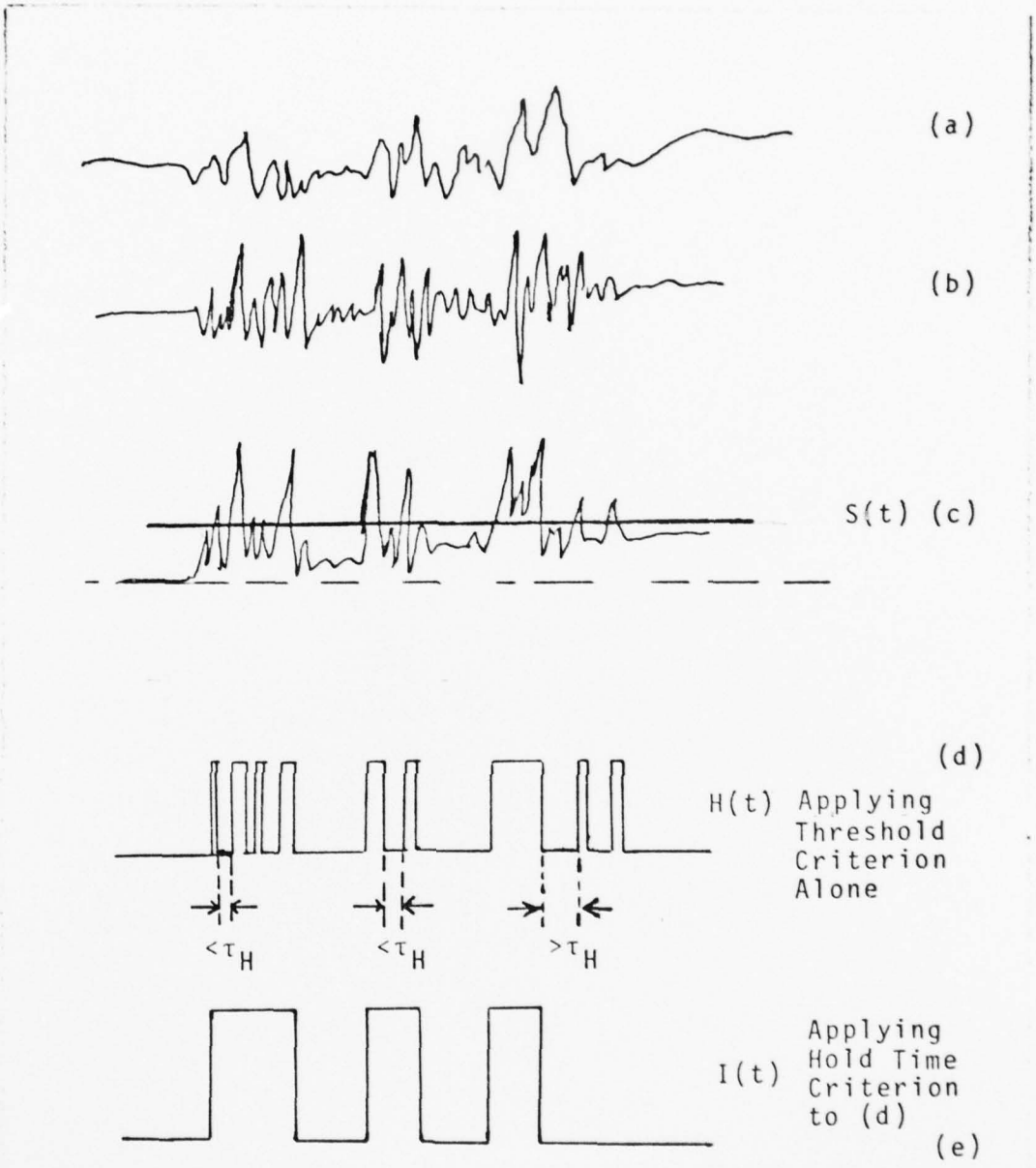

Figure 3-29. Sketches of Steps Taken to Form I(t).

the time derivative of (a). Both signals (a) and (b) are obtained by analog method. The square of (b) is shown in (c). This is obtained by the computer and is the input signal S(t). By applying the threshold criterion alone, figure (d) can be obtained. This is the intermediate signal, H(t). By applying the hold time criterion to (d), the I(t) function is obtained. Note that the intermediate signal, H(t), is actually not formed by the computer as programmed. In the program used, the threshold and hold time criteria are applied simultaneously so that the I(t) function is formed directly from S(t).

6. Fold-over

Fold-over (folding) was defined in Chapter I as the process by which a region of turbulent fluid has non-turbulent fluid between it and the fully turbulent region. A fold-over region is a region of turbulent fluid which has non-turbulent fluid between it and the fully turbulent region. This is what Paizis and Schwarz (1974) called a "fold." A fold-over event occurring at the front of the interface is that event whereby a probe, further from the axis of the jet than a second probe at the same longitudinal (x-direction) location, detects a turbulent burst before the second probe. Similarly, a fold-over event occurring at the back of the interface is that event whereby the probe further from the jet axis remains in the turbulent region longer than the probe closer to the axis of the jet. A minimum of one fold-over event is required to form

a fold-over region. However, as many as four fold-over events can form a single fold-over region. As will be discussed shortly, back and front fold-over events are also called back-fold-over and front-fold-over, respectively. This work did not investigate the actual shape or width of the fold-over region.

Mulej (1975) made the first attempt to measure fold-over events in a plane turbulent jet. Earlier attempts were made to quantify fold-over in other flow fields. In the boundary layer, for example, Paizis (1972) and Paizis and Schwarz (1974) observed that the turbulent-nonturbulent interface exhibited a significant amount of fold-over; (they used the word "folding" instead of fold-over). They described the interface position by two single valued functions: $H(x, z, t)$ and $H^*(x, z, t)$. $H(x, z, t)$ was the total width of turbulent fluid at (x, z) at time t. This was measured by summing the turbulence detector output (they used a linear array of twenty hot wire probes). The second function, $H^*(x, z, t)$, was the width of the turbulent fluid that was not part of the fold-over. This was obtained as the output of the counting circuit. The difference of those two functions was a measure of the total width of the fold-over region. They measured the mean value of that quantity to be 0.05δ, where δ is the boundary layer thickness. They noted that the total width of the turbulence was 1.5δ and that the standard deviation

AD-A071 262 PURDUE UNIV LAFAYETTE IND RAY W HERRICK LABS F/G 20/4
FOLD-OVER, INTERMITTENCY AND CROSSING FREQUENCY OF A PLANE JET --ETC(U)
FEB 77 C O AJAGU, V W GOLDSCHMIDT N00014-67-A-0226-0025
UNCLASSIFIED HL-76-22 NL

2 OF 3
AD A071262

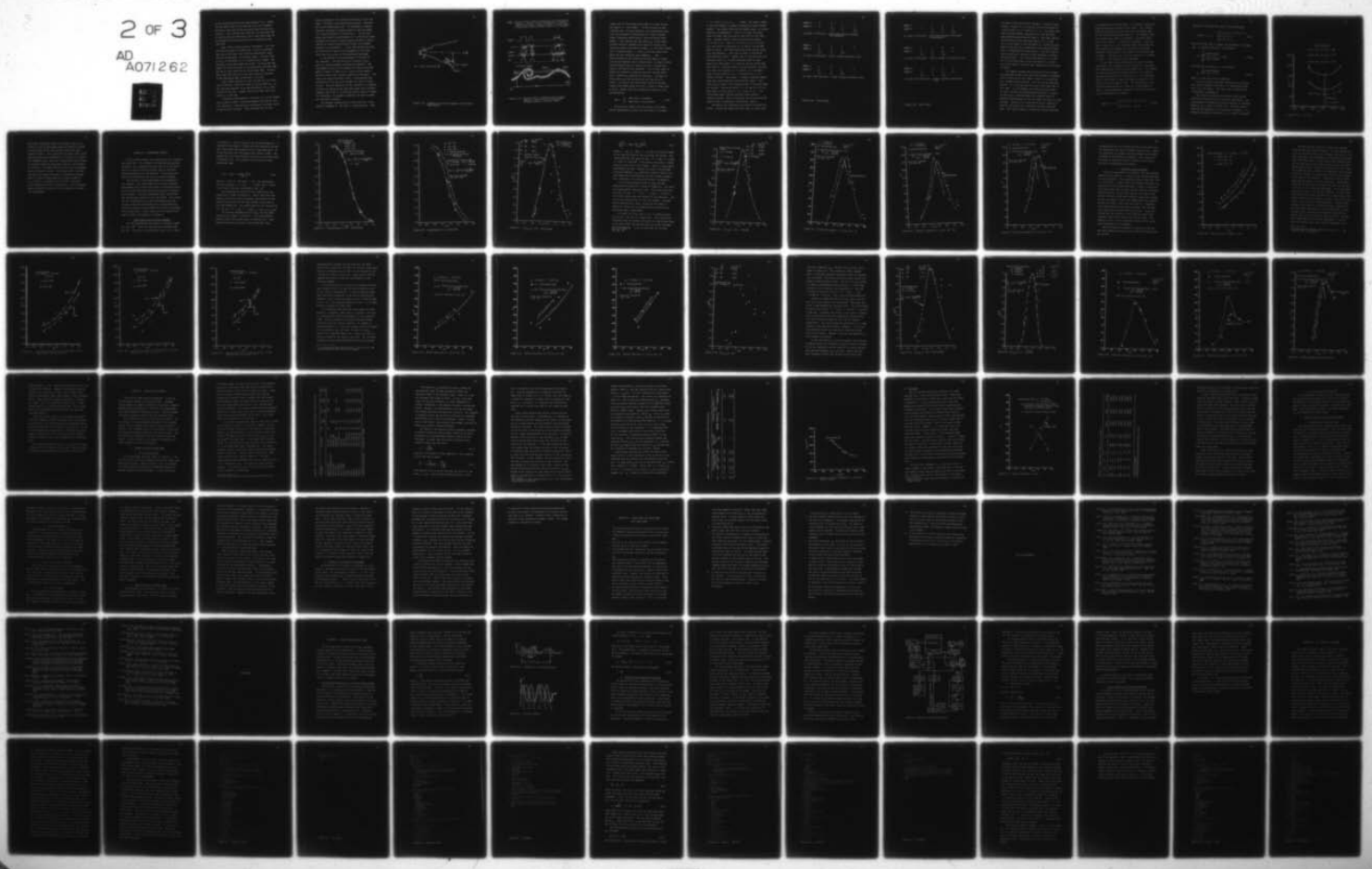

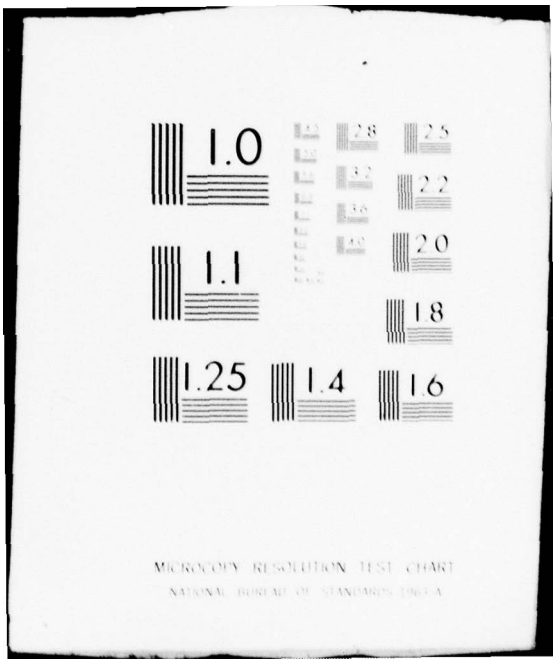
1.0
1.1
1.25
1.4
1.6
2.8
2.5
3.2
2.2
3.6
2.0
4.0
1.8
MICROCOPY RESOLUTION TEST CHART
NATIONAL BUREAU OF STANDARDS 1963-A

of the interface position was approximately 0.3δ. Comparing the total width of the fold-over with this standard deviation, they came to the conclusion that this was significant. They reported that fold-over occurred about 40% of the time but that fold-over with a total width equal to the standard deviation occurred with a probability less than 0.05.

LaRue (1973) called fold-over "overhangs." His flow field was the wake of a heated rod. He also recognized that due to fold-over, the turbulent-nonturbulent interface was multivalued. He used two probes: one was fixed at $y/\ell_c = 0.349$ where ℓ_c is a characteristic length. The position of the other probe was varied. He noted that the number of fold-over events at the downstream interface edge was two to four times that at the upstream edge. He estimated that the fraction of time that there was fold-over at the downstream edge varied from 0.1 to 0.5%.

Kohan (1969) noticed in a wall jet that for two transverse locations in the flow field, y_1 and y_2 where $y_2 > y_1$, the flow was turbulent at y_2 and nonturbulent at y_1 less than 5% of the time. Schwarz (1972) also made that observation in a wall jet.

Preliminary measurements of fold-over in a plane jet were taken by Mulej (1975). These measurements were made by visually examining a continuous and simultaneous visicoder record of two hot wire voltages. These voltages were for two

probes separated in the lateral direction by a small distance. In effect, the turbulent-nonturbulent interface was visually detected by him. His procedure to measure fold-over consisted in deciding which of the two probes first became turbulent or nonturbulent. The hot wire probes positioned at approximately 0.1 in (0.254 cm) apart displayed very similar voltage signals and hence, posed a problem of visually deciding which probe first became turbulent or nonturbulent. It has been pointed out that the difficulty of making those judgments at all times could lead to an error in the measurement technique.

ϕ_i was defined as the percentage of fold-over in the interface. This definition was retained in this work, but the measurement technique was improved. The arrangement of the hot wire probes for fold-over measurements is shown in Figure 3-30. Figure 3-31(b) shows a possible form of the interface emphasizing fold-over. This figure was taken from Mulej (1975). Corresponding time derivatives of the hot wire voltages are shown in Figure 3-31(a). The main objective of this research is to measure fold-over by analyzing the digitized signal with a digital computer and to see if a traveling acoustic wave can change its occurrence. No attempt, therefore, was made to model the interface structure.

The computer program used to study fold-over is presented in Appendix B. The logic is explained here. From

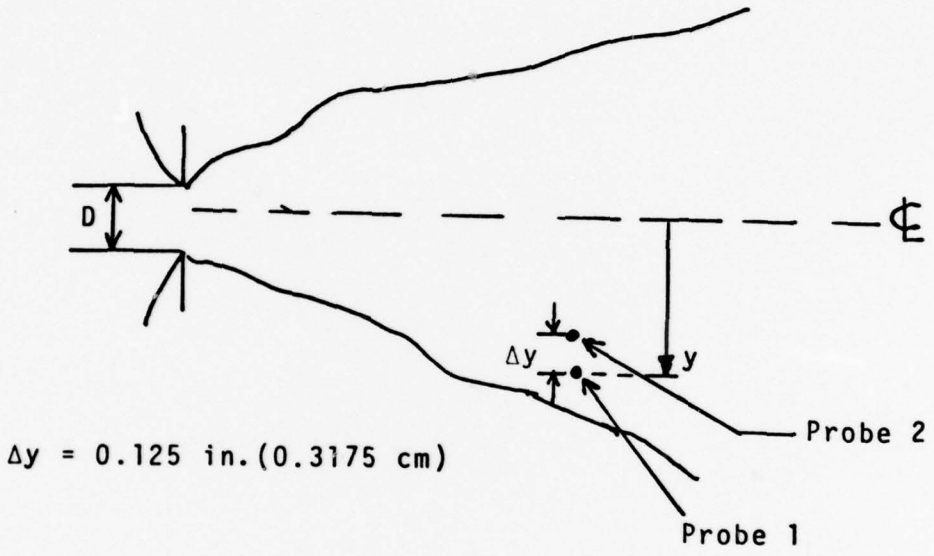

Figure 3-30. Schematic of Probe Arrangement for Fold-Over Measurements.

NOTE: Figure 3-31(b) could be interpreted as including two "bursts." Figures 3-31(a) by themselves, could be interpreted as due to three "bursts." In this work, either figure would identify a total of six "events."

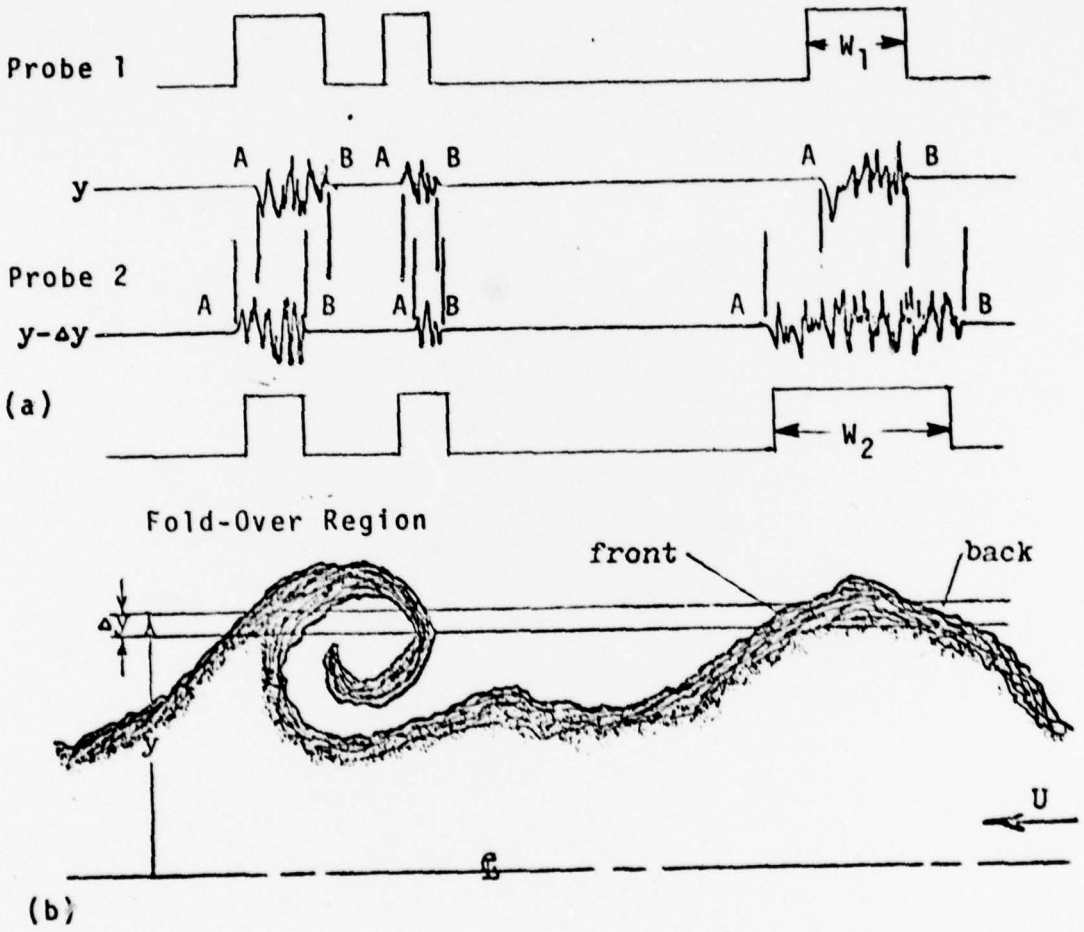

Figure 3-31. Possible Form of Interface with an Ideal Output of Time Derivatives of Hot Wire Voltages Showing a Fold-Over Region.

Figure 3-30 it can be seen that probe 2 is closer to the jet center-line than probe 1. If the structure of the interface does not have fold-over, the intermittency function, I(t), (properly constructed) will always indicate probe 2 turbulent before probe 1 and nonturbulent after probe 1. This implies that the width, w_2, of the intermittency function (random square wave) for probe 2 will always be greater than that of probe 1, w_1 (see Figure 3-31(a)). This is because probe 2 is closer to the jet center-line where the flow should be more turbulent. The front and back of the interface are also shown in Figure 3-31(b) and labeled A and B, respectively, in Figure 3-31(a). Three different types of events can occur in either the front or the back of the interface. Two of these types of events are defined as producing fold-over and the third type is defined as producing no-fold-over. The types of front events can best be explained with the aid of a sketch. As soon as the intermittency function has been formed, each sample point will have a value of either zero or unity. Recall that the intermittency function, I(t), was defined by:

$$I(t) = \begin{cases} 1 & \text{when flow is turbulent} \\ 0 & \text{when flow is nonturbulent} \end{cases} \qquad (3\text{-}15)$$

The digitized signals from the two hot wire probes can be represented by a matrix of the form [i x j] where

i = 1, 2 and j = 1, 2, 3, ... 42960. The number, 42960, is the total number of samples processed per tape recorder channel. The signals from the two channels were, of course, digitized simultaneously. Figure 3-32 shows the three types of events that can occur at the front of the interface. Consider Figure 3-32(a) and the set of points, (1, j) and (2, j). Both (1, j-1) and (2, j-1) are zero, while the points in question, (1, j) and (2, j), are both equal to unity. This means that both probes became turbulent simultaneously. This type of event is defined as front-fold-over type 1. Recall that if fold-over were not possible, point (1, j) would have been equal to zero. Recall also that probe 2 is closer to the jet center-line than probe 1. Fold-over type 2 can be explained similarly. This time, while points (1, j-1) and (2, j-1) are both equal to zero, point (1, j) = 1 and point (2, j) = 0 (Figure 3-32(b)). Here probe 1 becomes turbulent before probe two, thus producing front-fold-over type 2. The third type of event is the expected event if fold-over were not present. Here while points (1, j-1) and (2, j-1) are both equal to zero, point (1, j) = 0 and (2, j) = 1 implying that probe 2 became turbulent before probe 1 (Figure 3-32(c)). Here, no fold-over has occurred and the type of event is defined as no-fold-over, type 5.

The back of the interface also exhibits fold-over behavior. Figure 3-33 shows the three types of events that

PROBE 1→	0	0	1	1
PROBE 2→	0	0	1	1
		↑	↑	↑
		j-1	j	j+1

(a) Type 1 (Fold-over): Both probes become turbulent simultaneously

PROBE 1→	0	1	1	1
PROBE 2→	0	0	1	1
	↑	↑	↑	
	j-1	j	j+1	

(b) Type 2 (Fold-over): Probe 1 becomes turbulent first

PROBE 1→	0	0	1	1
PROBE 2→	0	1	1	1
	↑	↑	↑	
	j-1	j	j+1	

(c) Type 5 (No fold-over): Probe 2 becomes turbulent first.

Figure 3-32. Front Events

PROBE 1→	1	1	0	0
PROBE 2→	1	1	0	0
		↑	↑	↑
		j-1	j	j+1

(a) Type 3 (Fold-over): Both probes become nonturbulent simultaneously

PROBE 1→	1	1	0	0
PROBE 2→	1	0	0	0
	↑	↑	↑	
	j-1	j	j+1	

(b) Type 4 (Fold-over): Probe 2 becomes nonturbulent first

PROBE 1→	1	0	0	0
PROBE 2→	1	1	0	0
	↑	↑	↑	
	j-1	j	j+1	

(c) Type 6 (No fold-over): Probe 1 becomes nonturbulent first.

Figure 3-33. Back Events.

can occur at the back of the interface. Consider Figure 3-33(a). Points (1, j-1) and (2, j-1) are both equal to 1 while points (1, j) = 0 and (2, j) = 0. This means that the two probes become nonturbulent at the same time, thus producing back-fold-over type 3. The other type of back-fold-over occurs when both points (1, j-1) and (2, j-1) are equal to one and points (1, j) and (2,j) are equal to one and zero, respectively (see Figure 3-33(b)). This is termed back-fold-over type 4. The final type of event occurring at the back of the interface is no-back-fold-over type 6. This occurs when points (1, j-1) and (2, j-1) are both equal to one, and points (1, j) and (2, j) are equal to zero and one, respectively (see Figure 3-33(c)).

The computer program that analyzed fold-over events was developed to make those decisions whenever a turbulent burst crossed one of the probes. There is a possibility of a strange event occurring. This will be be explained shortly. It is obvious that for every front there has to be a back. If, for example, the front-fold-over event is type 1 and the corresponding back-fold-over is type 3, we shall get a situation where the turbulent burst is detected simultaneously by the two probes for both its front and back. This will be a burst which at the location of crossing the probes has a perfectly vertical front and back. This type of event is called the strange event and

is considered no-fold-over event. The computer program was purposely written to check for this event. This strange event was not detected in all the cases considered, both for the disturbed and undisturbed jet. This suggests that the interface was either in a perfect fold-over condition or in a perfect no-fold-over condition. Fold-over types 1 and 3 (i.e., the situations where both probes become respectively turbulent at the same time, and non-turbulent simultaneously) were found to be relatively few in number. Fold-over type 1 was on the order of 5 percent of type 2. The same was true at the back.

In the logic used to define the six types of events occurring at the interface, it was necessary to know what the immediate past history of the signal was. For example, in order to have front-fold-over type 1 at the location defined by the points (1, j) and (2, j), it is necessary, but not sufficient, to have the values of points (1, j-1) and (2, j-1) both equal to zero. The sufficiency is supplied by having points (1, j) and (2, j) both equal to unity. Using mathematical notation, front-fold-over type 1 can be defined by the relation:

$$\text{Type 1} = 1 \iff \begin{cases} (1)\ (1,\ j\text{-}1) = (2,\ j\text{-}1) = 0 \\ \\ (2)\ (1,\ j) \quad = (2,\ j) \quad = 1 \end{cases} \tag{3-16}$$

Similarly, front-fold-over type 2 can be defined by:

$$\text{Type } 2 = 2 \iff \begin{cases} (1)\ (1, j-1) = (2, j-1) = 0 \\ (2)\ (1, j) = 1 \\ (3)\ (2, j) = 0 \end{cases} \tag{3-17}$$

The rest of the types of events can be defined in the same way. ϕ_i (percent fold-over) is defined by:

$$\phi_i = \frac{\sum_{N=1}^{4} \text{Type N Events}}{\sum_{M=1}^{6} \text{Type M Events}} \times 100 \tag{3-18}$$

and fold-over frequency, F_θ, is defined by:

$$F_\theta = \frac{\sum_{N=1}^{4} \text{Type N Events}}{T} \tag{3-19}$$

where T is the total time of sampling.

As was previously remarked, the accuracy of the fold-over analysis depends on how well the intermittency function, I(t), was formed. The logic used in forming I(t) is presented in Appendix B.

The accuracy in measuring fold-over could also be affected by the choice of Δy (the probe separation). The relationship of the measured fold-over percent to different values of Δy is shown in Figure 3-34. The error associated with the choice of Δy is discussed in Chapter V. It should be pointed out here that at $\Delta y \leq 0.0625$ in. (0.15875

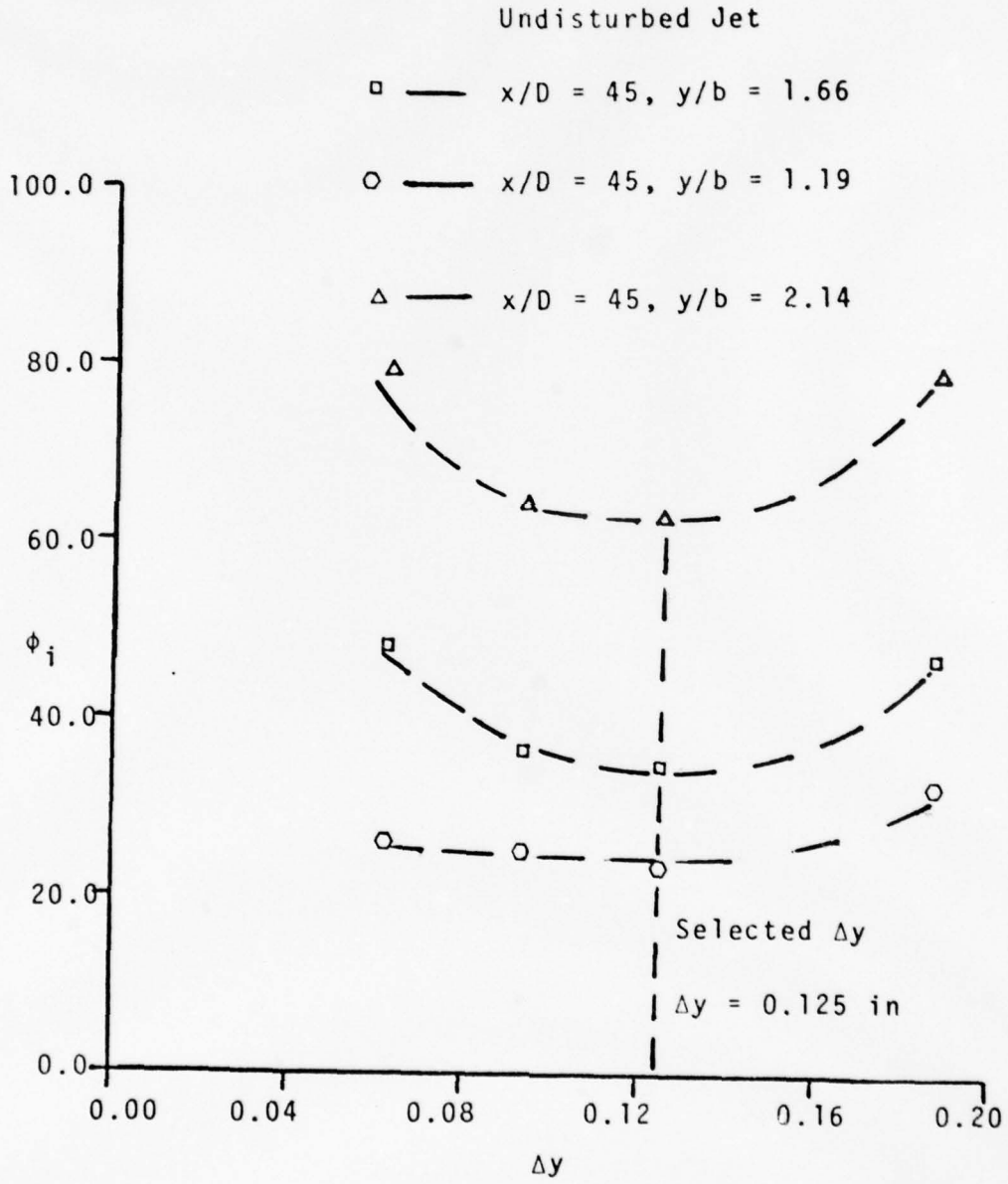

Figure 3-34. ϕ_i vs. Δy.

cm) probe interference seems to be present and at $\Delta y \geq$ 0.1575 in. (0.4 cm) the probe separation begins to exceed the microscale of the flow and the correlation fails (Jenkins (1974)). Favre, Gaviglio and Dumas (1958), while measuring Space-Time Correlations of velicity in a turbulent boundary layer, show that no appreciable errors exist by slightly displacing one probe laterally, with respect to the other. The same observation was made by Champagne, Harris and Corrsin (1970). From Figure 3-26, it can be seen that the percent fold-over is essentially constant within a range of probe separation given by 0.093 in. $\Delta y \leq$ 0.1575 in. (0.236 cm $\leq \Delta y \leq$ 0.4 cm). The final value selected was 0.125 in. (0.3175 cm). This was chosen based on Figure 3-34 and also for the purpose of convenient measurement.

CHAPTER IV. EXPERIMENTAL RESULTS

As was already stated, the objectives of this research are three-fold: (1) to detect the turbulent-nonturbulent interface, (2) to measure fold-over and (3) to see the effects of a plane traveling acoustic wave on fold-over, crossing frequency and intermittency. These objectives were to be fulfilled by the use of a digital computer.

The results of these measurements are presented in this chapter. The intermittency and crossing frequency measurements were possible only after a satisfactory technique for detecting the turbulent-nonturbulent interface was developed. Fold-over measurements were taken after the intermittency function, I(t), was formed. The results for the intermittency and crossing frequency with and without an acoustic disturbance will be presented first. Fold-over results with and without an acoustic disturbance will be given next. These results will be compared with those of other investigators in Chapter V.

1. Intermittency and Crossing Frequency

All the measurements were taken at a Reynolds number of 1.78×10^4. Three x/D stations were considered (35, 45, 55). The curve of intermittency versus y/b is shown

in Figure 4-1. This is the case for the undisturbed jet. A few points from Jenkins' (1974) curve are plotted to see how well the present work compared with his published work. It can be seen that the curve agrees with Jenkins (1974). The dashed line is an error function curve fit of the form given in equation 3-12. This equation can be written in non-dimensional form:

$$\gamma(y') = \frac{1}{2}\left[1 - \operatorname{erf}\left(\frac{y' - \bar{Y}'}{\sqrt{2}\ \sigma'}\right)\right] \qquad (4\text{-}1)$$

where $y' = y/b$, $\bar{Y}' = \bar{Y}/b$ and $\sigma' = \sigma/b$. The coefficients for the curve are: $\bar{Y}' = 1.61$, $\sigma' = 0.408$ and $\sigma = 0.670$ in.(1.70 cm). This was calculated at $x/D = 35$.

The intermittency profile for the acoustically disturbed jet is shown in Figure 4-2. Notice that while the shape of the curve remains unchanged, the profile for the acoustically excited jet has been shifted to the left of the undisturbed case. The coefficients for the curve fit at $x/D = 35$ are: $\bar{Y}' = 1.48$, $\sigma' = 0.369$, $\sigma = 0.69$ in. (1.75 cm).

The crossing frequency curve ($F_\gamma/F_{\gamma m}$) for the undisturbed case is shown in Figure 4-3. This approximates a Gaussian curve of the form given in Equation 3-13. This equation can also be written in non-dimensional form:

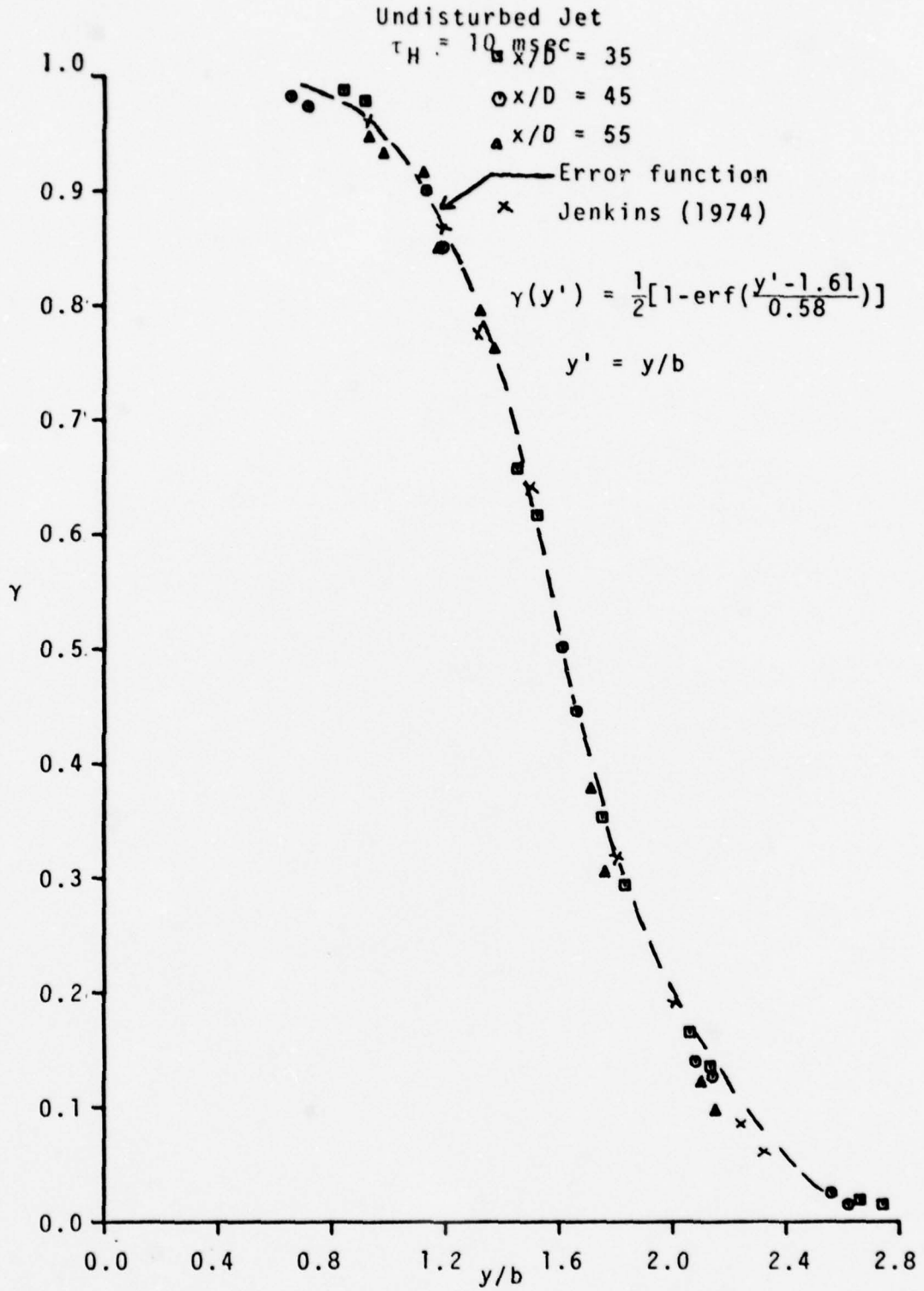

Figure 4-1. Intermittency vs y/b: Undisturbed.

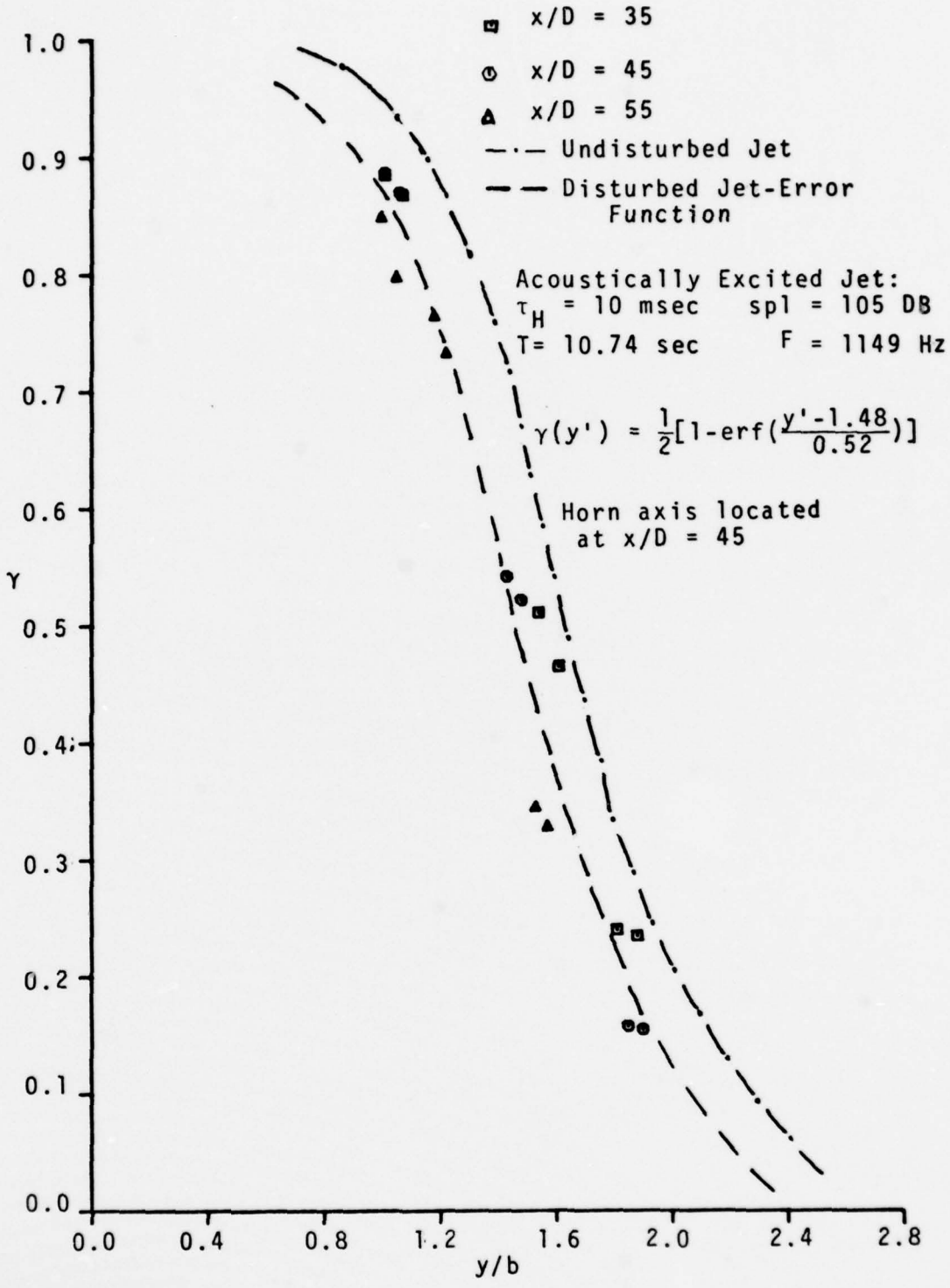

Figure 4-2. Intermittency vs. y/b:Excited.

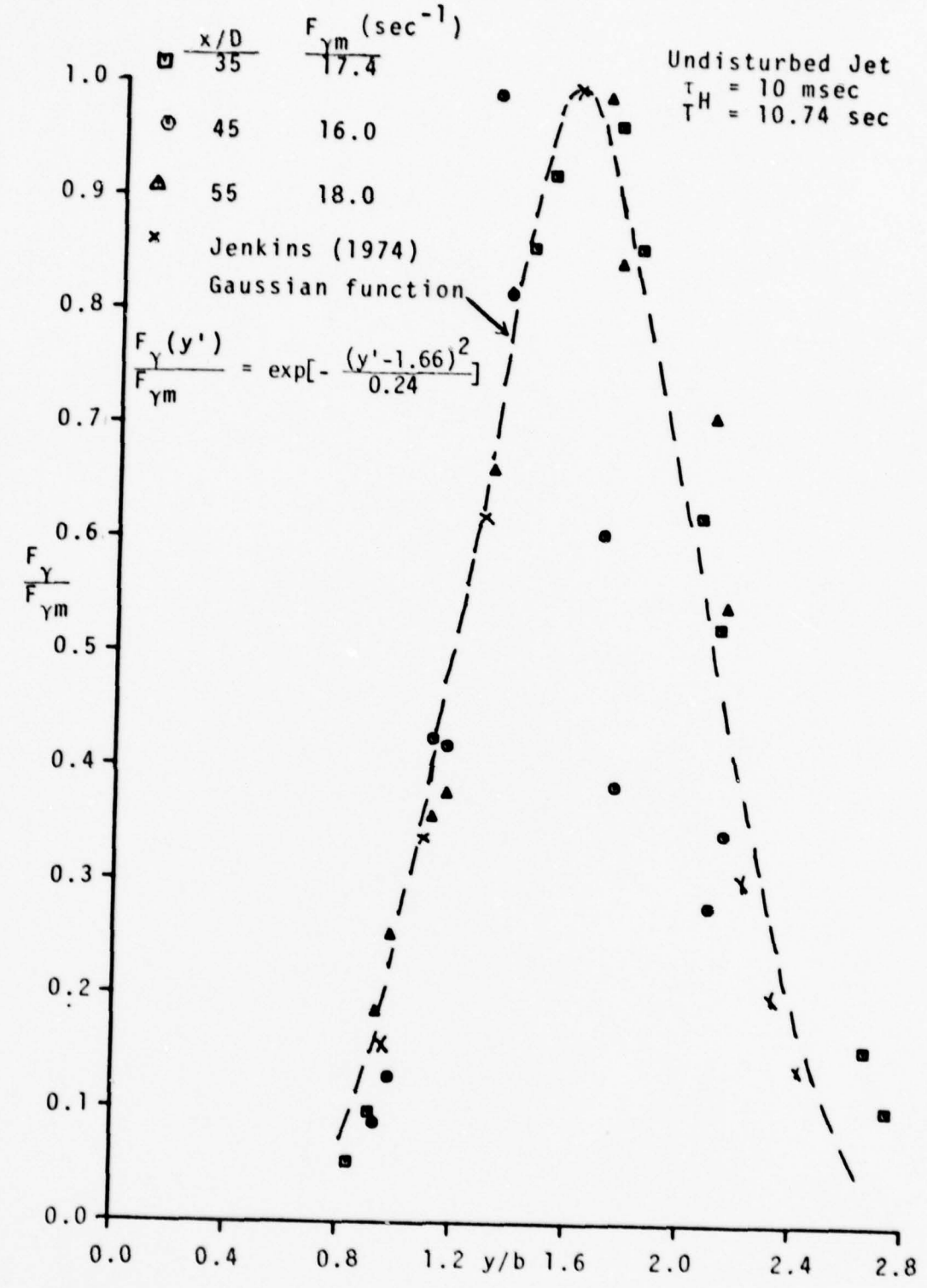

Figure 4-3. $F_\gamma/F_{\gamma m}$ vs. y/b: Undisturbed.

$$\frac{F_\gamma(y')}{F_{\gamma m}} = \exp\left[-\frac{(y' - \bar{Y}')^2}{2\sigma'^2}\right] \qquad (4\text{-}2)$$

where $y' = y/b$, $\bar{Y}' = \bar{Y}/b$, $\sigma' = \sigma/b$ and b is the half width of the velocity field of the jet at any x/D station. The coefficients for the curve fit are: $\bar{Y}' = 1.66$, $\sigma' = 0.345$, $\sigma = 0.567$ in. (1.44 cm)*. A few points from Jenkins' (1974) curve are also shown in the figure. There is a good agreement between the two. However the value of the maximum crossing frequency, $F_{\gamma m}$, obtained by Jenkins (1974) is almost double the value obtained from the present research. This difference will be discussed further in Chapter V.

The crossing frequency curve ($F_\gamma/F_{\gamma m}$) for the acoustically excited jet is shown in Figure 4-4. The curve also approximates a Gaussian curve. The coefficients for the curve fit are: $\bar{Y}' = 1.43$, $\sigma' = 0.329$, $\sigma = 0.613$ in. (1.56 cm)*. Notice that the location $\bar{Y}'$ has decreased. This will be discussed further in the next chapter. The data points used to plot γ and F_γ versus y/b are shown in Tables B-1 and B-2 for the undisturbed and acoustically disturbed cases, respectively.

In Figures 4-5, 4-6, and 4-7, F_γ is plotted against y/b for x/D = 35, 45, 55, respectively. The acoustically disturbed cases are plotted along with the undisturbed cases to see what effect the acoustic wave has on the interface crossing frequency. It can be seen that the crossing

*At x/D = 35.

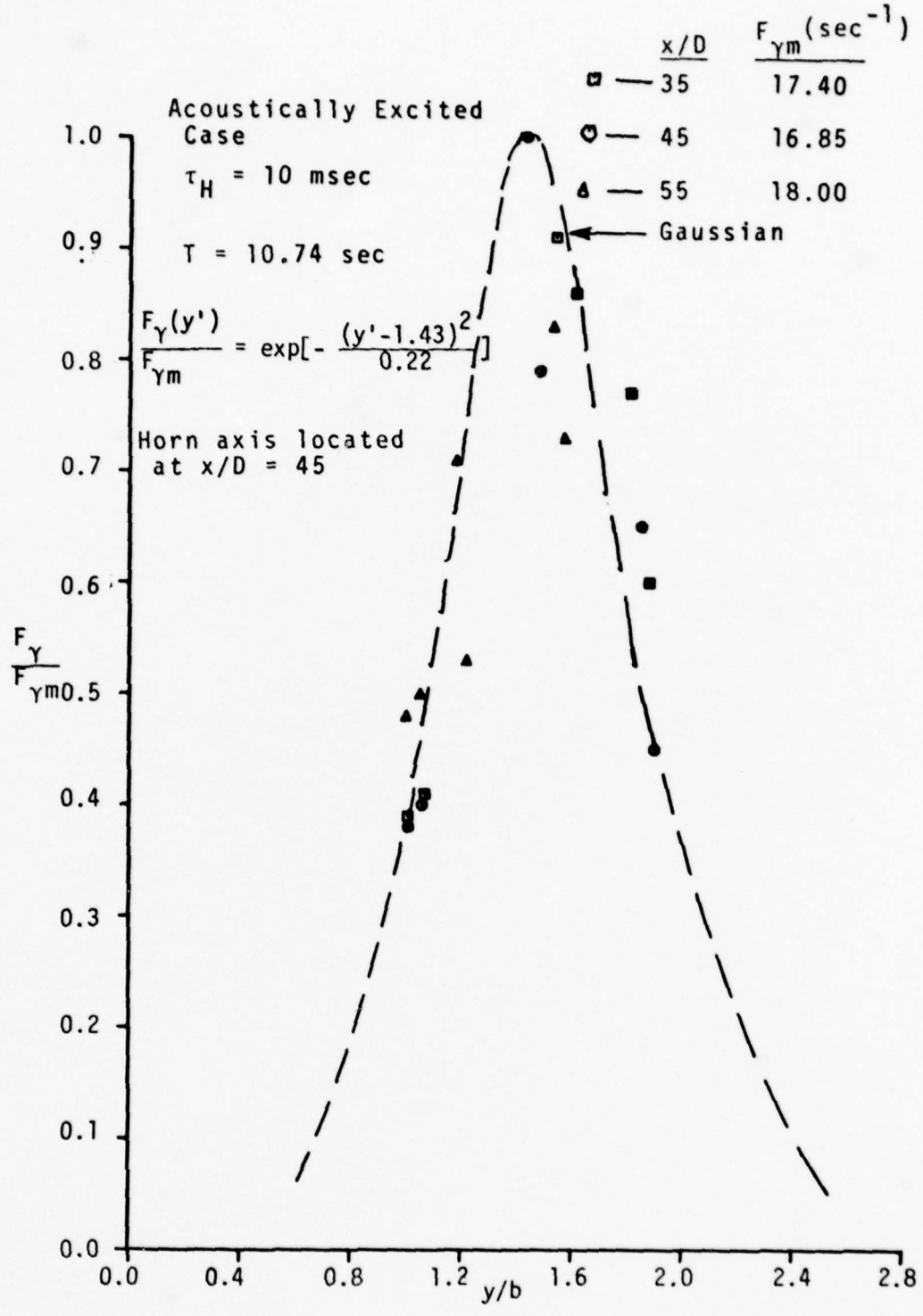

Figure 4-4. $F_\gamma/F_{\gamma m}$ vs. y/b : Excited.

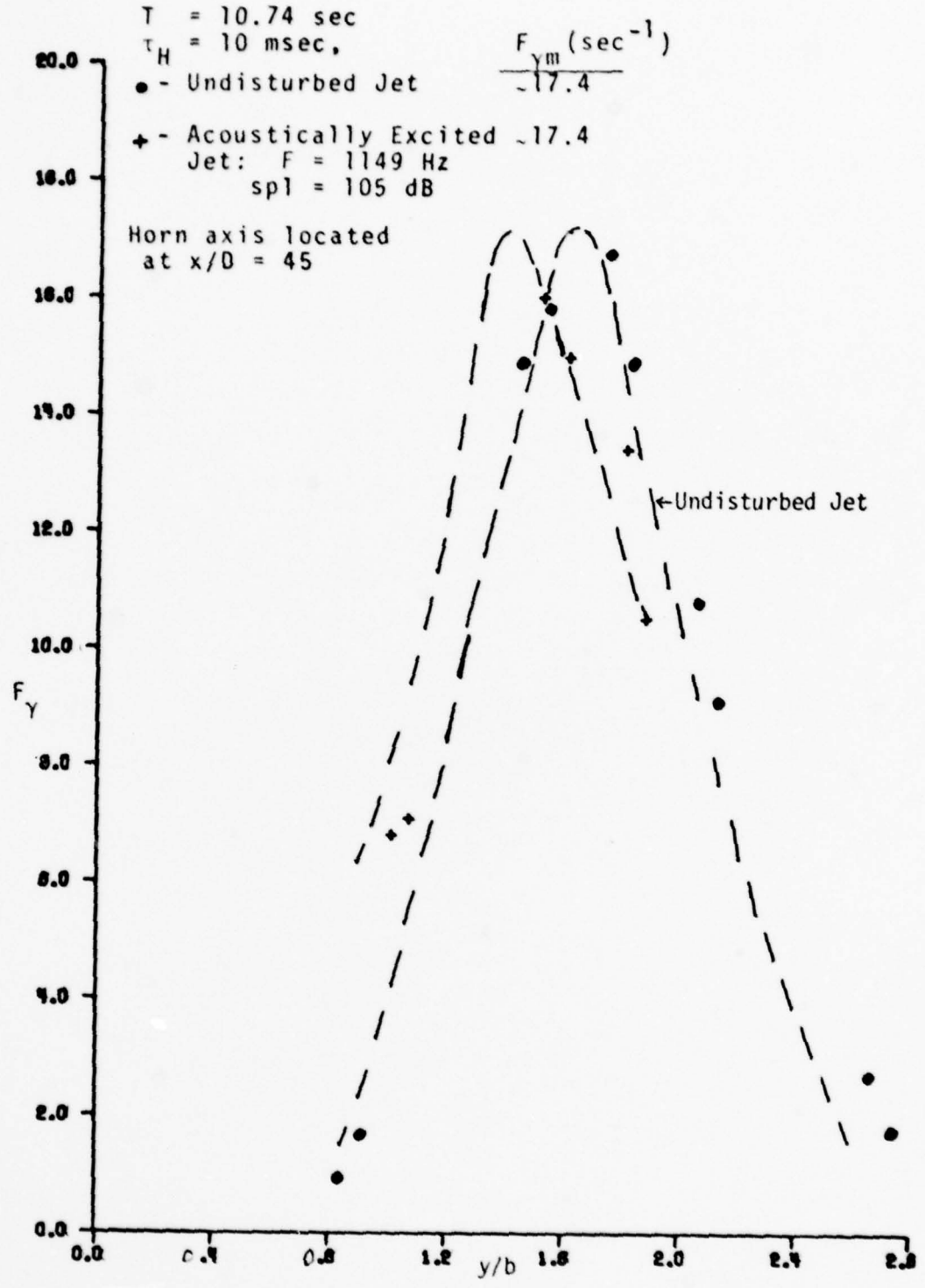

Figure 4-5. Crossing Frequency vs. y/b at x/D = 35

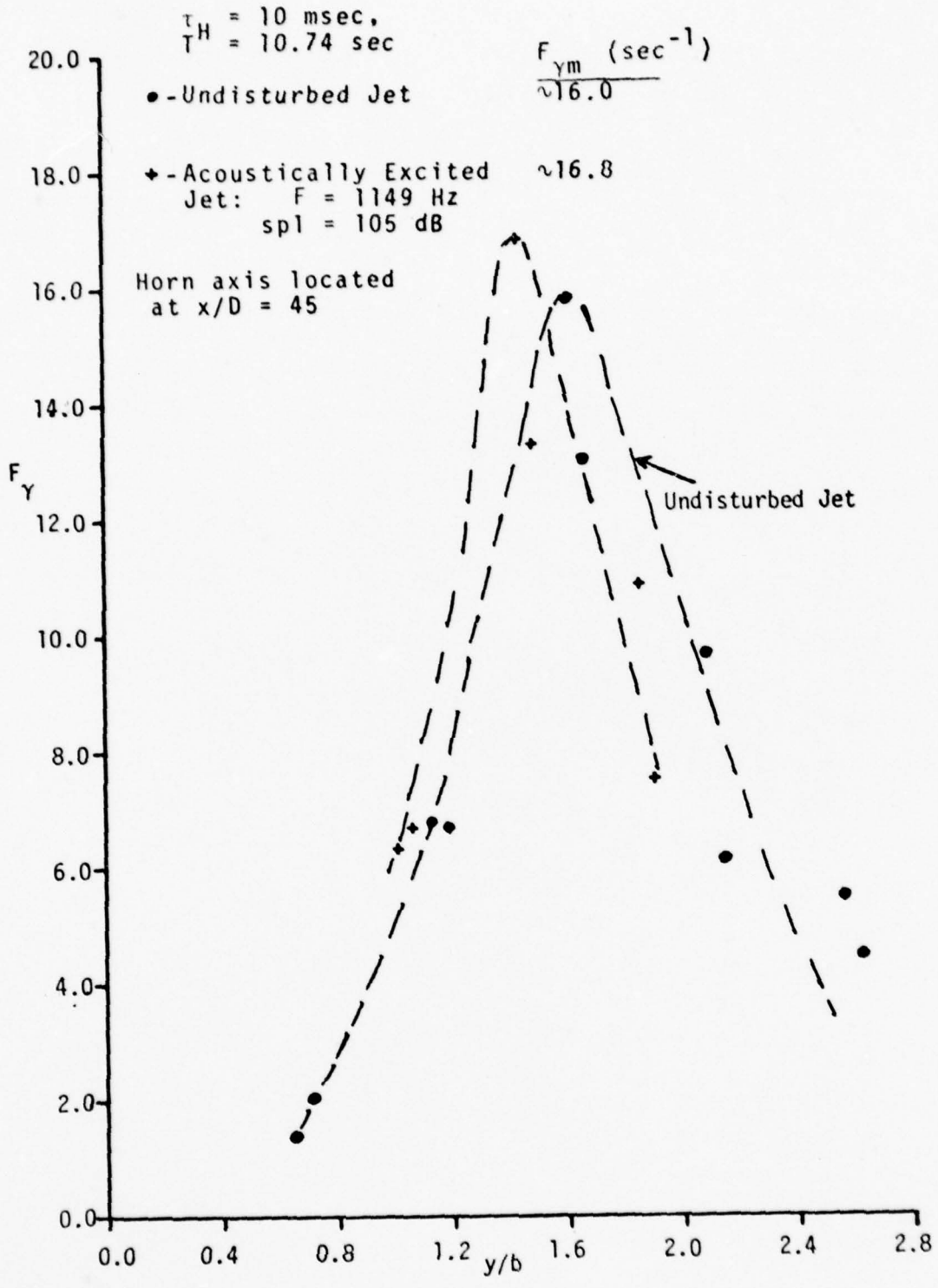

Figure 4-6. Crossing Frequency vs. y/b at x/D = 45.

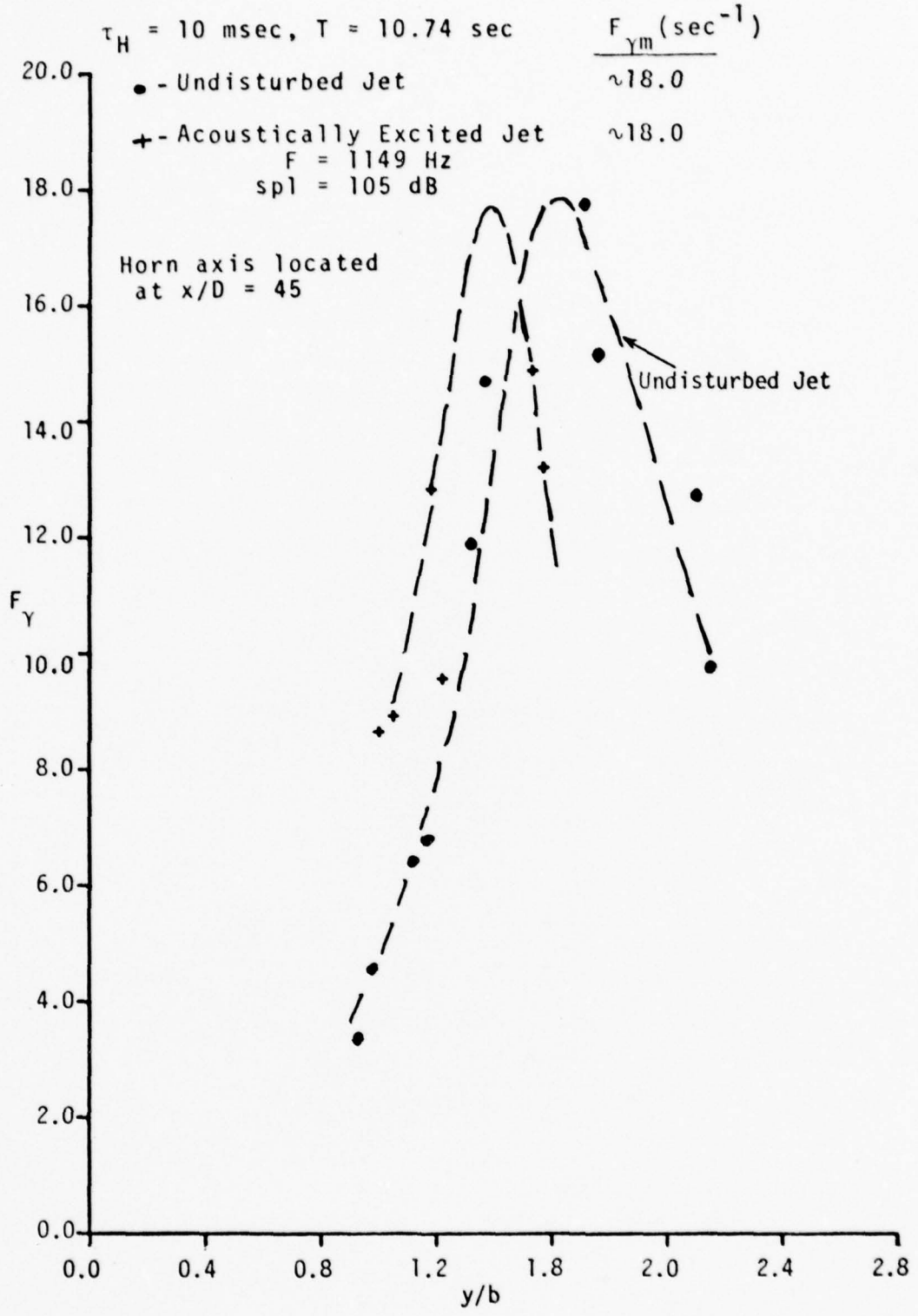

Figure 4-7. Crossing Frequency vs. y/b at x/D = 55.

frequency profiles are shifted, and that the maximum crossing frequencies now occur at smaller values of y/b. Figure 4-6 shows that the maximum crossing frequency was slightly increased by the acoustic disturbance. This increase is not noted in Figures 4-5 and 4-7 and this may be due to the lack of experimental data points.

2. Fold-over of the Interface

Fold-over measurements were taken at the same Reynolds number and x/D stations as those for the intermittency and crossing frequency. The separation between probes was 0.125 in. (0.3175 cm). A plot of the total percent fold-over, ϕ_i, versus y/b for the undisturbed case is shown in Figure 4-8. The result shows that the total percent fold-over increases with y/b and x/D. Using these figures, the range of the fraction of time during which fold-over events were recorded, was calculated. Recall that 42960 points were sampled and that the total record time was 10.74 sec. Assuming that 42960 fold-over events were recorded, then fold-over events would have occurred 100% of the time. It was calculated that the fraction of time fold-over events were recorded in this work varied from 0.02% to 0.42%. This compares with 0.1 to 0.5% reported by LaRue (1973) at the downstream edge of the interface.

When an acoustic disturbance was applied to the jet, the total percent fold-over was also found to increase with y/b and x/D.

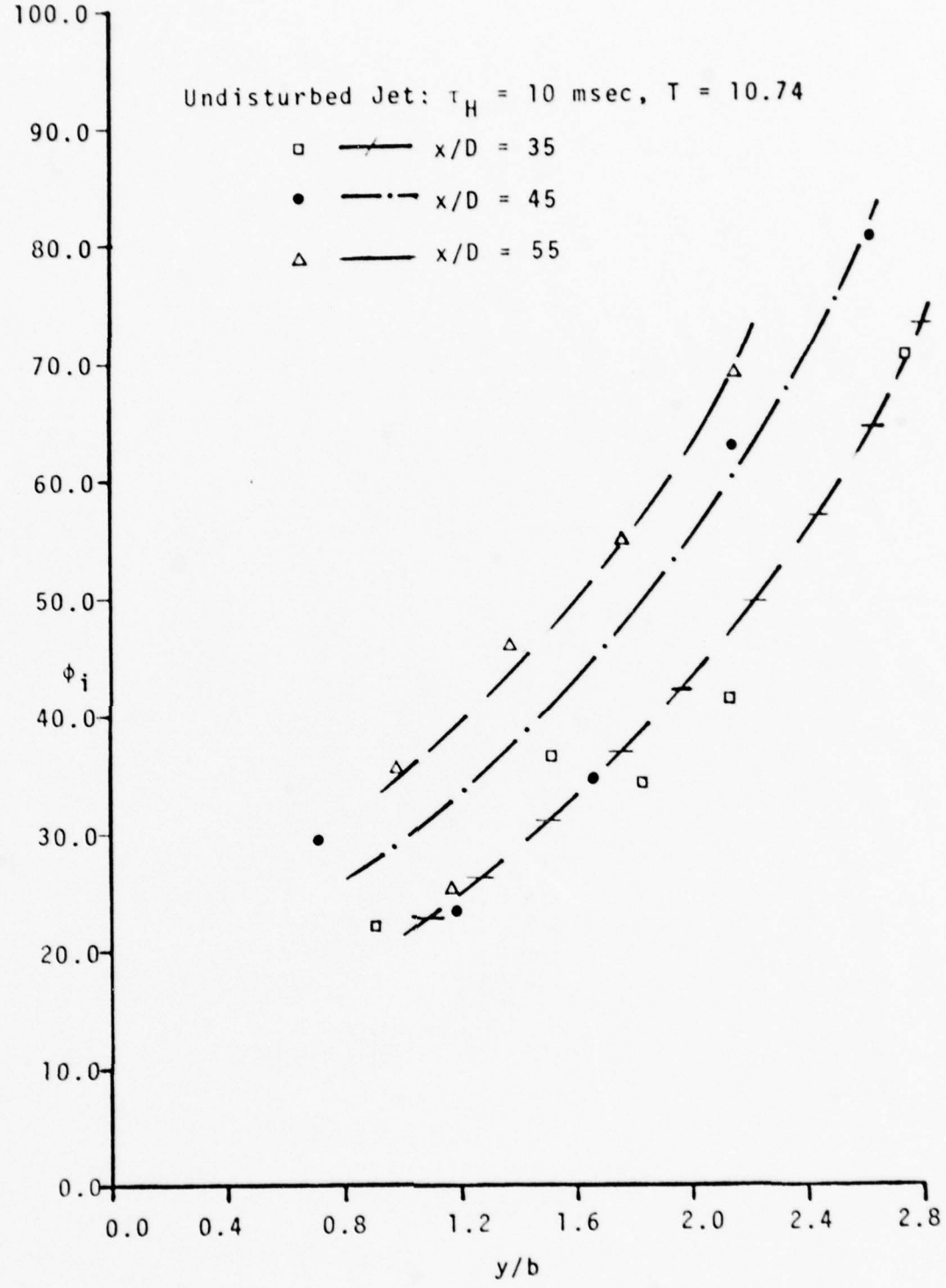

Figure 4-8. Total Percent Fold-Over vs. y/b.

The total percent fold-over accounts for both the front and the back fold-over events. To check whether the fronts or the backs have a more frequent occurrence of fold-over, the events are accordingly distinguished (see Figures 4-9a, 4-9b* and 4-9c*). These figures show separately the percent fold-over for the front and back of the interface. Whereas Mulej (1975) reported that fold-over is more likely to be detected at the front of the interface, these figures show that fold-over is actually more likely to be detected at the back of the interface. Specifically, Mulej (1975) measured fold-over at 11 lateral locations. The percent fold-over for the front was greater than that for the back in 10 out of the 11 cases he considered. The present work measured fold-over at 15 lateral locations. It can be seen from Figures 4-9a, 4-9b, and 4-9c that in the average, the percent fold-over for the back is greater than that for the front. This is for the undisturbed case. Fold-over measurements were taken at 9 different lateral locations for the acoustically excited jet. It was found that in 6 out of the 9 cases, the percent fold-over for the back was greater than that for the front (see Table B-4). Furthermore, examining each x/D station separately, it can be seen from Figures 4-9a, 4-9b, and 4-9c that there is an

---

*The data show an anomalous behavior at y/b = 1.2. The cause of this is uncertain.

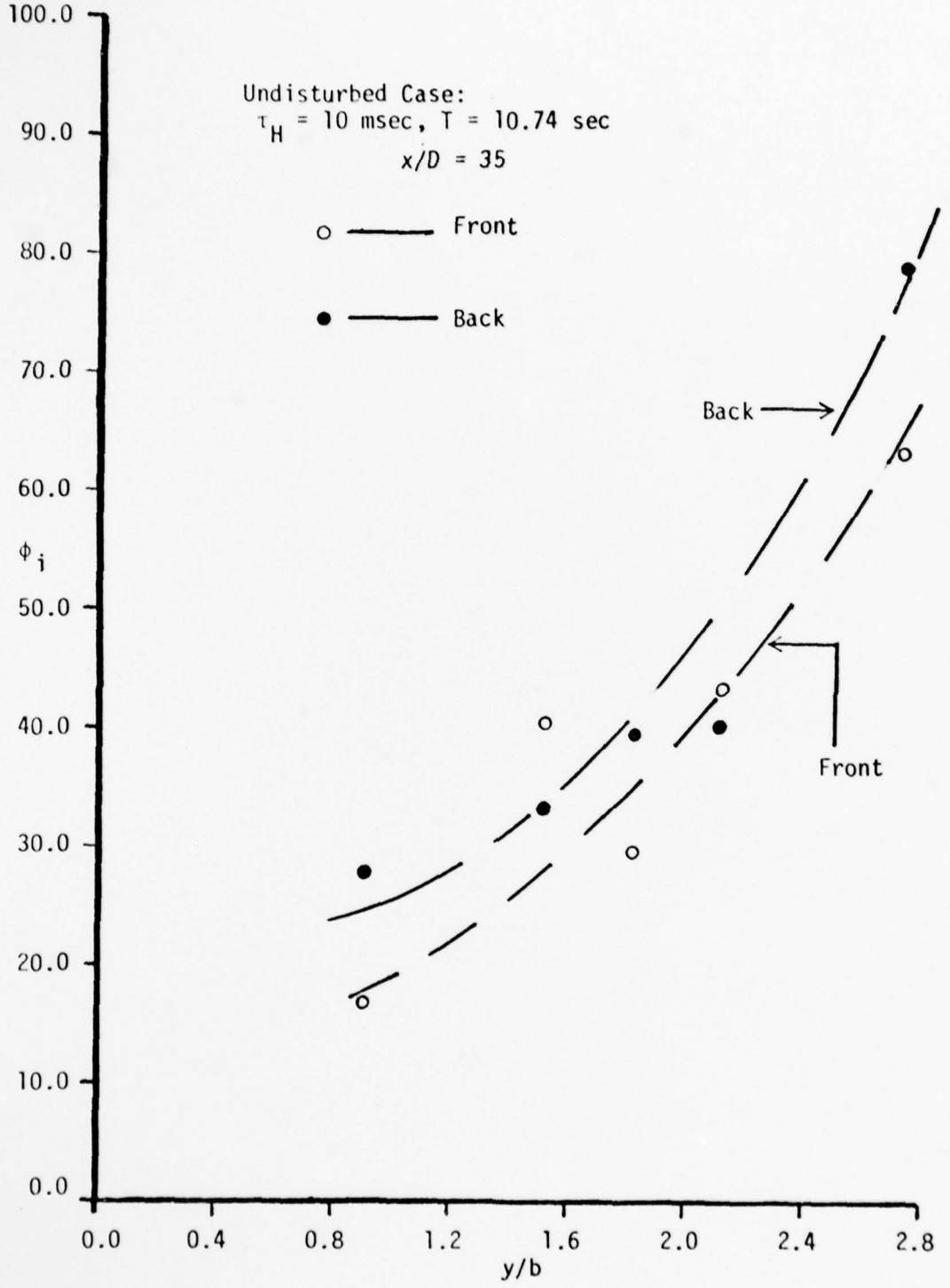

Figure 4-9a. Percent Fold-over for Fronts and Backs of the Interface vs. y/b at x/D = 35.

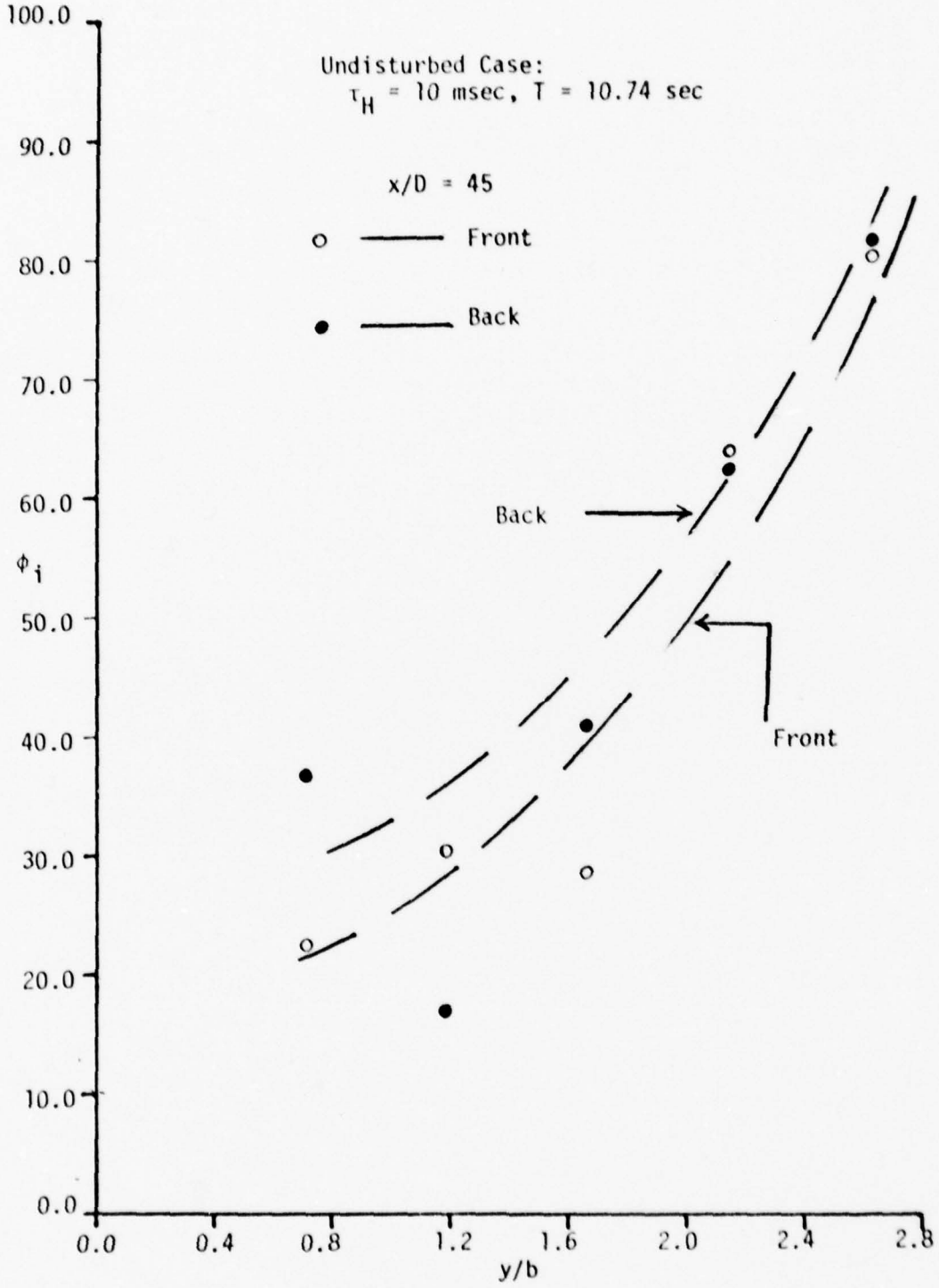

Figure 4-9b. Percent Fold-over for Fronts and Backs of the Interface vs. y/b at x/D = 45.

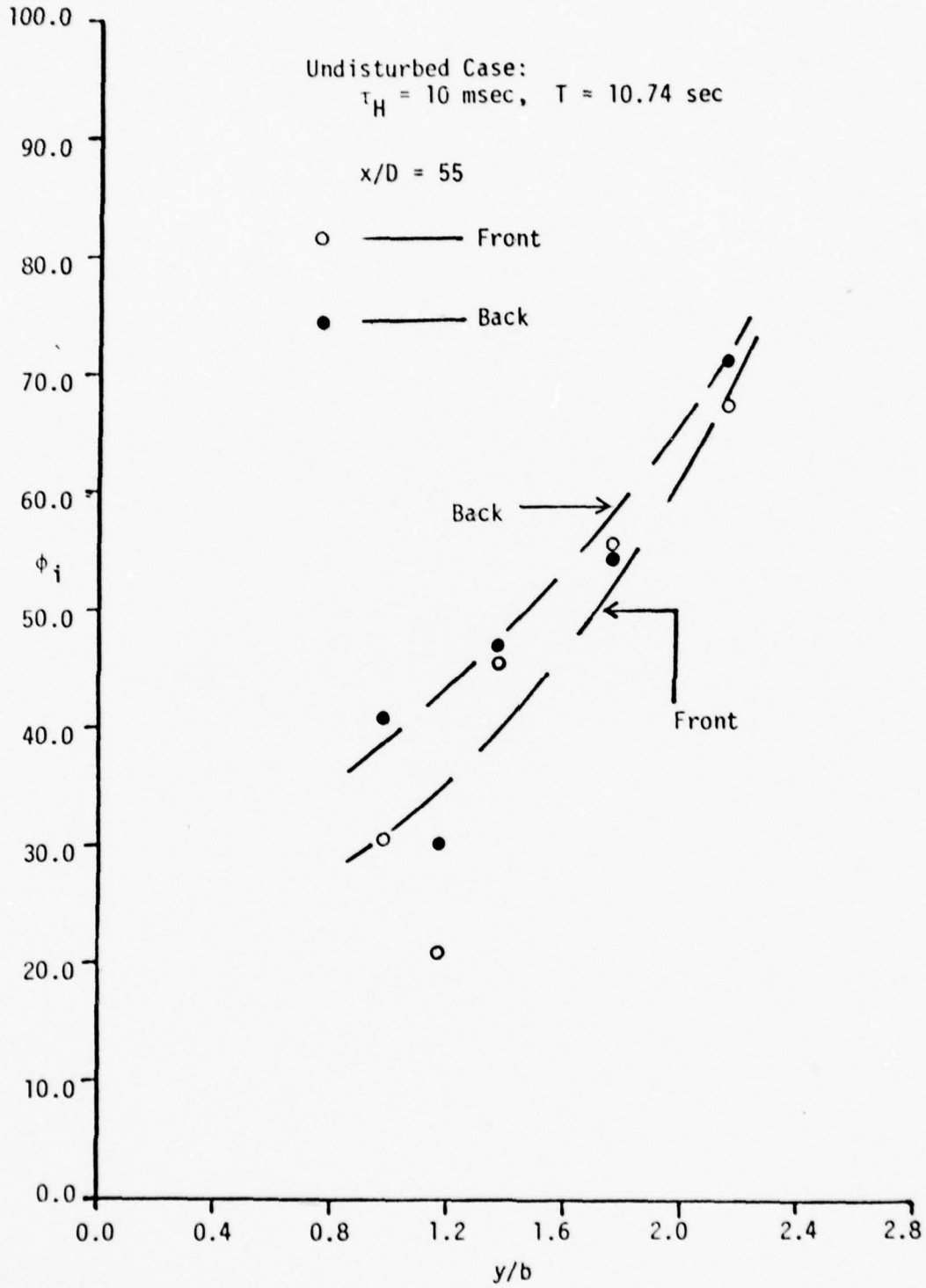

Figure 4-9c. Percent Fold-over for Fronts and Backs of the Interface vs. y/b at x/D = 55.

average percent increase for the front over the back. Specifically, going from the front to the back, there seems to be a 5% increase in ϕ_i at x/D = 35, 5% increase at x/D = 45 and 4% increase at x/D = 55. These results will be compared with those of previous investigators in the following chapter.

To see the effect of an acoustic disturbance on fold-over, Figures 4-10, 4-11, and 4-12 were plotted for x/D = 35, 45, and 55, respectively*. It can be seen that fold-over occurs more frequently in the case of acoustic disturbance. This is more noticeable at x/D = 35 and 45 than at x/D = 55. (The anomalous behavior at y/b = 1.2 is again noticed in Figures 4-11 and 4-12).

It is proposed that fold-over could better be represented as a frequency rather than as a percent. This led to a definition of fold-over frequency, F_θ (see equation 3-19). This was defined as the total fold-over events divided by the total time of sampling. An attempt to non-dimensionalize F_θ, using the maximum crossing frequency of the interface, $F_{\gamma m}$, was made. The plot of $F_\theta/F_{\gamma m}$ versus y/b is shown in Figure 4-13. Notice the lack of a universal trend for the shape of the curve. The fold-over frequency was then non-dimensionalized using the maximum

---

*X is always measured from the nozzle. The shift of the virtual origin is not taken into account.

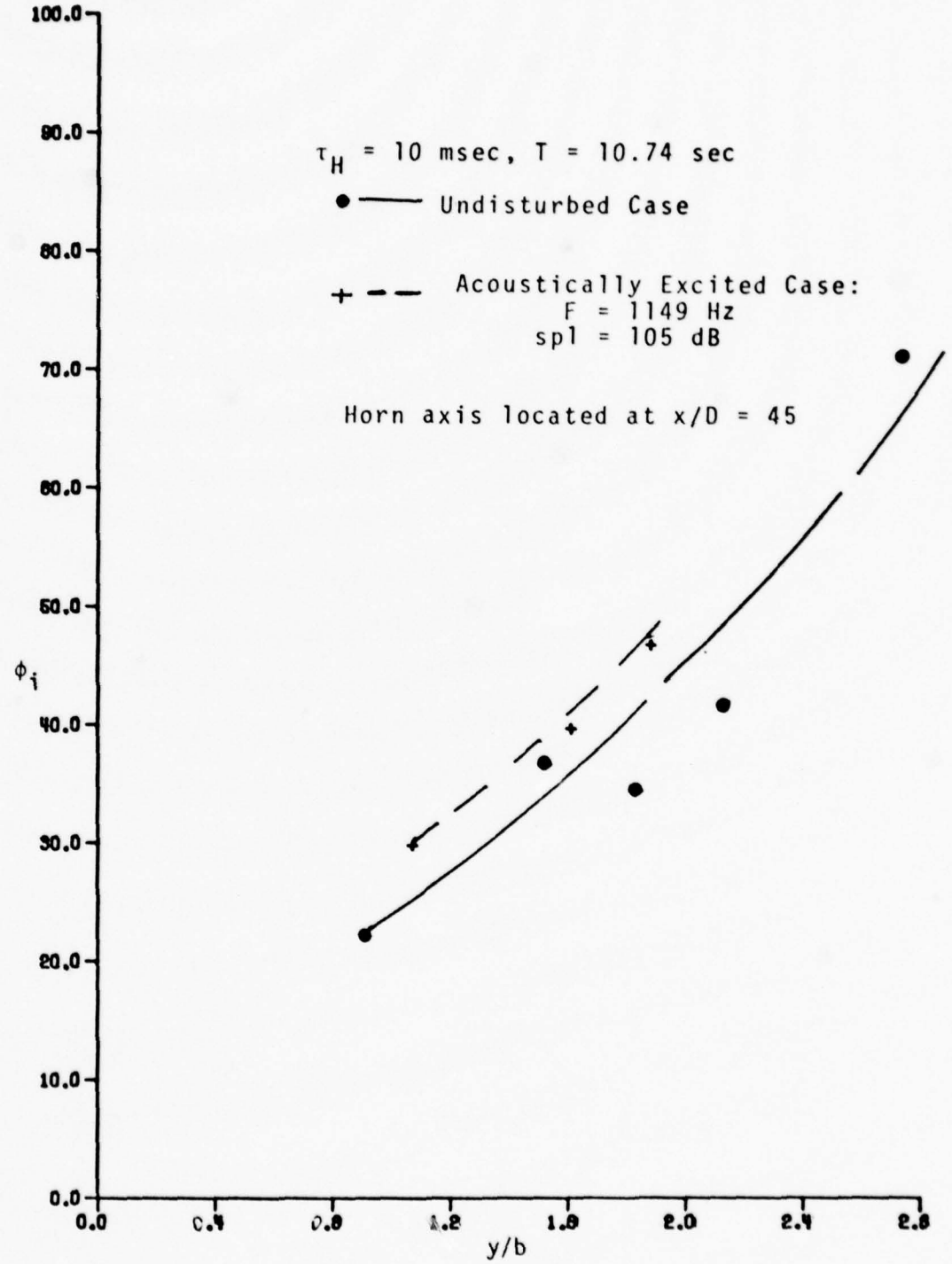

Figure 4-10. Percent Fold-Over vs. y/b at x/D = 35.

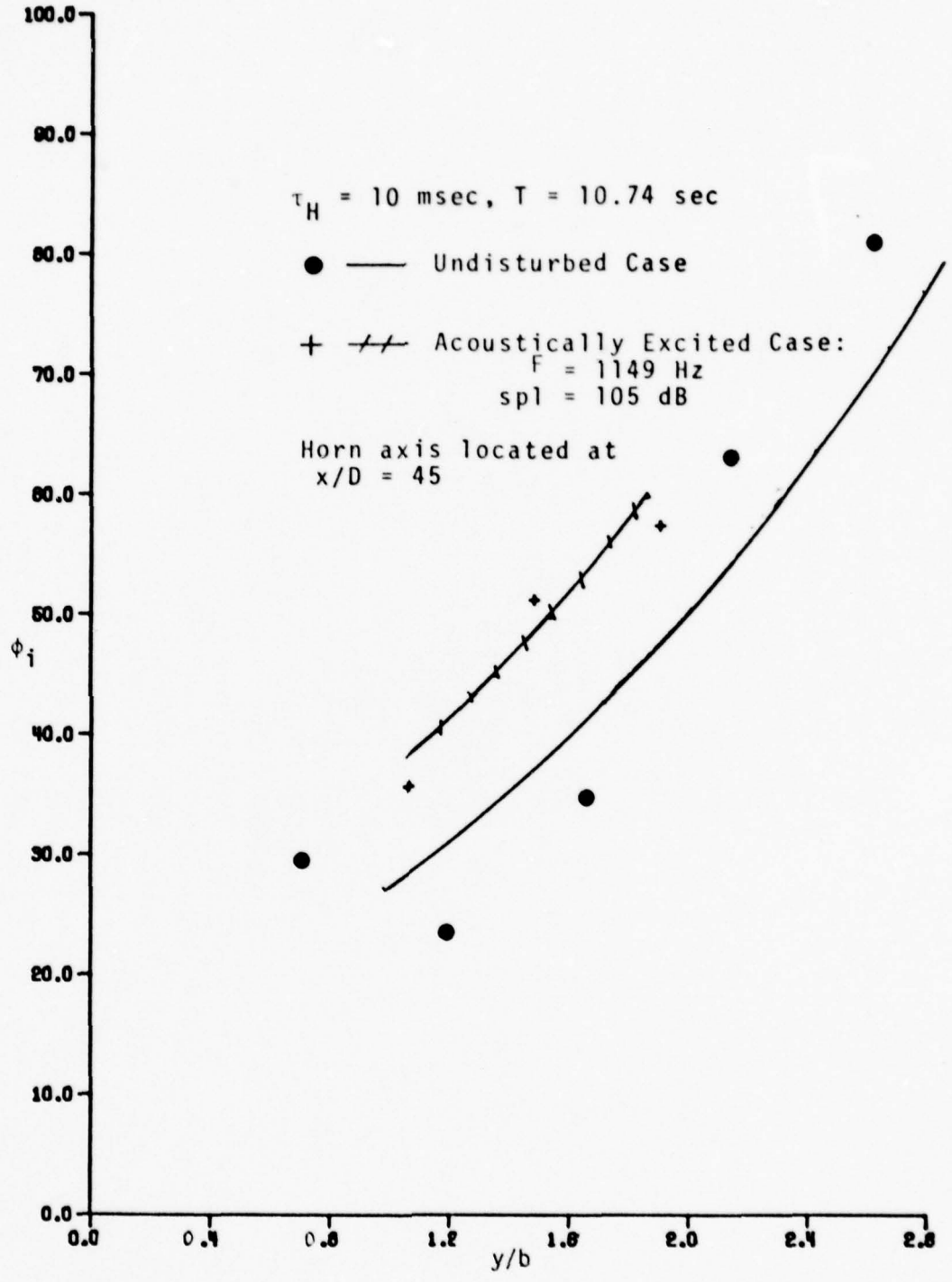

Figure 4-11. Percent Fold-Over vs. y/b at x/D = 45.

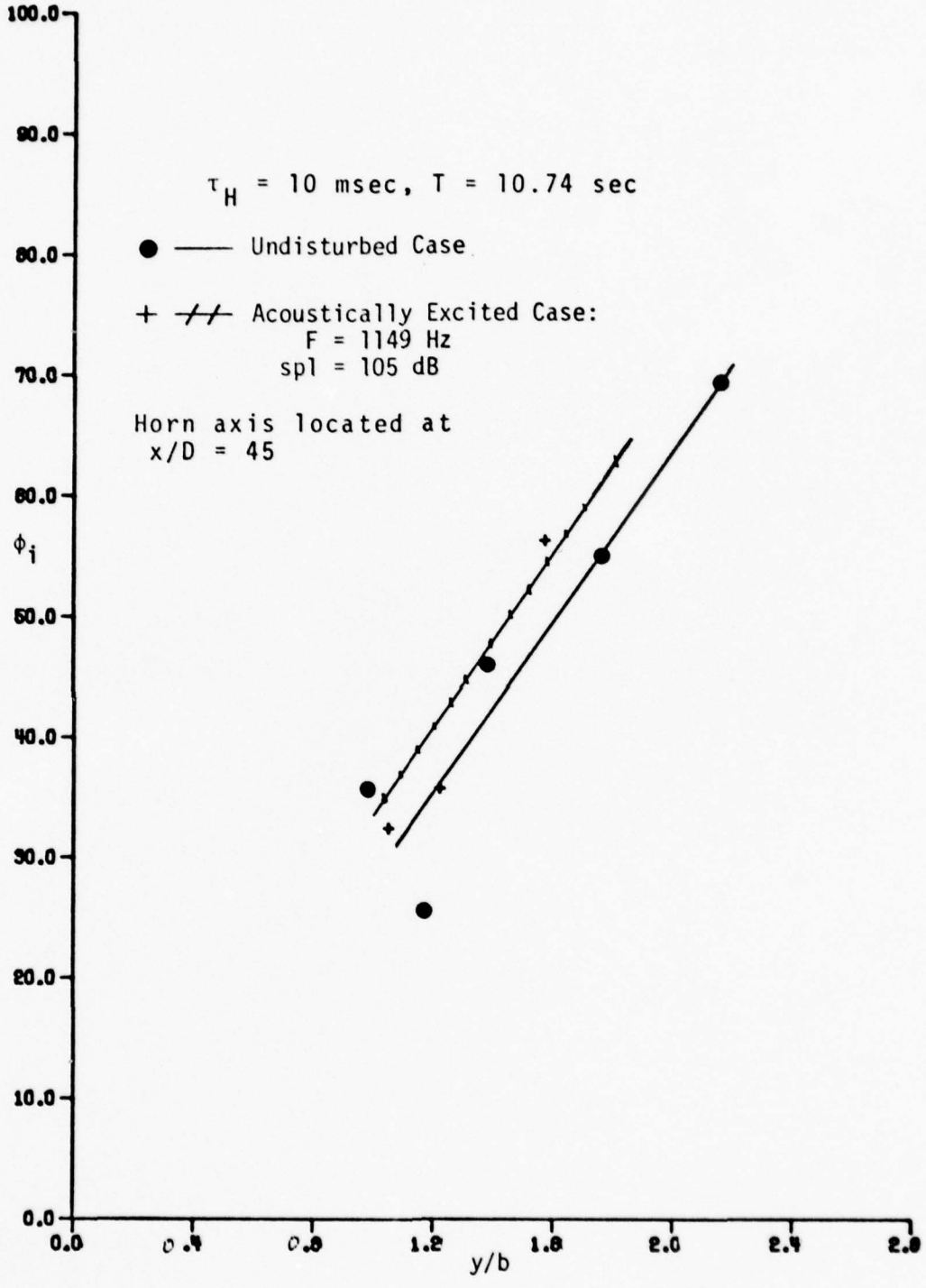

Figure 4-12. Percent Fold-Over vs. y/b at x/D = 55.

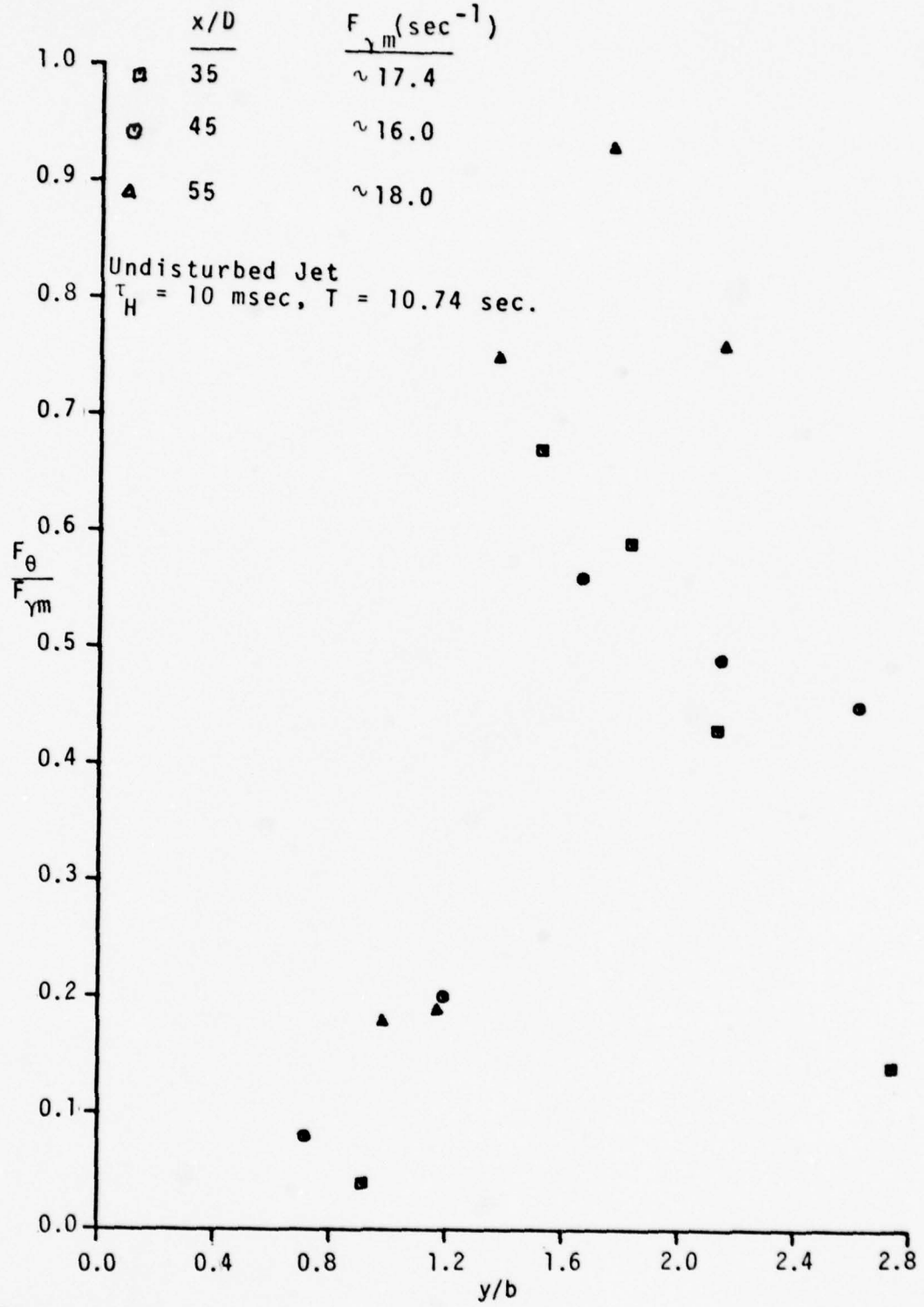

Figure 4-13. $F_\theta/F_{\gamma m}$ vs. y/b

fold-over frequency, $F_{\theta m}$. The plot of $F_{\theta m}$ versus y/b is shown in Figure 4-14. The results now show a general tend. The maximum fold-over frequencies were not obtained very accurately. More data points and larger samples are needed to obtain better values. The plot of $F_\theta/F_{\theta m}$ versus y/b seems to approximate a Gaussian curve. To this end, a curve fit was attempted using equation 4-2. The coefficients for the curve fit are: $\bar{Y}' = 1.58$, $\sigma' = 0.3$, $\sigma = 0.493$ in. (1.25 cm). This is for the undisturbed jet.

Figure 4-15 shows the plot of $F_\theta/F_{\theta m}$ versus y/b for the case of the acoustically excited jet. Here again the curve is approximated by a Gaussian curve. The coefficients for the curve fit are: $\bar{Y}' = 1.48$, $\sigma' = 0.275$, $\sigma = 0.513$ in. (1.302 cm). To observe the effect of the acoustic disturbance on the maximum fold-over frequencies, Figures 4-16, 4-17 and 4-18 were plotted for x/D = 35, 35, and 55, respectively. The results show the possibility of a slight increase in the maximum fold-over frequency. It is clear that more data points are required to study the actual shape of the curves. However, it was not the objective of this research to do this.

In the intermittency, crossing frequency and fold-over frequency curves just reported, the mean interface location $\bar{Y}_\gamma$ was not identical with the location, $\bar{Y}_f$, where the maximum crossing frequency, $F_{\gamma m}$, occurred. Recall that the mean interface location was defined arbitrarily as the

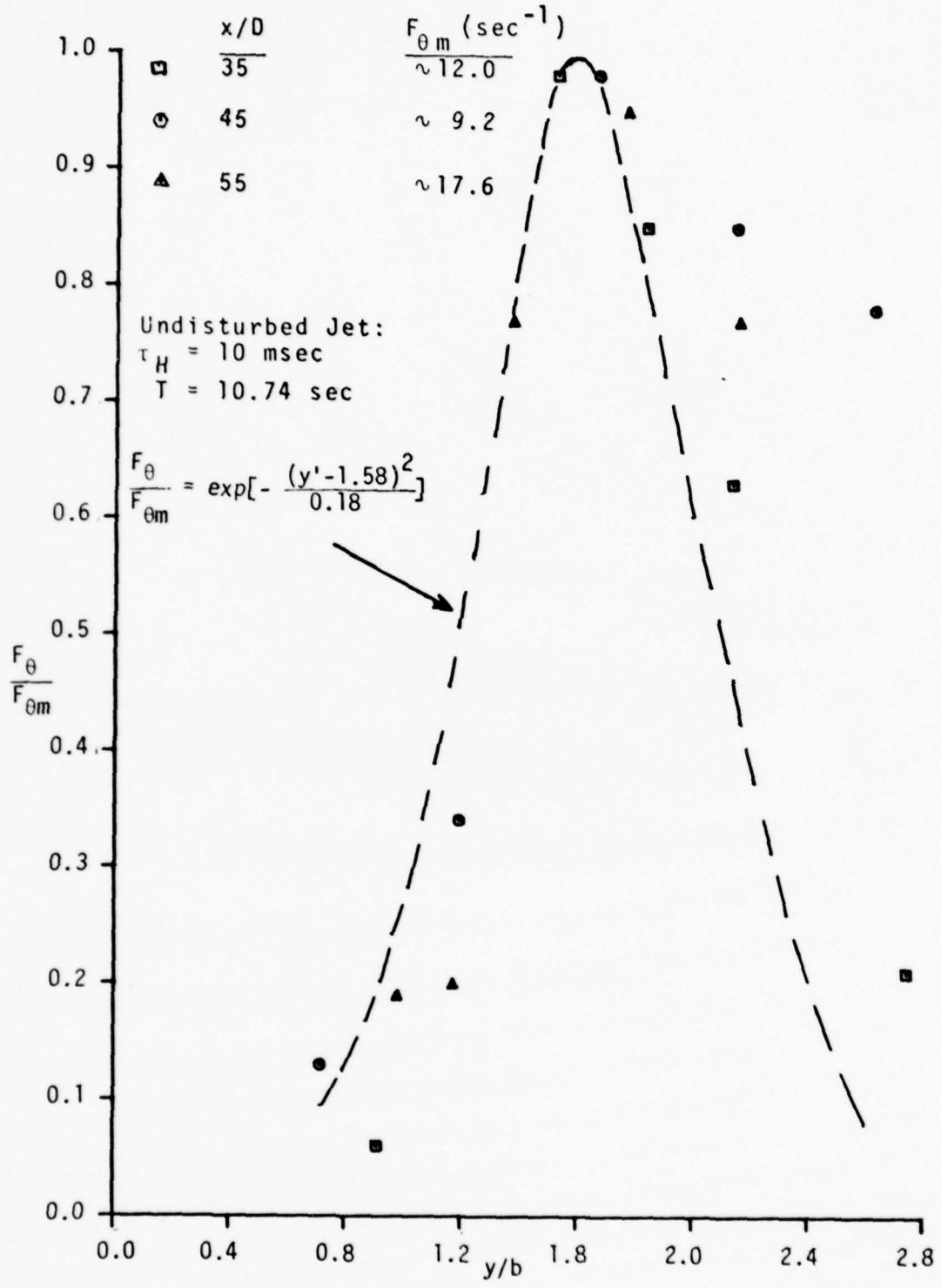

Figure 4-14. $F_\theta/F_{\theta m}$ vs. y/b: Undisturbed.

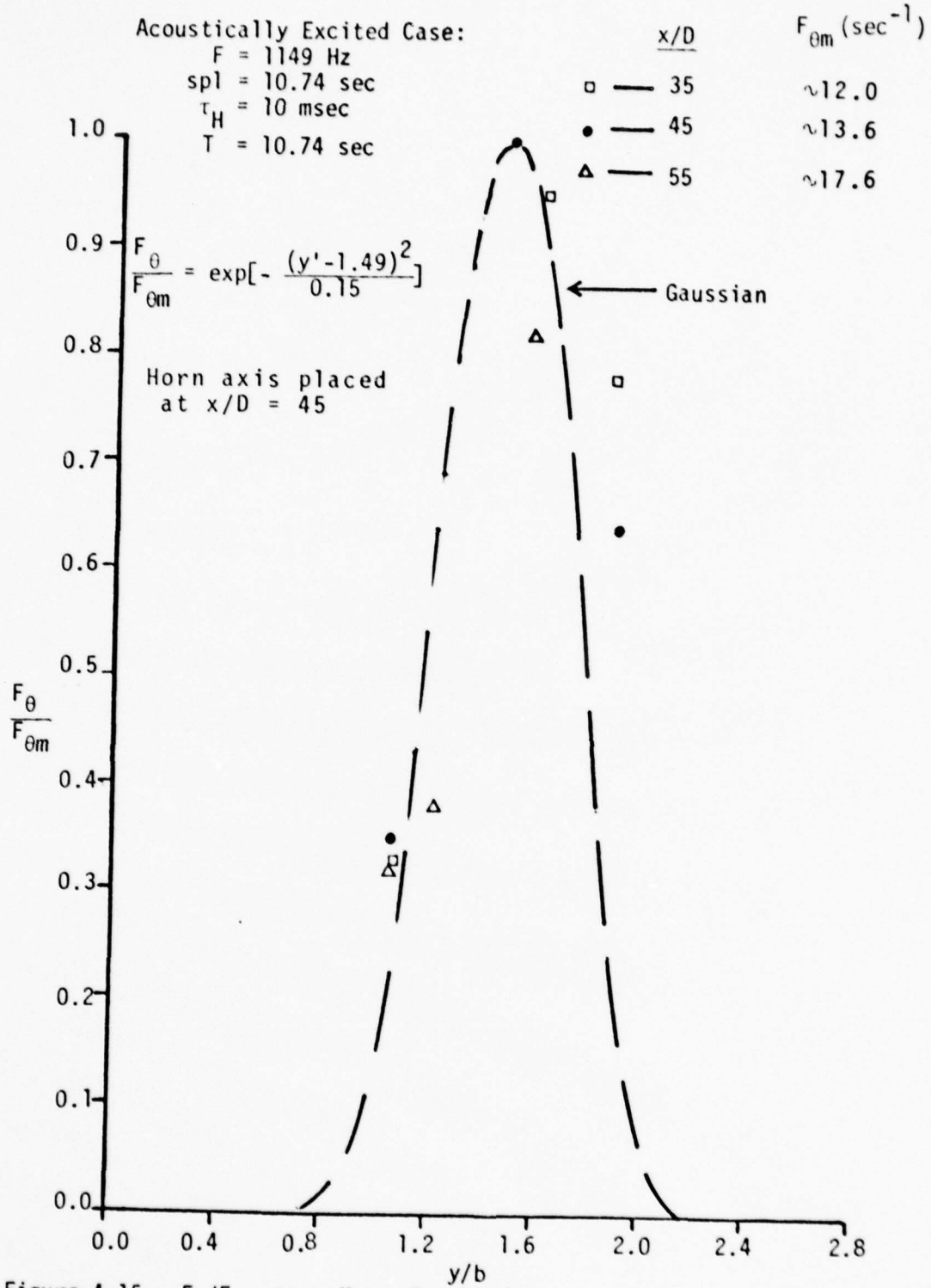

Figure 4-15. $F_\theta/F_{\theta m}$ vs. y/b: Excited.

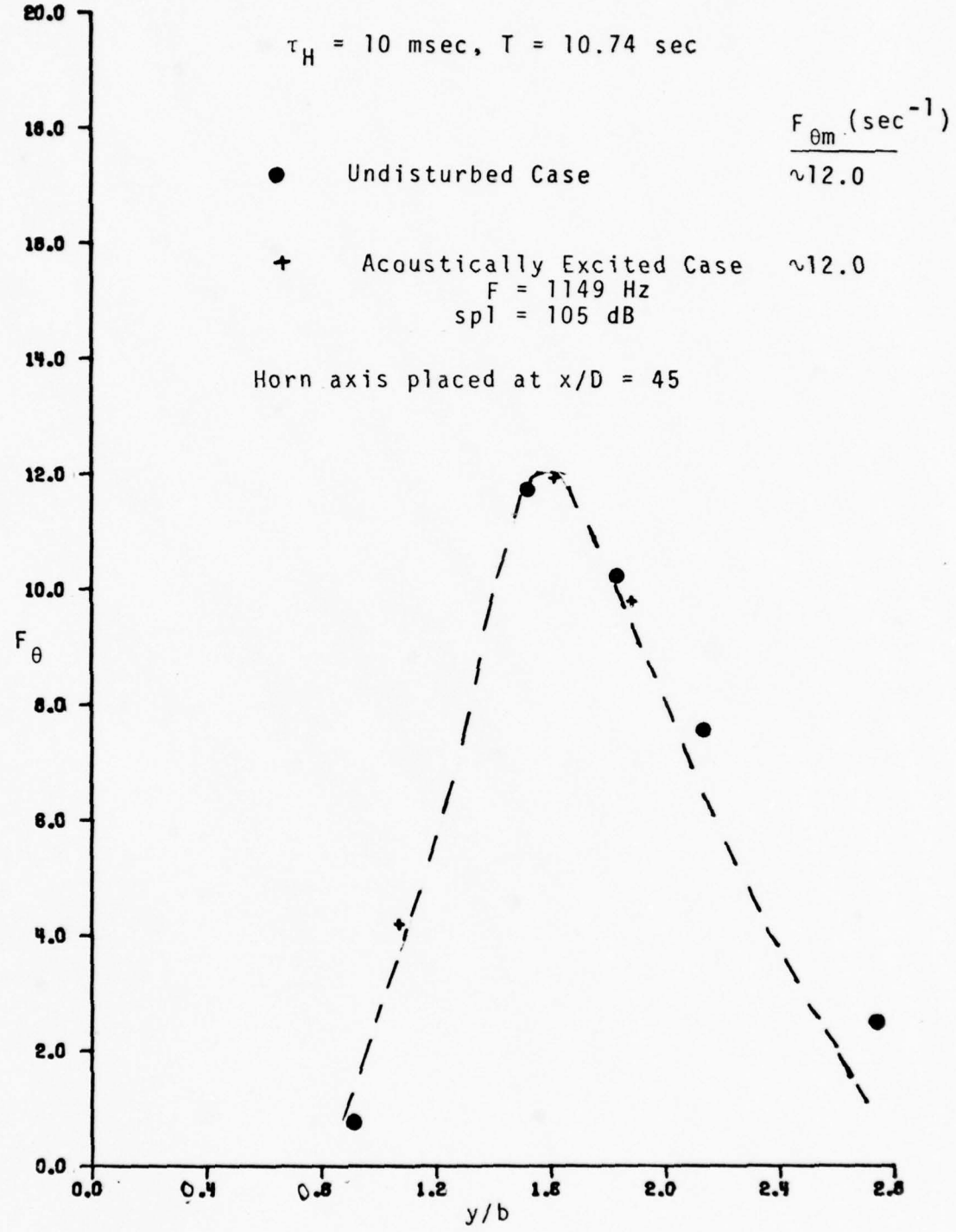

Figure 4-16. Fold-Over Frequency vs. y/b at x/D = 35.

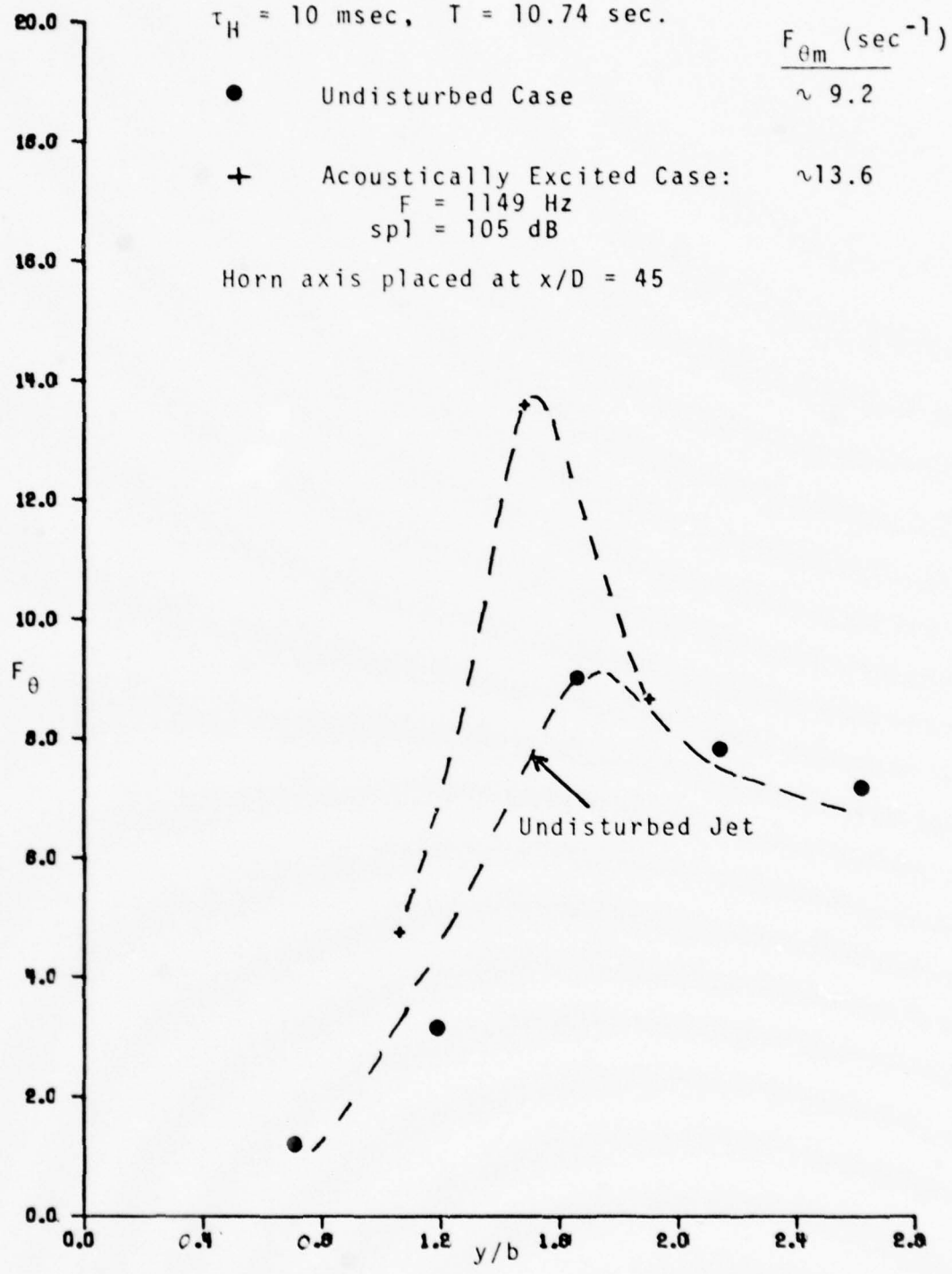

Figure 4-17. Fold-Over Frequency vs. y/b at x/D = 45.

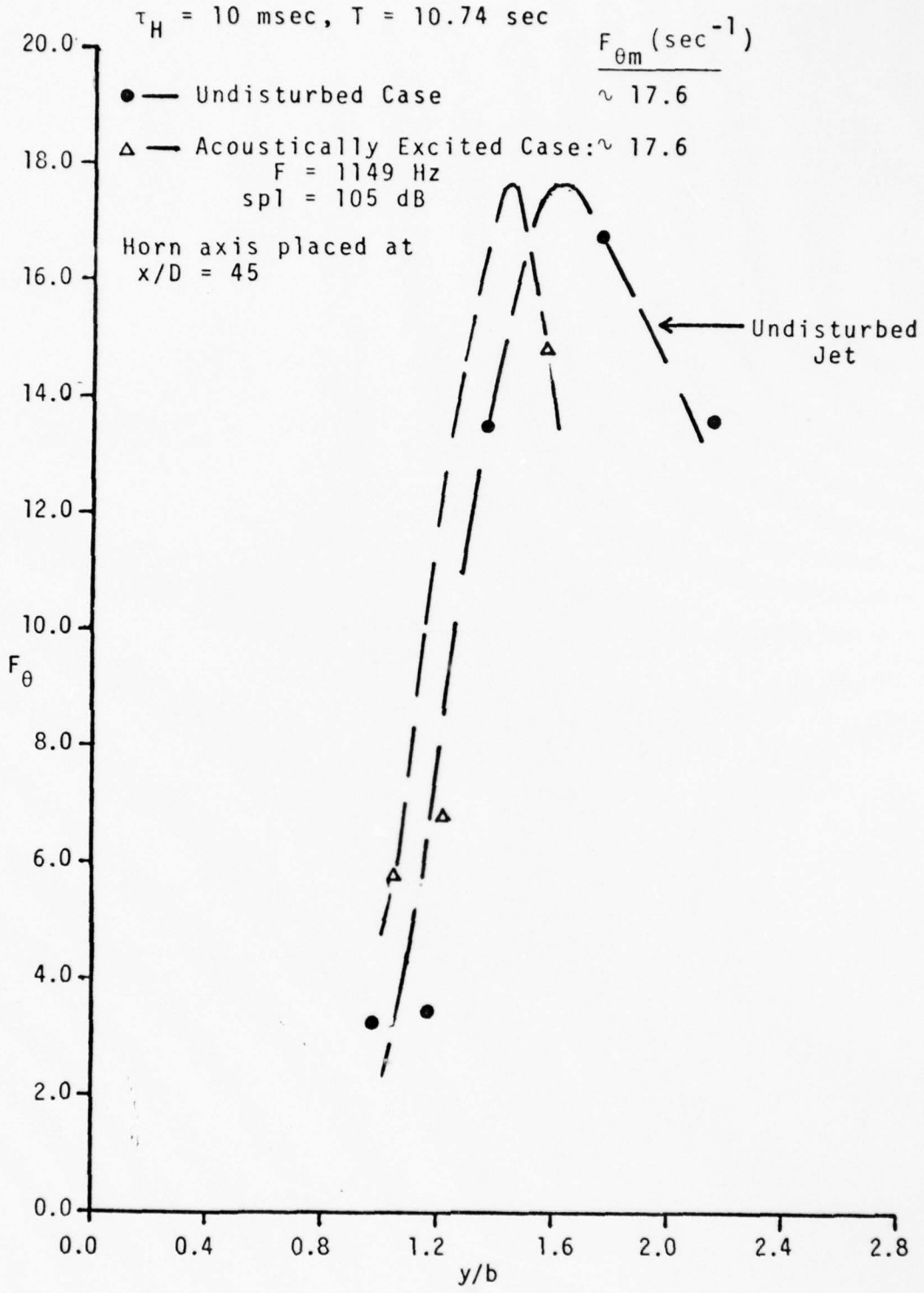

Figure 4-18. Fold-Over Frequency vs. y/b at x/D = 55.

location where $\gamma = 0.5$. Ideally the two locations ($\overline{Y}_\gamma$ and $\overline{Y}_f$) would be identical. However, experimenters have reported slight variations in those values (LaRue, 1973; Kibens and Kovasznay, 1969, 1970; Jenkins, 1974, and Mulej, 1975). LaRue (1973) for example obtained $\overline{Y}_\gamma = 4.89$ cm, $\overline{Y}_f = 4.68$. This is a variation of about 4.3%. In the present work, a 3% variation was obtained. This is well within the experimental scatter and not much should be concluded from it.

The cause of the increase in the maximum interface crossing frequency observed in Figure 4-17 is not certain. It may be due to the positioning of the exponential horn. Recall that the axis of the horn was fixed at x/D = 45 for all the acoustically excited cases. Note that the curves shown in Figures 4-16, 4-17, and 4-18 were not approximated by a Gaussian curve (the nondimensional frequencies were).

The anomalous behavior at y/b = 1.2 is again noticed in Figure 4-18. The choice of $\overline{Y}'_\theta$ in this figure was made to agree with those obtained from Figures 4-16 and 4-17.

CHAPTER V. DISCUSSION OF RESULTS

This work has been purely experimental. It has explored digital methods to analyze the data. Although analog methods are equally acceptable, the digital computer methods have the advantage of using less instrumentation that would otherwise contribute to error. Digital methods also permit repeated analysis with the same base data.

This discussion will be divided into four parts: (1) the results of the measurements presented in the previous chapter will be compared with those of previous experimenters. (2) Possible sources and estimates of error will be presented following comparison with previous work. (3) A discussion on entrainment and the interface slope will follow. (4) The effects of an acoustic distrubance on a plane turbulent jet will be discussed.

1. Comparison with Previous Work

a. The Undisturbed Jet

The intermittency curve was shown in Figure 4-1. The results of this curve were compared with Jenkins (1974) and were found to agree. Jenkins (1974) in turn had compared his results with those obtained by Heskestad (1965) and Bradbury (1965) and found agreement. It was pointed out

in Chapter IV that the shape of this curve is approximated by an error function of the form given in equation (4-1). The coefficients of the curve fit were also given. Libby (1975) proposed a model equation which described the intermittent turbulent flow. Assuming that the unconditioned flow was known, he showed that the properties of the conditioned mean velocity and of the intermittency could be predicted. He compared predicted and experimental quantities for two mixing layers and a simulated boundary layer and found the agreement satisfactory. This model could also be applied to a plane jet.

The crossing frequency was compared with Jenkins (1974) and the plot of $F_\gamma/F_{\gamma m}$ vs. y/b agreed. However, as was previously noted, the values of the maximum crossing frequency, $F_{\gamma m}$, obtained in this research did not compare favorably with Jenkins' (1974), even though $F_\gamma/F_{\gamma m}$ vs. y/b did agree(*). No other paper has been published that gives values for the maximum crossing frequency of the interface for a two dimensional plane turbulent jet. The values obtained in this research are shown compared with Jenkins' (1974) in Table 5-1. Similar values obtained for other shear flows are also shown in Table 5-1. The nondimensional variance obtained from an error function curve fit is denoted by $\sigma_\gamma/\overline{Y}_\gamma$. The other two nondimensional variances, $\sigma_F/\overline{Y}_F$ and $\sigma_\theta/\overline{Y}_\theta$ are for the crossing and fold-over frequencies, respectively.

(*) This could be due to the different hold times used.

Table 5-1. Maximum Interface Crossing Frequency and Parameter for the Curve Fit.

Investigator	Flow Field	x/D	$F_{\gamma m}$ (Hz)	$\frac{\sigma_\gamma}{\lvert\overline{\gamma}_\gamma\rvert}$	$\frac{\sigma_F}{\lvert\overline{\gamma}_F\rvert}$	$\frac{\sigma_\theta}{\lvert\overline{\gamma}_\theta\rvert}$
Bradbury (1965)	Plane Jet	35		~0.24	~0.24	--
Kibens & Kovasznay (1970)	Boundary Layer		~30			
Antonia (1972)	Boundary Layer		~125			
LaRue (1973)	Heated Wake	400	122	0.26	0.27	--
Jenkins (1974)	2-Dim. Plane Jet	35	31	~0.24		
Jenkins (1974)	Plane Jet	45	30			
Jenkins (1974)	Plane Jet	55	31			
Present	2-Dim. Plane Jet	35	17.4	0.25	0.21	0.19
Present	2-Dim. Plane Jet	45	16.0	0.25	0.27	0.17
Present	2-Dim. Plane Jet	55	18.0	0.26	0.24	0.21
Present*	2-Dim. Plane Jet	35	~17.4	0.25	0.23	0.19
Present*	2-Dim. Plane Jet	45	~16.8	0.26	0.21	0.20
Present*	2-Dim. Plane Jet	55	~18.0	0.26	0.25	0.19

*Acoustically excited case: F = 1149 Hz, SPL = 105 dB.

The values of $F_{\gamma m}$ obtained by Jenkins (1974) are approximately equal to that obtained by Kibens and Kovasznay (1970) in the boundary layer. There is no reason to expect the values to agree. In fact, since the flows are entirely different, it seems reasonable to expect a difference in the maximum interface crossing frequency. Besides, the intermittency curves do not match even though they obey the same error function. The constants in equations (3-12) and (3-13) are different for different flow fields since σ and $\overline{\gamma}$ are different. Hence, it would not be surprising if the values of the maximum crossing frequency $F_{\gamma m}$, would be indeed different.

The values of the maximum crossing frequency obtained by Jenkins (1974) were used by Mulej (1975) in his final presentation of the determined lateral velocity of the interface. He shows that the lateral velocity of the interface should take the form:

$$V_i = - \frac{2F_\gamma}{\partial\gamma/\partial y} \qquad (5\text{-}1)$$

Equation (5-1)is Mulej's (1975) equation 6. This equation can be rewritten to give:

$$\frac{V_i}{b} = - \frac{2F_\gamma}{\partial\gamma/\partial(y/b)} = - \frac{2F_\gamma}{b\,\frac{\partial\gamma}{\partial y}} \qquad (5\text{-}2)$$

From equation (5-2) it can be seen that the sign of V_i depends on $\partial\gamma/\partial y$. Mulej (1975) plotted $b(\partial\gamma/\partial y)$ vs. y/b.

This is actually a plot of the magnitude of $b(\partial\gamma/dy)$ vs. y/b. From the equation for γ (equation 3-12) and its shape shown in Figure 4-1, it is obvious that the slope of γ, given by $\partial\gamma/\partial(y/b)$, is either zero or negative all the time; i.e., $\partial\gamma/\partial(y/b) \leq 0$. Applying this condition to equation 5-2 it can be seen that V_i will always be positive.

Mulej (1975) measured the lateral velocity of the interface in three ways. He defined V_{i1} as a measure of the interface velocity neglecting the effects of fold-over and V_{i2} as the velocity of the interface considering the effects of fold-over. He claims that V_{i2} takes no account of the direction of the velocity of the interface and thus was not a good representation of the velocity. He finally defined a third velocity of the interface, V_{i3}, as that velocity which takes into account the direction of the velocity of the interface. It has been argued earlier in this chapter that the lateral velocity of the interface, as defined by the equation (5-2) cannot be negative.* Hence V_{i3} does not seem to be the best measure of the velocity of the interface. It was, however, not the objective of this research to measure the velocity of the interface. The measurements of V_i by Mulej (1975) offer a means of comparing the maximum interface crossing frequency, $F_{\gamma m}$, obtained in this research to that obtained by Jenkins (1974). Since V_i was defined as a function of F_γ it is possible to

*This applies to the average value of V_i. The instantaneous value might be negative.

compare the measured V_i with the predicted value using Jenkins' (1974) F_γ and that obtained from the present work. Since $F_\gamma = F_{\gamma m}$ at $\gamma = 0.5$ the comparison has been made at $\gamma = 0.5$ at three x/D stations. The results are tabulated in Table 5-2. Notice that V_i/b computed with $F_{\gamma m}$, obtained from the present research, agrees with the measured values V_{i1}/b and V_{i2}/b much better than that computed using Jenkins' (1974) values. However V_{i3}/b agrees better with V_i/b computed using Jenkins' (1974) $F_{\gamma m}$. Since V_{i1} takes no account of fold-over, and V_{i3} defines the velocity of the interface as both positive and negative, it is assumed here that both defintions could give incorrect values of the velocity of the interface. It is suggested here that a reasonable definition of the lateral velocity of the interface, as measured by Mulej (1975), is that given by V_{i2}. The relative good agreement between the measured velocity, V_{i2}, and the predicted, V_i, using the present $F_{\gamma m}$ suggests that the values of $F_{\gamma m}$ obtained from this research are probably the "correct" values.

Both Kibens and Kovasznay (1970) and LaRue (1973) report that F_γ is very sensitive to the variations in the technique used to construct the intermittency function, I(t). To show how $F_{\gamma m}$ varies with the hold time, τ_H, in this work, Figure 5-1 is shown. Notice that $\tau_H \simeq 5$ msec, $F_{\gamma m} = 31\ \text{sec}^{-1}$. The method used to choose τ_H was presented in Chapter III. $\tau_H = 5$ msec was found to be unacceptable.

Table 5-2. V_i Obtained Using $F_{\gamma m}$ Obtained by Jenkins (1974) and Present Work.

		Measured by Mulej (1975) Figures 27-30			Mulej (1975) Figure 8	Predicted Value Equation 5-2 V_i/b	
x/D	γ	V_{i1}/b	V_{i2}/b	V_{i3}/b	$b\frac{\partial\gamma}{\partial y}$	Jenkins' (1974) $F_{\gamma m}$	Present Work $F_{\gamma m}$
35	.5	25.42	29.45	54.25	1	62	34.8
45	.5	25.5	30.0	67.5	1	60	32.0
55	.5	23.3	32.6	52.7	1	62	36.0

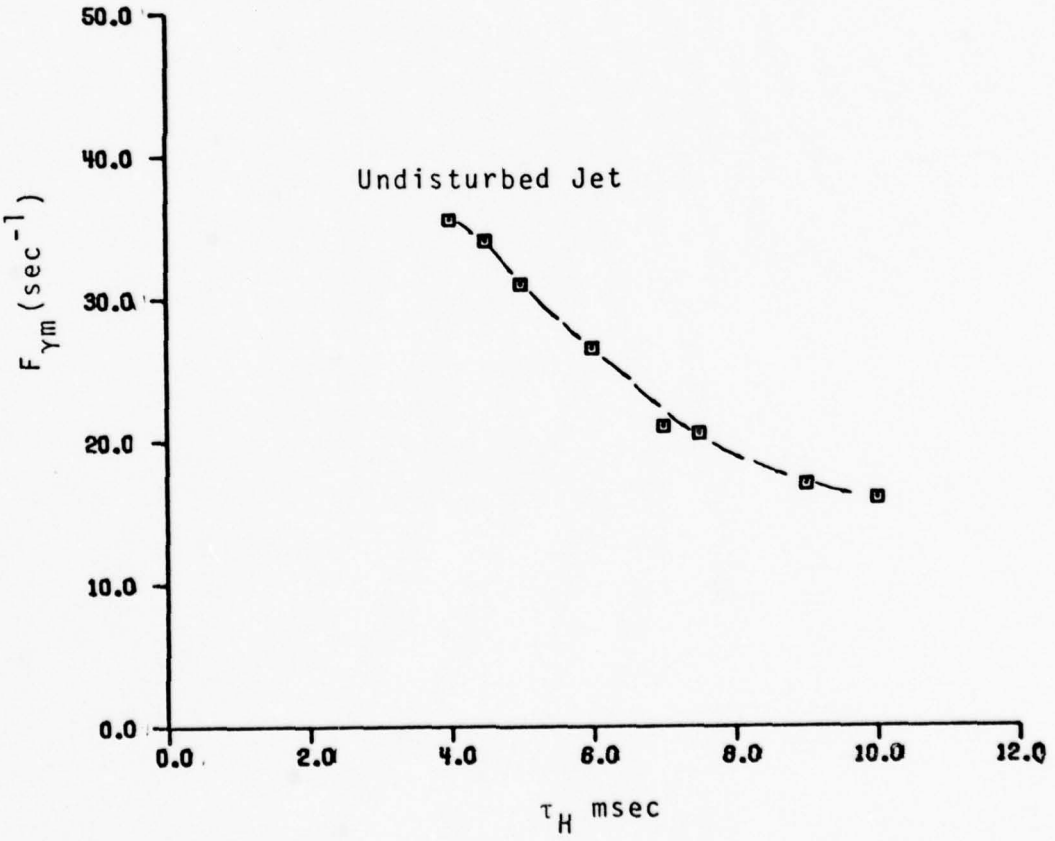

Figure 5-1. Maximum Crossing Frequency vs. τ_H at y/b = 1.61, γ = 0.5.

(i) Fold-Over

The only reported measure of fold-over in a plane turbulent jet is that given by Mulej (1975). Other measurements of fold-over in other shear flows were discussed in Chapter III. It was pointed out earlier that the method used by Mulej (1975) could lead to erroneous measurements of fold-over. It has been stated that fold-over can be measured only after the intermittency function, I(t), has been formed. Whereas, Mulej (1975) reported that fold-over decreased with y/b, this research shows that it increases with y/b instead. There is no theory to support this claim. However, it is shown here that a decreasing function can be obtained by using incorrect threshold levels. These values of the threshold level would give incorrect values of γ and F_γ. Figure 5-2 shows the two trends. The data points used to plot those curves are shown in Table 5-3. Notice that different values of ϕ_i (percent fold-over accounting for both the fronts and the backs of the interface) can be obtained by different settings of P*. Only three locations were checked and these were found to be sufficient to show the trend (see Figure 5-2).

The fold-over frequency, F_θ, reported in this research appears to be unique in the sense that it has not been found to have been reported by any other investigator. This frequency seems to be a good measure of fold-over.

*These values of P were selected purposely to exhibit the "wrong" trend.

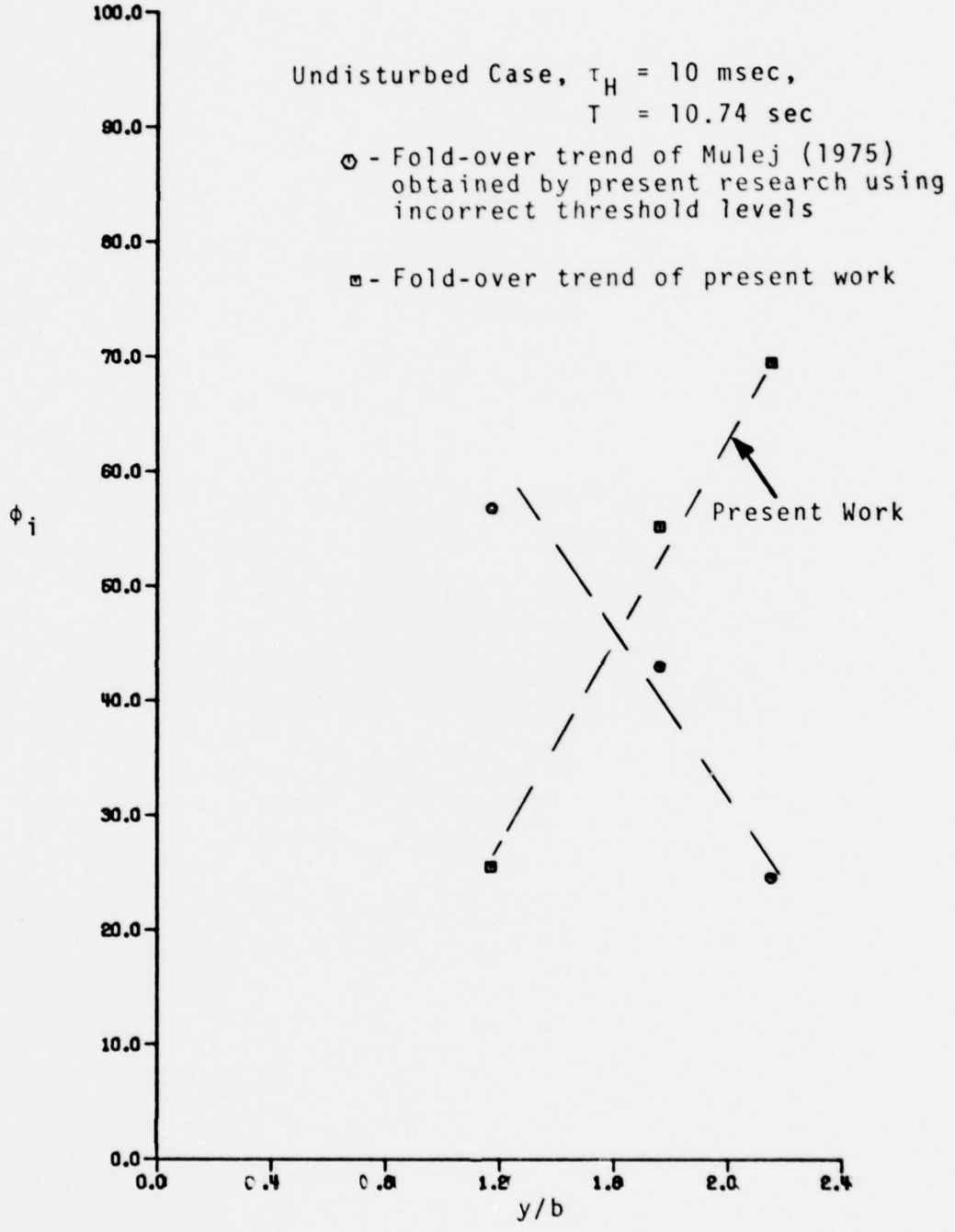

Figure 5-2. Percent Fold-Over vs. y/b.

Table 5-3. Comparing Mulej's (1975) ϕ_i: τ_H = 10 msec.

x/D	y/b	P1	P2	γ_1	$F_{\gamma 1}$	ϕ_{Front}	ϕ_{Back}	$\phi_{Average}$
55*	2.15	3.5	2.9	.098	9.78	67.62	71.43	69.52
55**	2.15	5.2	2.5	.076	5.31	22.81	26.32	24.56
55	2.15	5.2	2.9	.076	5.31	36.64	42.11	39.47
55*	1.76	1.50	1.7	.306	15.18	55.83	54.60	55.21
55**	1.76	1.75	1.7	.290	12.20	44.27	43.51	43.89
55*	1.17	.15	.45	.850	6.80	20.83	30.14	25.52
55	1.17	.8	1.3	.673	11.82	44.0	50.39	47.22
55**	1.17	.05	.45	.975	1.77	55.56	57.89	56.76

* Values used presently

** Data plotted which shows Mulej's (1975) fold-over trend.

The plot of $F_\theta/F_{\theta m}$ vs. y/b appears to approximate a Gaussian curve of the form given in equation 4-2.

It was reported earlier that Paizis and Schwarz (1974) measured the total width of the fold-over. Fold-over widths were not measured in this research. LaRue (1973), and also LaRue and Libby (1974) measured the fraction of time that there is fold-over at the downstream edge of the interface of the wake of a heated rod. They also reported that the number of fold-over events at the downstream interface edge was two to four times the value measured at the upstream interface edge. This means that fold-over is more likely to be detected at the downstream edge of the interface than at the upstream. The downstream interface edge of a wake corresponds to the back of the interface in a jet and the upstream corresponds to the front. This work also reports that fold-over is more frequent at the back than at the front of the interface, but not as much as reported by LaRue and Libby (1974).

Kohan (1969) and Paizis (1974) reported that in the plane wall jet in which they were measuring, fold-over events occurred less than 5% of the time. LaRue (1973) and LaRue and Libby (1974) reported that fold-over events occurred at the downstream edge of the interface between 0.1 to 0.5% of the time. In the present work, fold-over events were found to occur between 0.2 to 0.42% of the time. This seems to show agreement with previous workers.

b. The Acoustically Excited Jet

It was mentioned in Chapter II that no previous work has been reported concerning the effects of an acoustic disturbance on intermittency, fold-over and crossing frequency of the turbulent-nonturbulent interface of a shear flow. These measurements appear to be unique and hence are not compared with other results.

2. Possible Sources of Error and Estimates

a. Threshold Level and Hold Time

The arbitrariness used in selecting the criteria for detecting the turbulent-nonturbulent interface could lead to some error in constructing the intermittency function, I(t). The method used to select the hold time was discussed in Chapter III. It was suggested earlier that the error involved in selecting τ_H was small. This error is estimated at $\pm$ 0.5% of τ_H. However the threshold level presented some problems. A range of threshold level existed that gave relatively constant F_γ values. However, the problem was in deciding what value of threshold level to choose within the acceptable range. The calibration curve, Figure 3-28, showed that the selected threshold level was close to the start of the acceptable range. Within this acceptable range, γ varied by about 21% and F_γ by 3%. However, when the threshold level was chosen close to the start of the acceptable range of F_γ, the intermittency, γ,

varied by 3% and F_γ by 0.5%. This method of choosing the threshold level close to the start of the acceptable range of F_γ was adopted for the rest of the experiment. The uncertainty in the present data (based on the estimated error in constructing I(t)) is believed to be $\pm$3%.

b. Probe Separation, Δy

The measurement of Δy is accurate to about 0.01 in. (0.0254 cm). It was discussed in Chapter III how this separation was achieved and how Δy was chosen for fold-over measurements. The curve of ϕ_i vs. Δy was shown in Figure 3-34. Using the value of Δy (0.125 in. or 0.3175 cm), the error in measuring percent fold-over was found to be $\pm$4%. However, better results might have been obtained by taking measurements with different Δy and extrapolating the results to zero separation.

c. Errors Due to Digital Analysis

These sources of error are discussed in Appendix A. Some of those errors could be due to (1) the sampling rate, (2) total time of sampling, (3) aliasing. Other errors could be due to the calibration of the tape recorder and the choice of the differentiator circuit parameters. The differentiator circuit is discussed in Appendix C.

d. Cost Estimate

A cost estimate of using the digital computer is made here. In Chapter III, the method of selecting the threshold level was discussed. Recall that in order to select the "correct" P, different values of P were used and curves

of γ and F_γ versus P were drawn. Up to 33 different values of P had been used to plot one of those curves (however, fewer points were used in many cases). This means that the computer program, Thold 10 (see Appendix B) iterates 33 times. Of course, this was not done at one time. Ten values of P could be selected at first; then γ and F_γ could be plotted against P. The shape of the F_γ curve would decide whether to select more values of P and where to select them. The cost for each iteration is approximately $2.00. Thirty-three iterations would cost $66.00. This is for one y/b location. Fifteen locations were examined for the fold-over measurements for the undisturbed jet; nine locations were considered for the acoustically excited jet. This gives a total of 24 locations or approximately $1584.00. After the "correct" P is chosen, the fold-over program, FOLD, is used to compute the fold-over events. Each fold-over program cost approximately $2.20. This gives a total of about $52.80. The cost of using the other two programs, SKIP3 and MSQ, is approximately $200.00. The total computer cost is approximated at $1800.00. This does not include the cost encountered when each program was being developed.

3. Entrainment and Interface Slope

The phenomenon of entrainment is a feature of all free turbulent shear flows. The entrainment process is that whereby ambient nonturbulent fluid is being assimilated

by the turbulence. The exact process of this mechanism is still not fully understood. However, it is generally accepted that the originally irrotational fluid acquires vorticity by viscous diffusion and this vorticity is amplified by the rate-of-strain field. Paizis and Schwarz (1975) argue that this process must lead to a sharp interface which separates the turbulent and the nonturbulent regions. They defined the rate of entrainment of ambient fluid across a turbulent interface as the mean rate of increase of turbulent fluid in the flow direction. The flow field considered in their experiment was a two dimensional wall jet. They assumed that the interface is a continuous surface whose location is a random function of space and time.

Many researchers (Kaplan and Laufer, 1967; Kohan, 1969; Townsend, 1970; LaRue, 1973; Davies and Yule, 1974; Paizis and Schwarz, 1974; Jenkins, 1974; Mulej, 1975; and others) agree that fold-over of the interface is an important part of the entrainment mechanism. Furthermore, LaRue (1973) argues that fold-over events are intimately related to the mean interface slope. His measurements show that the mean slope at the downstream (back) interface edge is steeper than the mean slope at the upstream (front) interface edge. He attributed this to the larger number of fold-over events that were observed at the back of the interface. Mean interface slope measurements were not taken in this work. However, from the measurements taken,

the sign of the interface can be inferred. Whenever a fold-over event (fold-over type 2) occurs at the front of the interface, the interface slope is negative at that point. On the other hand the slope of the interface is positive when a fold-over event (fold-over type 4) occurs at the back of the interface. Hence the total number of fold-over events type 2 is a measure of the total number of times the front of the interface is negative at that location. Similarly, the total number of fold-over events type 4 is a measure of the total number of times the back of the interface is positive at the location considered. Finally, the total number of fold-over events type 1 and 3 is a measure of total number of times the slope of the interface is infinite at that location. Recall that the types of fold-over events were defined in Chapter III.

4. Effects of an Acoustic Disturbance

The application of an acoustic disturbance at a frequency of measurable sensitivity seems to have two effects on the flow: (1) the location at which $\gamma = 0.5$ ($\overline{\gamma}$) is reduced for the intermittency, crossing frequency and fold-over frequency curves. Recall that the widening rate of the jet increased by 8.7%. It appears that the reduction in the mean interface locations is of the same order as the

increase in the widening rate of the jet. (2) The other effect of an acoustic disturbance on the flow in the increase of the maximum crossing frequency and fold-over frequency. Although this increase could not be inferred at x/D = 35 and 55, it was clearly noticed that x/D = 45. Only three locations (and hence three data points) were examined for each x/D station. It is obvious that more data points will be needed to establish this effect at all x/D stations. At x/D = 45 where the increased was noticed, the maximum crossing frequency, $F_{\gamma m}$, increase by 5.3% and the fold-over frequency increased by 47.8%. The total percent fold-over was also increased by the acoustic disturbance. These increases are approximately: 9%, 4%, and 6% at x/D = 35, 45, and 55%, respectively. These increases are of the order of the increase in the widening rate of the jet.

The mechanism by which an acoustic wave interacts with a plane turbulent jet is still unknown. Simcox (1969) proposed that the mechanism was a direct interaction of the acoustic wave with the turbulence. Hussain and Zaman (1975) seem to believe that the interaction is at the initial region of the jet. (Recall that their acoustic excitation was at the plenum chamber.) The present work was conducted entirely in the fully developed region (and in the similarity region). The location and/or mechanism of the interaction cannot be inferred from this work. Besides, since the period between turbulent bursts were not measured, it

is difficult to infer whether the period between bursts was more structured in the presence of an acoustic excitation than in its absence. A study of this interaction is presently being conducted by Chambers (1976). The present research is related to his work.

CHAPTER VI. CONCLUSIONS AND SUGGESTIONS FOR FUTURE STUDY

The following conclusions are made based on this work:

1. The FORTRAN IV program developed for this research satisfactorily detected the turbulent-nonturbulent interface.
2. The sign of the slope of the interface can be deduced from the types of fold-over events.
3. The maximum fold-over frequencies $F_{\theta m}$ were found to be less than the maximum interface crossing frequencies, $F_{\gamma m}$.
4. The presence of fold-over, especially at the back of the interface edge, is consistent with the hypothesis that one of the entrainment mechanisms is large scale "engulfment" of the nonturbulent ambient fluid by the turbulent fluid. However, the presence of fold-over is inconsistent with the Gaussian interface model. This model assumes that there are no fold-over events at the fronts and backs of the interface (LaRue (1973)).
5. The total percent fold-over increased with the lateral location (y/b). Both the total percent fold-over and the number of fold-over events increased as the longitudinal distance (x/D) increased. This is consistent

with the suggestion (Phillips, 1972), that the slower moving eddies are responsible for the entrainment of ambient fluid. A larger number of these eddies are more likely to be found further from the mouth of the jet than close to it.

6. Fold-over events were more likely to be detected at the backs rather than the fronts of the interface.
7. An acoustic disturbance at a frequency corresponding to the first sensitive frequency was found to reduce the mean interface locations, for the intermittency, crossing frequency and fold-over frequency curves. The percent reductions were on the order of the percent increase in the widening rate of the jet. The total percent fold-over also increased and was also on the order of the percent increase in the widening rate of the jet. The maximum values of the crossing frequency and fold-over frequency were also found to increase (observed only at $x/D = 45$ where the axis of the horn was positioned).
8. In detecting the turbulent-nonturbulent interface by this method, it was convenient to select a fixed hold time and vary the threshold level. However, the decision of the detection criteria is left to the researcher.

The following are suggestions for future study.

1. The times between turbulent bursts were not computed in the work just completed. The computer program can be adjusted easily to measure this time. The number of points between the (1-0) and the following (0-1) level changes can be computed. Dividing this number by the sampling rate, the required time between bursts can be computed.
2. The probe separation, Δy, was fixed for the fold-over measurements in this work. It would be interesting to know what results would be obtained by fixing one probe location (preferably at the mean interface location, $\overline{Y}$) and varying the other probe location.
3. It might also be interesting to try using four probes instead of two. These probes can be located in pairs. One pair could be positioned at one x/D station while the other pair is positioned at another x/D station. The lateral positions should be such that two lines joining the probes are parallel and form an angle of 45° or less with the axis of the jet. This angle should be measured in the counterclockwise direction. However all the probes should be perpendicular to the flow. This exercise might help in determining the shape of the interface, and possibly the width of the fold-over region.

4. The effect of an acoustic disturbance could be examined further to check whether the percent increase in fold-over is exactly equal to the percent increase in the jet widening rate. Since this work considered only one Reynolds number, the Reynolds number could be varied in the future.
5. It was pointed out earlier that the jet widening rate decreased with increasing Reynolds number at frequencies of measurable sensitivity; it would be interesting to know whether this relationship is linear or not.

LIST OF REFERENCES

Corrsin, S., and Kistler, A.L., "Free-stream Boundaries of Turbulent Flows," NACA TN 3133, 1954. Also published in NACA Rep. 1244, 1955.

Davies, P.O.A.L., and Yule, A.J., "Coherent Structures in Turbulence," Proceedings of Colloquium on Coherent Structures in Turbulence, Southampton, March, 1974.

Favre, A.J., Gaviglio, J.J., and Dumas, R.J., "Further Space-Time Correlations of Velocity in a Turbulent Boundary Layer," JFM, 3, pp. 344-356, 1958.

Fiedler, H., and Head, G.R., "Intermittency Measurements in the Turbulent Boundary Layer," JFM, 25, part 4, pp. 719-735, 1966.

Flora, J.J., and Goldschmidt, V.W., "Virtual Origins of a Free Plane Turbulent Jet," AIAA Journal, vol. 7, no. 12, pp. 2344-2346, December, 1969.

Foss, J.J., "A Study of Incompressible Bounded Turbulent Jets," Ph.D. Thesis, Purdue University, January, 1965.

Glass, D.R., "The Effects of Acoustic Feedback on the Spread and Decay of Supersonic Jets," AIAA Journal, vol. 6, no. 10, p. 1890, October, 1968.

Goldschmidt, V.W., and Kaiser, K.F., "Interaction of an Acoustic Field and a Turbulent Plane Jet: Mean Flow Measurements," Sonochemical Engineering Symposium Series, vol. 67, no. 109, pp. 91-98, 1971.

Gortler, H., "Berechnung von Aufgaben der freien Turbulenz auf Grund eines neuen Näherungsansatzes, ZAMM, vol. 22, pp. 244-254, 1942.

Hedley, T.B., and Keffer, J.F., "Intermittency Measurements in a Turbulent Flow," Proceedings of the Fourth Canadian Congress of Applied Mechanics, Montreal, Canada, May 28-June 1, 1973.

Hedley, T.B., and Keffer, J.F., "Turbulent/Non-Turbulent Decisions in an Intermittent Flow," JFM, 64, part 4, pp. 625-644, 1974.

Heskestad, G., "Hot Wire Measurements in a Plane Turbulent Jet," Journal of Applied Mechanics, 32, pp. 721-739, December, 1965.

Hinze, J.O., Turbulence, An Introduction to Its Mechanism and Theory, McGraw-Hill Book Co., 1959.

Householder, M.K., and Goldschmidt, V.W., "Turbulent Diffusion of Small Particles in a Two-Dimensional Free Jet," Report submitted to the Nat. Sci. Foundation, Tech. Rpt. FMTR-68-3, Purdue Research Foundation 5307, pp. 132-143, 1968.

Hussain, A.K.M.F., and Zaman, K.B.M.Q., "Effect of Acoustic Excitation on the Turbulent Strcuture of a Circular Jet," Proceedings, Third Interagency Symposium on University Research in Transportation Noise, University of Utah, Salt Lake City, Utah, pp. 314-326, November 12-14, 1975.

Jenkins, P.E., and Goldschmidt, V.W., "Mean Temperature and Velocity in a Plane Turbulent Jet," ASME Transactions, Journal of Fluids Engineering, pp. 581-584, December 1973.

Jenkins, P.E., "A Study of the Intermittent Region of a Heated Two-Dimensional Plane Jet," Ph.D. Thesis, Purdue University, December, 1974.

Kaiser, K.F., "An Experimental Investigation of the Interaction of an Acoustic-Field and a Plane Turbulent Jet," MS Thesis, Purdue University, Feburary, 1971.

Kaplan, R.E., and Laufer, J., "Concerning the Large Scale Motion in the Turbulent Boundary Layer," Fourth Euromech. Colloquium "The Structure of Turbulence," Southampton, March, 1967.

Kaplan, R.E., and Laufer, J., "The Intermittently Turbulent Region of the Boundary Layer," University of Southern California, Report USCAE 110, 1968.

Kibens, V., "The Intermittent Region of a Turbulent Boundary Layer," Ph.D. Thesis, The Johns Hopkins University, 1968.

Kibens, V., and Kovasznay, L.S.G., "The Intermittent Region of a Turbulent Boundary Layer," Interim Technical Report No. 1, Department of Mechanics, The Johns Hopkins University, January, 1969.

Kibens, V., and Kovasznay, L.S.G., "Detection of the Turbulent-Non-Turbulent Interface," Interim Tech. Rept., No. 1, Dept. of Mechanics, The Johns Hopkins University, June, 1970.

Kohan, S.M., "Some Studies of the Intermittent Region and the Wall Region of a Two-Dimensional Plane Wall Jet," Ph.D. Thesis, Stanford University, 1969.

Kovasznay, L.S.G., "Structure of the Turbulent Boundary Layer," The Physics of Fluids Supplement, vol. 10, no. 9, pp. 25-30, September, 1967.

Kovasznay, L.S.G., Kibens, V., and Blackwelder, R.F., "Large Scale Motion in the Intermittent Region of a Turbulent Boundary Layer," JFM, 41, part 2, pp. 283-325, 1970.

LaRue, J.C., "The Temperature Characteristics in the Turbulent Wake of a Heated Rod," Ph.D. Thesis, University of California, San Diego, California, 1973.

LaRue, J.C., "Detection of the Turbulent-Nonturbulent Interface," The Physics of Fluids, vol. 17, no. 8, pp. 1513-1517, August, 1974.

LaRue, J.C., and Libby, P.A., "Temperature and Intermittency in the Turbulent Wake of a Heated Cylinder," The Physics of Fluids, vol. 17, no. 5, pp. 873-878, May, 1974.

Libby, P.A., "On the Prediction of Intermittent Turbulent Flows," JFM, 68, part 2, pp. 273-295, March, 1975.

Lin, C.C., Turbulent Flows and Heat Transfer, Princeton University Press, Princeton, New Jersey, 1959.

Merkine, L., and Liu, J.T.C., "On the Development of Noise-Producing Large Scale Wavelike Eddies in a Plane Turbulent Jet," JFM, vol. 70, part 2, pp. 353-368, 1975.

Miller, D.R., and Commings, B.W. "Static Pressure Distribution in the Free Turbulent Jet," JFM, 3, part 1, pp. 1-16, October, 1957.

Mulej, D.J., "Velocity and Fold-Over of the Turbulent Non-Turbulent Interface in a Plane Jet," MS Thesis, Purdue University, September, 1975.

Ott, E.S., III, "Convective velocities in a Turbulent Plane Jet," MS Thesis, Purdue University, December, 1972.

Paizis, S.T., "The Turbulent Interface," Ph.D. Thesis, The Johns Hopkins University, 1972.

Paizis, S.T., and Schwarz, W.H., "An Investigation of the Topography and Motion of the Turbulent Interface," JFM, vol. 63, part 2, pp. 315-343, 1974.

Paizis, S.T., and Schwarz, W.H., "Entrainment Rates in Turbulent Shear Flows," JFM, 68, part 2, pp. 297-308, March, 1975.

Phillips, O.M., "The Entrainment Interface," JFM, 51, part 1, pp. 97-118, 1972.

Powell, A., Ph.D. Thesis, University of Southampton, England, 1953. (Referred to by Chanaud and Powell (1962).)

Rockwell, D.O., "The Macroscale Nature of Jet Flows Subjected to Small Amplitude Periodic Disturbances," Chemical Engineering Progress Symposium Series, Lehigh University, Bethlehem, Pennsylvania, pp. 99-107, 1971.

Roffman, G.L., and Toda, K., "A Discussion of the Effects of Sound on Jets and Flueric Devices," Trans. of ASME, J. of Eng. Industry, pp. 1161-1167, November, 1969.

Schlichting, H., Boundary Layer Theory, 6th Ed., McGraw-Hill Book Co., 1968.

Schwarz, W.H., "Turbulence in Liquids," Proceedings of Symposia on Turbulence in Liquids, p. 1, 1972.

Simcox, C.D., "A Theoretical Investigation of Acoustic-Turbulent Interactions with Application to Free-Jet Spreading," Ph.D. Thesis, Purdue University, January 1969.

Simcox, C.D., and Hoglund, R.F., "Acoustic Interactions with Turbulent Jets," Trans. of the ASME, J. of Basic Engineering, vol. 93, pp. 42-46, 1971.

Spencer, B.W., "Statistical Investigation of Turbulent Velocity and Pressure Fields in a Two-Stream Mixing Layer," Ph.D. Thesis, University of Illinois, Urbana, May 1970.

Stiffler, A.K., "Signal Transit Velocities in a Turbulent Plane Jet," ASME Paper, No. 75-WA/FE-1, 1975.

Tennekes, H., and Lumley, J.L., A First Course in Turbulence, The MIT Press, Cambridge, 1972.

Thomas, R.M., "Conditional Sampling and Other Measurements in a Plane Turbulent Wake," JFM, 57, part 3, pp. 549-582, 1973.

Townsend, A.A., "Local Isotropy in the Turbulent Wake of a Cylinder," Aust. Jour. Sci. Res. Series A, vol. 2, pp. 161-174, 1948.

Townsend, A.A., "The Fully Developed Turbulent Wake of a Circular Cylinder," Aus. Jour. Sci. Res. Series A, vol. 2, pp. 451-468, 1949.

Townsend, A.A., The Structure of Turbulent Shear Flow, Cambridge University Press, 1956.

Townsend, A.A., "The Mechanism of Entrainment in Free Turbulent Flows," JFM, vol. 26, part 4, pp. 689-715, 1966.

Townsend, A.A., "Entrainment and the Structure of Turbulent Flows," JFM, 41, part 1, pp. 13-46, 1970.

Uberoi, M.S., and Freymouth, P., "Spectra of Turbulence in Wakes Behind Circular Cylinders," The Phys. of Fluids, vol. 12, no. 7, pp. 1359-1363, July, 1969.

Van der Hegge Zijnen, "Measurements of Heat and Matter in a Plane Turbulent Jet of Air," Appld. Sci. Res., vol. 7, Section A, pp. 277-292, 1957.

Weinger, S.D., "The Effect of Sound on a Reattaching Jet at Low Reynolds Numbers," Harry Diamond Laboratories Fluid Amplification Symposium, vol. IV, pp. 29-46, 1965.

Williams, K.C., "An Experimental Investigation of the Interaction of a Developing Turbulent Flow with a Longitudinally Resonant Acoustic Field in a Horizontal Pipe," Ph.D. Thesis, Purdue University, January, 1969.

Wygnanski, I., and Fiedler, H.E., "The Two-Dimensional Mixing Region," JFM, 41, part 2, pp. 327-361, 1970.

Young, M.F., "A Turbulence Study: Convective Velocities, Energy Spectra, and Turbulence Scales in a Plane Air Jet," MS Thesis, Purdue University, 1973.

APPENDICES

APPENDIX A. DIGITAL PROCESSING OF DATA

The technique used to digitize the tape recorded analog signal will be presented here. A complete block diagram of the hybrid computer used for this process will also be given. The description here will be sufficiently detailed so as to initiate future experimenters who want to use the system. The hybrid computer used in this research is located at the Electrical Engineering building. This computer is the CDC 1700. Before the actual process is described, the theory underlining discrete representation of an analog signal will be given.

1. Discrete Representation of a Recorded Analog Signal

Digitization is made up of two separate and distinct operations: (a) sampling and (b) quantization. Sampling is the process of defining the instantaneous points at which the data are to be observed. Quantization is the conversion of data values at the sampling points into numerical form. Sampling for digital data analysis is usually performed at equally spaced intervals (see Figure A-1). The sampling interval is represented by h. A problem arises in how to choose h. On one hand, sampling at points which are too close together will yield correlated and

highly redundant data, and thus, unnecessarily increase the labor and cost of calculations. On the other hand, sampling at points which are too far apart will lead to confusion between the low and high frequency components of the original data. This latter problem, called aliasing (see Figure A-2), constitutes a potential source of error which does not arise in direct analog data processing. This will be discussed further, when errors associated with digital data analysis will be given.

A continuous random record $x(t)$ to be sampled at points $\Delta t = h$ apart, can be seen in Figure A-1. The Nyquist sampling criterion is given by the relation:

$$h \leq \frac{1}{2F_c} \qquad \text{(A-1)}$$

where F_c is the Nyquist folding frequency (see Bendat and Piersol (1971)). Two practical methods exist for handling the aliasing problem. The first is to choose h sufficiently small so that it is physically unreasonable for data to exist above the associated cutoff frequency, F_c. The second method is to filter the data prior to sampling so that information above a maximum frequency of interest is no longer contained in the filtered data. Then choosing F_c equal to the highest frequency of interest will give accurate results for frequencies below F_c. This second method is recommended since it saves on computing time and costs.

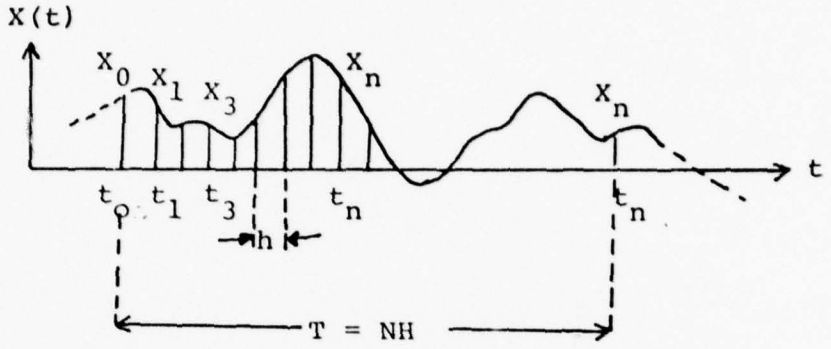

Figure A-1. Sampling of a Continuous Record.

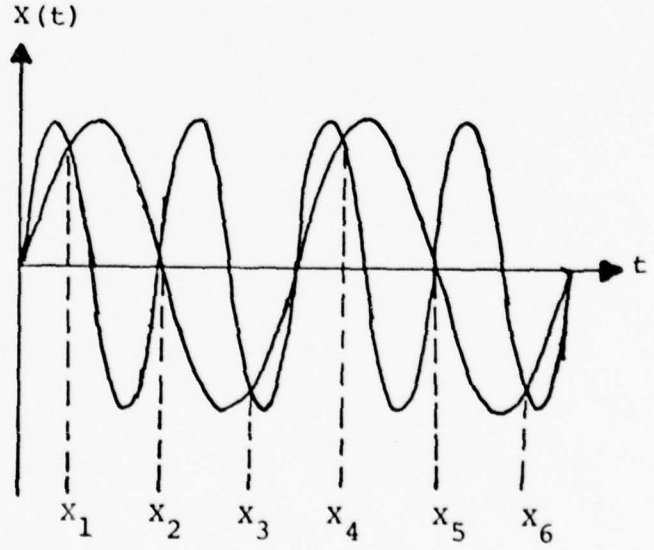

Figure A-2. Aliasing Problem.

Let $\{X_n\}$ represent a set of data values found at the N points where n = 1,2, ..., N. Then

$$t_n = t_0 + nh \qquad \text{for } n = 1, 2, \ldots, N$$

where t_0 is the initial point chosen and N is the sample size. This sample size is selected on the basis of the desired accuracy. The analog signal can now be represented by the set:

$$X_n = X(t_0 + nh) \quad n = 1, 2, \ldots, N \tag{A-2}$$

The record length, T must satisfy the equation

$$T = Nh \tag{A-3}$$

2. Analog-Digital Conversion Technique

The description of the technique used to convert an analog signal to a digital representation is presented here. Care is taken to describe the steps to be taken starting from the laboratory, where the data is tape recorded, to the hybrid computer facilities, and finally, to the computing center at the Mathematical Science building. Researchers at Purdue University who intend to digitize their data and process them in the computer will find this section extremely valuable.

In the last section, mention was made about the method to use to avoid the problem of aliasing and yet to be economical. Using that method, it would be necessary to

first filter the signal before tape recording. In this research the maximum frequency of interest was found, using a spectral analyzer, to be below 2 KHz. To see what effect filtering the signal had on the digitization process, two signals were recorded. One was low passed at 2 KHz and the other was not. No difference was observed after the digitization process. This was because the maximum frequency of the signal as obtained by the spectral analysis was below 2 KHz. It was not necessary, therefore, to filter the signal before digitizing.

The tape recorder used was an FM tape recorder model PI6104 (see Figure 3-4 in Chapter III). This was calibrated before any recording process. It should be pointed out that the hybrid computer used was capable of quantizing voltages in the range $-10V \leq V_i \leq 10V$. Any signal outside this range will be treated as $\pm$10 volts. The hybrid computer assigns a six digit number to the full scale value. The sign ($\pm$) is included in the number. Specifically, $\pm$10 volts = $\pm$32764. However if the signal is positive, the sign is assumed. If the nominal voltages of the signal were significant, they can be obtained by graphing the computer numbers against voltages. The computer number for zero voltage is zero. It is necessary, therefore, to calibrate the tape recorder so that on play back the voltages fall appreciably within $\pm$10 volts.

The block diagram of the hybrid computer system used in the digitization process is shown in Figure A-3. A simplified version of this figure was shown in Chapter III (Figure 3-5). A description of the patching process is given using Figure 3-5.

The FM tape recorder used to record the signal should be used here. The two channels were connected to the interface rack labeled Trunk 070 and 071, using the available patch cords. The Analog trunk lines labeled EAI 680 #1 should be used. This is internally connected to the digital computer. On the Patch Board, ADC-0 was connected to Trunk 070 and ADC-1 to Trunk 071, using the appropriate cords. Also on the Patch Board, a special logic cord was used to connect Sense-line-0 to Pushbutton #5. The patching process was now complete. However, the signal could be viewed on the oscilloscope provided for the purpose, since one of the oscilloscopes is internally connected to the EAI 680 #1 Analog computer. The patching could be checked by connecting Trunk 070 or 071 to Trunk 110. The signal should appear automatically on the scope if the scope was turned on and the tape recorder playing. The hybrid computer consultants should be consulted in case of problem.

The rest of the process involved reading a set of cards and manipulating the CDC 1700 console. The Teletype (1711) was used to give command to the rest of the

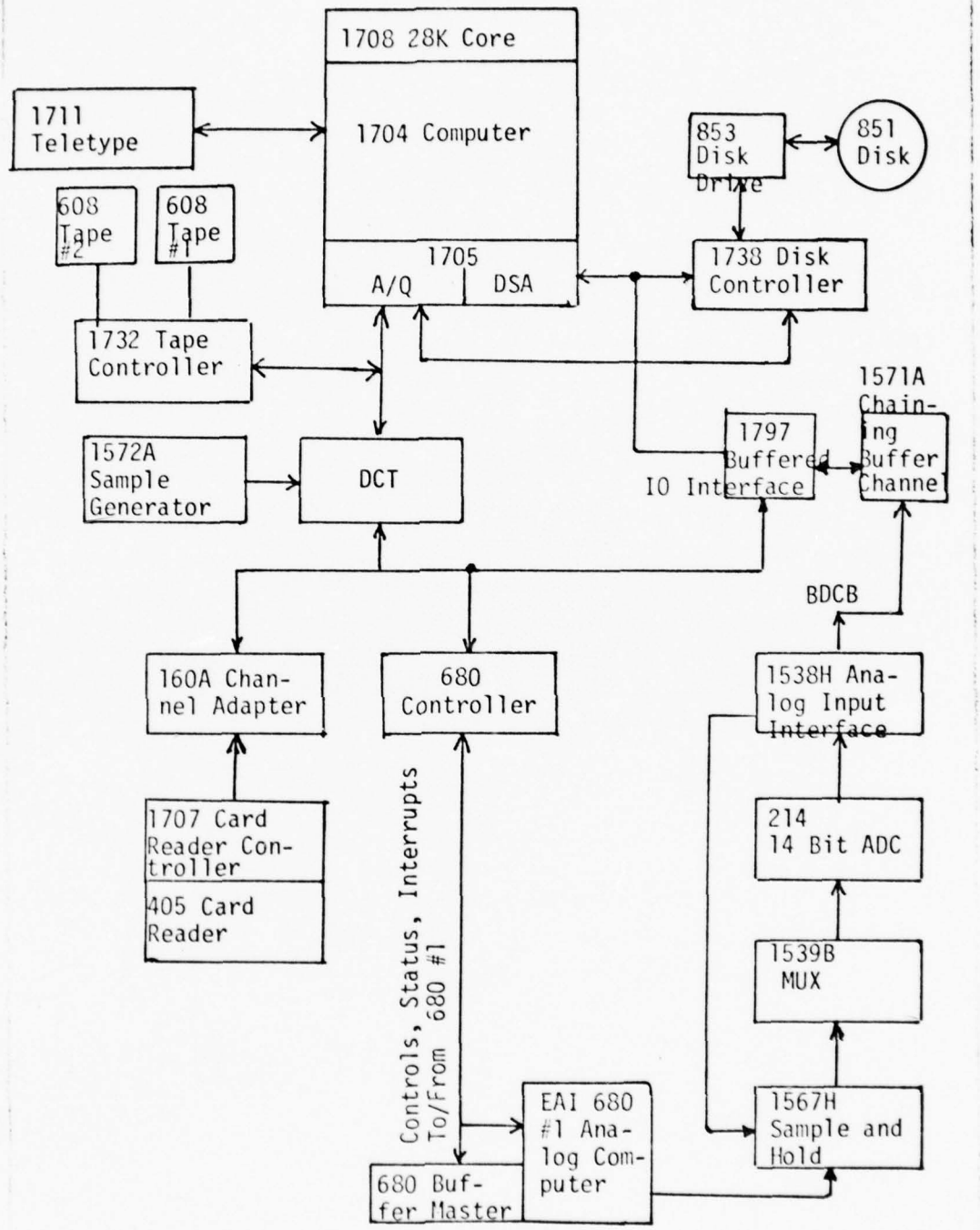

Figure A-3. Schematic of Hybrid Computer System.

equipment. A step-by-step procedure on manipulating the CDC 1700 console is available at the console shelf.

The program used to digitize the analog signal was due to the Hybrid computer consultants. The program was capable of digitizing up to 4 channels of analog data using the 1538 in conjunction with the 1571 (see Figure A-3). The program was modified to accomplish the present task. Figure A-3 will be used to describe the logic used in the program.

The hybrid system was capable of sampling at 40 KHz. The actual sampling rate was determined by the number of analog channels, NCH, and the number of 5 microsecond intervals per sample, NS. For example: Assume that two analog channels of data will be digitized, and that the maximum frequency of interest was 2 KHz. The sync pulse interval is equal to the h used in equation (A-1). So:

h = sync pulse interval

i.e., $h = NS \times 5\ \mu s$ (A-4)

Applying equation A-1:

$$h = \frac{1}{2F_c} = \frac{NS}{2 \times 10^5} \quad \text{(A-5)}$$

Since F_c was already determined in the laboratory to be 2 KHz, NS can be computed. This value, 50, is plugged into the program and the sampling rate per channel will be 1/h or 4000 samples per second. Two buffers of length 2500 words were used to store the data before writing on the

magnetic tape. Since the two analog channels were digitized simultaneously, a buffer of 2500 words will contain 1250 words per channel. It is important to know how the data is arranged in the user's buffer (the magnetic tape). Since two channels were digitized using ADC #0 and ADC #1, the output will read ADC #1 before ADC #0. However, if 4 channels were digitized using ADC #0, ADC #1, ADC #2 and ADC #3, the system will put the last unit digitized first, i.e., ADC #3 and the rest in series. So the output should be interpreted as: ADC #3, ACD #0, ADC #1 and ADC #2. Other subroutines used by this program are explained in the hybrid program documentation.

A second program was required to reformat the digitized data for CDC 6500 input. This program can also be obtained from the consultants.

3. Errors Associated with Digital Analysis

In section one, it was mentioned that one of the problems encountered in digital data analysis was that due to aliasing. Figure A-2 was drawn to illustrate this problem. Assuming the sample interval was chosen to be h, say, the sampling rate will be 1/h samples per second. However, at least two samples per cycle are required to define a frequency component in the original data. Hence, the highest frequency which can be defined by sampling at a rate of 1/h samples per second is 1/2h cps. Frequencies in the original

data above 1/2h cps will be folded back into the frequency range from 0 to 1/2h cps, and be confused with data in this lower range. This describes how aliasing arises (see Figure A-2). The methods of handling the aliasing problem were described in section one of this Appendix. Other errors of importance are: (a) Aperture error: This arises from the fact that the data sample is taken over a finite period of time rather than instantaneously; (b) Jitter: This arises from the fact that the time interval between samples can vary slightly in some random manner; and (c) Nonlinearities: This is due to many sources such as misalignment of parts, bit dropouts, quantization spacing, zero discontinuities, etc.

The errors a, b, c mentioned above cannot be corrected by the experimenter. It should be pointed out that digitization process merely approximates a continuous analog signal to discrete points. Further discussion can be found in Bendat and Piersol (1971).

APPENDIX B. THE FORTRAN IV PROGRAMS

The computer programs used to analyze the digitized analog data are presented and described here. It is obvious that after a digitization process, a means of evaluating the quality of the data is essential. Two programs were used for this purpose. They were coded SKIP3 and MSQ. SKIP3 displays any portion of the tape. This is accomplished by specifying the lines at which to start and end. Notice that in the control card that requested the tape, the parameter C was set to 60. This was because the data was in a binary coded format which used 6 bits to represent one character. There were ten characters per line in the tape. The F = E is used to describe the type of format to be used (external). A regular size magnetic tape can store up to 90 buffers of words. Each buffer contains exactly 2500 words. Since 42960 points were analyzed for each location (x/D, y/b), in the flow field, a little over 17 buffers will be required to hold these data points. However, since two channels of data were digitized simultaneously, 17 buffers would contain 8-1/2 buffers per channel. This would in effect mean that only 21480 data points were analyzed. So in order to analyze 42960 words

per channel, 34.4 buffers would be needed. Since a magnetic tape can hold up to 90 buffers, it can be seen that only four locations in the flow field can be analyzed per magnetic tape. A means of separating the data for each pair of location and to check the goodness of data points was developed. Since the properties of a sine or triangular wave were known, either of these signals was used. Hence in a magnetic tape, the first buffer was filled with either a sine wave or a triangular wave, and the negative full scale values. In the buffer containing 2500 words, 1250 words from ADC #1 would be either a sine wave, or a triangular wave, depending on which signal was connected to Trunk line 071. The other 1250 words would be from ADC #0, depending on what signal was connected to Trunk line 070. Usually nothing was connected to Trunk line 070. This would have the effect of digitizing the negative full scale value of -32764. The next 44 buffers contain data at two locations in the flow field, say ($x/D = 35$, $y_1 = 3.5$ in (8.89 cm), $y_2 = y_1 - \Delta y = 3.5 - .125 = 3.375$ in (8.5725 cm)). Recall that the probe separation was $\Delta y = 0.125$ in (0.3175 cm). Probe #1 was located at y_1, and probe #2 was located at y_2, closer to the jet center-line. So 44 buffers will contain 22 buffers for y_1 and 22 buffers for y_2. However, only 42960 points (about 17.2 buffers) were processed per channel as was already noted. The other test signals were contained in the 46th buffer, and finally 44 more buffers

contained the other pair of location in the flow field. These second test signals separate the first set of data from the second.

The FORTRAN IV program, SKIP3, lists any portion of the magnetic tape. The line number is also printed. From the printed output, the data were examined to see if an overlap of data existed. This is accomplished by noting where the test signals started and stopped. Figure B-1 is a print out of program SKIP3.

The mean square of the voltage signals were computed using the program MSQ. These mean square values, S1 and S2, were required for the programs that constructed the intermittency function, I(t), and computed the fold-over events. Due to the limitation in the core memory of the CDC 6400-6500 dual MACE system, (maximum core memory 150K), it was necessary to break the program into four parts, as given by NTIMES = 4 in the program MSQ (see Figure B-2). This program also located the maxima for each set of 42960 points. The ratio of the maxima to the mean square was computed. As discussed in Chapter III, this helped to check the goodness of the data points. If the maxima equaled the square of the full scale values $(\pm 32764)^2$, it would be obvious that the data were bad. The location at which the maxima occurred was also printed. With this information, data points surrounding this point were printed using SKIP3. Visually checking these points will show where the data became bad.

```
15114,0(1,1,2000,T40,T6,P20.
FORTRAN.
REL(300000)
REQUEST(AJAGU2,1(0),5%6,C=60,F=E)
REWIND(AJAGU2)
LOAD(LGO=BURLIB2)
EXECUTE(...,AJAGU2)
*EOR
      PROGRAM SKIP3(INPUT,OUTPUT,AJAGU2,TAPE3=AJAGU2,
     1TAPE6=OUTPUT)

         THIS PROGRAM SKIPS N LINES OF A MAGNETIC TAPE,
         THEN READS AND PRINTS DESIRED PORTIONS STARTING
         FROM N+1 LINE.

 SOUND CASE :%/D=45, YS=46
      COMMON I(10),ISTART(5),IEND(5),IDATA1(10),IDATA2(10)

      NLINE=10500
      DO 10 I=1,NLINE
      CALL READBK(3,AJAGU2,1,K)
      IF(K.LE.0) GO TO 99
10    CONTINUE

 CHOOSE THE ROWS TO BE PRINTED WITH DESIRED VALUES BY
 SPECIFYING ISTART(J) AND IEND(J).

      JLAST=2
      ISTART(1)=NLINE+1
      IEND(1)=NLINE+750
      ISTART(2)=NLINE+8000
      IEND(2)=NLINE+8750
      ISTART(3)=8750
      IEND(3)=11250

      DO 2 J=1,JLAST
      IF(J.EQ.1)GO TO 3
      II=IEND(J-1)+1
      III=ISTART(J)-1
      DO 4 K=II,III
      READ(3,33) (I(N),N=1,10)
      DO 11 N=1,10,2
11    IDATA1(N)=I(N)
      DO 12 N=2,10,2
12    IDATA2(N)=I(N)
      IF(EOF,3)99,4
 4    CONTINUE
 3    M1=ISTART(J)
      M2=IEND(J)
      DO 5 K=M1,M2
      READ(3,33) (I(N),N=1,10)
      DO 13 N=1,10,2
13    IDATA1(N)=I(N)
      DO 14 N=2,10,2
14    IDATA2(N)=I(N)
      IF(EOF,3)99,7
 7    CONTINUE
      PRINT 34,(IDATA1(N),N=1,10,2),(IDATA2(N),N=2,10,2),K
 5    CONTINUE
 2    CONTINUE
33    FORMAT(10I6)
34    FORMAT(2%,5(I6,2%),5%,5(I6,2%),I10)
98    PRINT 97
97    FORMAT(5%,*LAST FINISHED*)
```

Figure B-1. Program: SKIP3.

```
99  PRINT 95
95  FORMAT(5X,'EOF READ')
96  CONTINUE
    STOP
    END
```

Figure B-1. Continued.

```
15114,001,L200,140,103,P20.
FORTRAN.
REL(C'800)
FILE(L2V)
ATTACH(AJ2,L2V)
LOAD(GO,RUN,LB2)
EXECUTE(,,AJ2)
EOR
      PROGRAM MSQ(OUTPUT,AJAGU2,TAPE3=AJAGU2,
     1TAPE6=OUTPUT)

         THIS PROGRAM SKIPS N LINES OF A MAGNETIC TAPE,
         THEN READS AND PROCESSES DESIRED PORTIONS STARTING
         FROM N+1 LINE.

 SOUND CASE: X/D=45, Y/S=46
      COMMON I(10),V1(10780),V2(10780)

      NLINE=10300
      DO 10 I=1,NLINE
      CALL READN(3,AJAGU2,1,K)
      IF(K.LE.0) GO TO 99
10    CONTINUE


 CHOOSE THE RUNS TO BE PROCESSED WITH DESIRED VALUES BY
 SPECIFYING ISTART AND IEND.

      NLINE=2156
      MSUM1=0
      MSUM2=0
      V1MAX=0.0
      V2MAX=0.0

      NTIMES=4
      DO 77 NCOUNT=1,NTIMES
      IF(NCOUNT.EQ.1) GO TO 40
      NLINE=IEND
      ISTART=NLINE+1
      IEND=NLINE+NLINE
      M1=ISTART
      M2=IEND
      GO TO 41
40    ISTART=NLINE+1
      IEND=NLINE+NLINE
      M1=ISTART
      M2=IEND
 COMPUTE THE VARIANCE AT EACH POINT AND SUM THEM FOR ALL POINTS
41    KK=0
      LL=0
      DO 5 K=M1,M2
      READ(3,33) (I(N),N=1,10)
      DO 13 N=1,10,2
      KK=KK+1
      V1(KK)=FLOAT(I(N))**2
13    MSUM1=MSUM1+I(N)**2
      DO 14 N=2,10,2
      LL=LL+1
      V2(LL)=FLOAT(I(N))**2
14    MSUM2=MSUM2+I(N)**2
      IF(EOF,3)99,5
 5    CONTINUE
33    FORMAT(10I6)
      GO TO 96
```

Figure B-2. Program: MSQ.

```
95  FORMAT(5X,'EOF READ')
96  CONTINUE
 COMPUTE THE MEAN SQUARE OF VARIANCE SIGNAL

    KKK=NCOUNT*KK
    S1=FLOAT(MSUM1)/FLOAT(KKK)
    S2=FLOAT(MSUM2)/FLOAT(KKK)
 FIND THE LOCAL MAX. OF VARIANCE SIGNAL
42  DO 11 N=1,KK
    IF(V1(N).LE.V1MAX) GO TO 18
    V1MAX=V1(N)
    NCHECK1=N
18  IF(V2(N).LE.V2MAX) GO TO 11
    V2MAX=V2(N)
    NCHECK2=N
11  CONTINUE

    RATIO1=SQRT(V1MAX/S1)
    RATIO2=SQRT(V2MAX/S2)

    NSAMPL=NTIMES*(KK-40)
    NRATE=4000
    T=FLOAT(NSAMPL)/FLOAT(NRATE)

    IF(NCOUNT.NE.NTIMES) GO TO 76
    PRINT 8,NSAMPL,NRATE,T,S1,S2
 8  FORMAT(///,5X,'TOTAL SAMPLES PER CHANNEL =',I10,2X,'SAMPLING-RATE
   1=',I8,2X,'TOTAL TIME =',F8.4,2X,'SECS',//,5X,'MEAN SQUARE :1 =',
   2F15.2,5X,'MEAN SQUARE :2 =',F15.2)
76  CONTINUE

    PRINT 35,V1MAX,V2MAX,NCHECK1,NCHECK2,RATIO1,RATIO2,NCOUNT
77  CONTINUE

35  FORMAT(//,5X,'V1MAX =',F15.1,10X,'V2MAX =',F15.1,//,5X,
   1'MAXIMUM POINT:1 =',I10,10X,'MAXIMUM POINT:2 =',I10,/,5X,
   2'MAX :1/RMS =',F6.2,2X,'MAX :2/RMS =',F6.2,10X,'NCOUNT =',I2)
    STOP
    END
```

Figure B-2. Continued.

After checking the data points and computing the mean square values, S1 and S2, the next step involved finding the correct threshold level to use in order to construct the "correct" intermittency function, I(t). This exercise is performed using the program THOLD10. The ratio of the threshold level to the mean square was given by P = TH1/S1 or P = TH2/S2 (see Figure B-3). This program varies P at will. For each P, the I(t) function is constructed. The hold time was varied by the equation:

$$MM = KK - NT \tag{B-1}$$

where KK denotes the number of points examined, and NT denotes the number of points that govern the hold time parameter. If NT = 0, the hold time will be zero and if NT = 40, the hold time will be computed by:

$$\tau_H = \frac{40}{NRATE} = .01 \text{ sec} = 10 \text{ msec} \tag{B-2}$$

where NRATE is the sample rate which was determined to be 4000 samples /sec. Notice that if NT = 20, the hold time, τ_H, will be equal to 5 msec. This was how the program varied τ_H. When the correct τ_H was obtained, 10 msec, NT was set equal to 40 for the rest of the experiment.

The intermittency function, I(t), was formed within the "DO LOOP":

$$DO\ 20\ N = 1, MM \tag{B-3}$$

(see Figure B-3). Essentially, the program compares a given

```
15114,0*1,CM50000,L2000,T200,TC3,P20,TU0000.
FUNCTION.
RFL(22000)
REQUEST(AJAGU2,1605,556,C=60,F=E)
REWIND(AJAGU2)
LOAD(LGO,RUNLIB2)
EXECUTE(,,AJAGU2)
+EOR
      PROGRAM THOLD10(OUTPUT,AJAGU2,TAPE3=AJAGU2,
     1TAPE6=OUTPUT)

          THIS PROGRAM SKIPS N LINES OF A MAGNETIC TAPE,
          THEN READS AND PROCESSES DESIRED PORTIONS STARTING
          FROM N+1 LINE.

 SOUND CASE : X/D=35, YS=46
      COMMON I(10),V1(10780),V2(10780)

      P=-0.2
      DO 75 NIT=1,5
      P=P+.3
      IF(NIT.EQ.1) GO TO 74
      REWIND 3

74    NLINE=300
      DO 10 I=1,NLINE
      CALL READH(3,AJAGU2,1,K)
      IF(K.LE.0) GO TO 99
10    CONTINUE


 CHOOSE THE ROWS TO BE PROCESSED WITH DESIRED VALUES BY
 SPECIFYING ISTART AND IEND.

      NLINE=2156
      J1=0
      J2=0
      F1=0.
      F2=0.

      NTIMES=4
      DO 77 NCOUNT=1,NTIMES
      IF(NCOUNT.EQ.1) GO TO 40
      NLINE=IEND
      ISTART=NLINE+1
      IEND=NLINE+NLINE
      M1=ISTART
      M2=IEND
      GO TO 41
40    ISTART=NLINE+1
      IEND=NLINE+NLINE
      M1=ISTART
      M2=IEND
 COMPUTE THE VARIANCE
41    KK=0
      LL=0
      DO 5 K=M1,M2
      READ(3,33) (I(N),N=1,10)
      DO 13 N=1,10,2
      KK=KK+1
13    V1(KK)=FLOAT(I(N))**2
      DO 14 N=2,10,2
      LL=LL+1
14    V2(LL)=FLOAT(I(N))**2
```

Figure B-3. Program: THOLD10.

```
 5  CONTINUE
33  FORMAT(1016)
    GO TO 96
99  PRINT 95
95  FORMAT(5X,'EOF READ')
96  CONTINUE

    S1=304240.07
    S2=374832.59
    TH1=P*S1
    TH2=P*S2
    NT=40
    MM=KK-NT
    NSAMPL=NTIMES*MM
    NRATE=4000
    T=FLOAT(NSAMPL)/FLOAT(NRATE)

    IF(NCOUNT.NE.1) GO TO 43
    PRINT 8,NSAMPL,NRATE,T,S1,S2,P
 8  FORMAT(///,5X,'TOTAL SAMPLES PER CHANNEL =',I10,2X,'SAMPLING-RATE
   1=',I8,2X,'TOTAL TIME =',F8.4,2X,'SEC'//,5X,'MEAN SQUARE :1 =',
   2F15.2,5X,'MEAN SQUARE:2 =',F15.2,10X,'THRESHOLD/MEAN SQ. =',F5.3)
43  DO 20 N=1,MM
    IF(N.NE.1) GO TO 21
    IF(V1(N).GE.TH1) GO TO 22
    DO 60 JJ=1,40
60  IF(V1(N+JJ).GE.TH1) GO TO 22
    GO TO 23
22  V1(N)=1.
    J1=J1+1
    GO TO 24
23  V1(N)=0.
24  IF(V2(N).GE.TH2) GO TO 25
    DO 61 JJ=1,40
61  IF(V2(N+JJ).GE.TH2) GO TO 25
    GO TO 26
25  V2(N)=1.
    J2=J2+1
    GO TO 20
26  V2(N)=0.
    GO TO 20
21  IF(V1(N).GE.TH1) GO TO 27
    IF(V1(N-1).NE.0.) GO TO 28
    V1(N)=0.
    GO TO 29
28  DO 62 JJ=1,40
62  IF(V1(N+JJ).GE.TH1) GO TO 27
    GO TO 30
27  V1(N)=1.
    J1=J1+1
    GO TO 29
30  V1(N)=0.
    F1=F1+1.
29  IF(V2(N).GE.TH2) GO TO 31
    IF(V2(N-1).NE.0.) GO TO 32
    V2(N)=0.
    GO TO 20
32  DO 63 JJ=1,40
63  IF(V2(N+JJ).GE.TH2) GO TO 31
    GO TO 34
31  V2(N)=1.
    J2=J2+1
    GO TO 20
34  V2(N)=0.
```

Figure B-3. Continued.

```
      F2=F2+1.
   20 CONTINUE
   77 CONTINUE

      Y1=FLOAT(J1)/FLOAT(NSAMPL)
      Y2=FLOAT(J2)/FLOAT(NSAMPL)
      FY1=F1/T
      FY2=F2/T

      PRINT 35,TH1,TH2,J1,J2,Y1,Y2,F1,F2,FY1,FY2

   35 FORMAT(//,5X,'THRESHOLD-LEVEL:1 =',F15.3,
     35X,'THRESHOLD:2 =',F15.3,/,5X,'TURBULENT SAMPLES:1 =',I10,5X,
     4'TURB SAMPLES:2 =',I10,5X,'INTERMITTENCY FACTOR:1 =',F5.3,5X,
     5'INT FACTOR:2 =',F5.3,/,5X,'LEVEL CHANGES:1 (1-0) =',F10.0,5X,
     6'L-CHANGES:2 (1-0) =',F10.0,/,5X,'CROSSING FREQ.:1 =',F10.2,5X,
     7'CROSSING FREQUENCY:2 =',F10.2////)
   75 CONTINUE
      STOP
      END
```

Figure B-3. Continued.

point, V1(N) to the threshold level, TH1. If

$$V1(N) \geq TH1, \quad V1 = 1 \tag{B-4}$$

Otherwise V1(N) will not be allowed to change level until it passes the hold time criterion. This criterion checks 40 future points to see if any of them is greater than TH1. If all of the 40 points are each less than TH1, V1(N) will be set equal to zero. Recall that the 40 points were tantamount to a hold time of 10 msec. Notice from the program that before the hold time criterion is applied to the point, V1(N), it first checks the value assigned to V1(N-1). Obviously, if V1(N-1) = 0, V1(N) would automatically be set equal to zero. This is because in order to set V1(N-1) = 0, V1(N) was found to be less than TH1. The hold time criterion is applied to V1(N) only when V1(N-1) = 1. The obvious question would be: What happens when N = 1?; that is, when the first point is examined since the computer "blows up" at V1(0). The program accounts for this by checking if N = 1. This time it compares V1(N), which is V1(1), to TH1. If V1(1) $\geq$ TH1, V1(1) = 1. Otherwise, the hold time criterion will be applied.

The program, THOLD10, computes γ and F_γ for each value of P. As was discussed in Chapter III, curves of γ and F_γ vs. P are drawn to determine the range of P where F_γ remains relatively constant and γ begins to approach an asymptotic value. From these curve, the "correct" P is chosen.

As soon as the "correct" P is selected (actually P1 and P2 for channels 1 and 2, respectively) the values are plugged into the fold-over program, FOLD. The logic in choosing the type of fold-over event was discussed in Chapter III and will not be repeated here. A listing of program, FOLD is shown in Figure B-4. Tables B-1 and B-2 show the values used to plot γ and F_γ vs. y/b for the undisturbed and acoustically excited cases, respectively.

```
1SIII,OCT,L2000,T40,IC3,P20.
FORTRAN.
REL,270000
FILES(L2V)
ATTACH(AJ1,L2V)
LDR(LGO,MUNLIB2)
EXECUTE(,,AJ1)
+EOR
      PROGRAM FOLD(OUTPUT,AJAGU2,TAPE3=AJAGU2,
     1TAPE6=OUTPUT)

          THIS PROGRAM SKIPS N LINES OF A MAGNETIC TAPE,
          THEN READS AND PROCESSES DESIRED PORTIONS STARTING
          FROM N+1 LINE.

 NO SOUND CASE: X/D=55, YS=47.0
      COMMON I(10),V1(10780),V2(10780)

      NLINE=10800
      DO 10 I=1,NLINE
      CALL READH(3,AJAGU2,1,K)
      IF(K.LE.0) GO TO 99
10    CONTINUE


 CHOOSE THE ROWS TO BE PROCESSED WITH DESIRED VALUES BY
 SPECIFYING ISTART AND IEND.

      NLINE=2156
      J1=0
      J2=0
      F1=0.
      F2=0.

      NTIMES=4
      DO 77 NCOUNT=1,NTIMES
      IF(NCOUNT.EQ.1) GO TO 40
      NLINE=IEND
      ISTART=NLINE+1
      IEND=NLINE+NLINE
      M1=ISTART
      M2=IEND
      GO TO 41
40    ISTART=NLINE+1
      IEND=NLINE+NLINE
      M1=ISTART
      M2=IEND
 COMPUTE THE VARIANCE AT EACH POINT
41    KK=0
      LL=0
      DO 5 K=M1,M2
      READ(3,33) (I(N),N=1,10)
      DO 13 N=1,10,2
      KK=KK+1
13    V1(KK)=FLOAT(I(N))**2
      DO 14 N=2,10,2
      LL=LL+1
14    V2(LL)=FLOAT(I(N))**2
      IF(EOF,3)99,5
 5    CONTINUE
33    FORMAT(10I6)
      GO TO 96
99    PRINT 95
95    FORMAT(5X,'EOF READ')
```

Figure B-4. Program: FOLD.

```
      S1=70161.75
      S2=112261.74
      P1=2.4
      P2=2.2
      TH1=P1*S1
      TH2=P2*S2
      NT=40
      MM=LK-NT
      NSAMPL=NTIMES*MM
      NRATE=4000
      T=FLOAT(NSAMPL)/FLOAT(NRATE)

      IF(NCOUNT.NE.1) GO TO 43
      PRINT 8,NSAMPL,NRATE,T,S1,S2
    8 FORMAT(///,5X,'TOTAL SAMPLES PER CHANNEL =',I10,2X,'SAMPLING-RATE
     1=',I8,2X,'TOTAL TIME =',F8.4,2X,'SECS',///,5X,'MEAN SQUARE :1 =',
     2F15.2,5X,'MEAN SQUARE :2 =',F15.2)
   43 DO 20 N=1,MM
      IF(N.NE.1) GO TO 21
      IF(V1(N).GE.TH1) GO TO 22
      DO 60 JJ=1,40
   60 IF(V1(N+JJ).GE.TH1) GO TO 22
      GO TO 23
   22 V1(N)=1.
      J1=J1+1
      GO TO 24
   23 V1(N)=0.
   24 IF(V2(N).GE.TH2) GO TO 25
      DO 61 JJ=1,40
   61 IF(V2(N+JJ).GE.TH2) GO TO 25
      GO TO 26
   25 V2(N)=1.
      J2=J2+1
      GO TO 20
   26 V2(N)=0.
      GO TO 20
   21 IF(V1(N).GE.TH1) GO TO 27
      IF(V1(N-1).NE.0.) GO TO 28
      V1(N)=0.
      GO TO 29
   28 DO 62 JJ=1,40
   62 IF(V1(N+JJ).GE.TH1) GO TO 27
      GO TO 30
   27 V1(N)=1.
      J1=J1+1
      GO TO 29
   30 V1(N)=0.
      F1=F1+1.
   29 IF(V2(N).GE.TH2) GO TO 31
      IF(V2(N-1).NE.0.) GO TO 32
      V2(N)=0.
      GO TO 20
   32 DO 63 JJ=1,40
   63 IF(V2(N+JJ).GE.TH2) GO TO 31
      GO TO 34
   31 V2(N)=1.
      J2=J2+1
      GO TO 20
   34 V2(N)=0.
      F2=F2+1.
   20 CONTINUE

  FOLD-OVER ANALYSIS:FRONT AND BACK OF THE INTERFACE
```

Figure B-4. Continued.

AD-A071 262 PURDUE UNIV LAFAYETTE IND RAY W HERRICK LABS F/G 20/4
FOLD-OVER, INTERMITTENCY AND CROSSING FREQUENCY OF A PLANE JET --ETC(U)
FEB 77 C O AJAGU, V W GOLDSCHMIDT N00014-67-A-0226-0025
UNCLASSIFIED HL-76-22 NL

3 OF 3
AD A071262

END
DATE FILMED
8-79
DDC

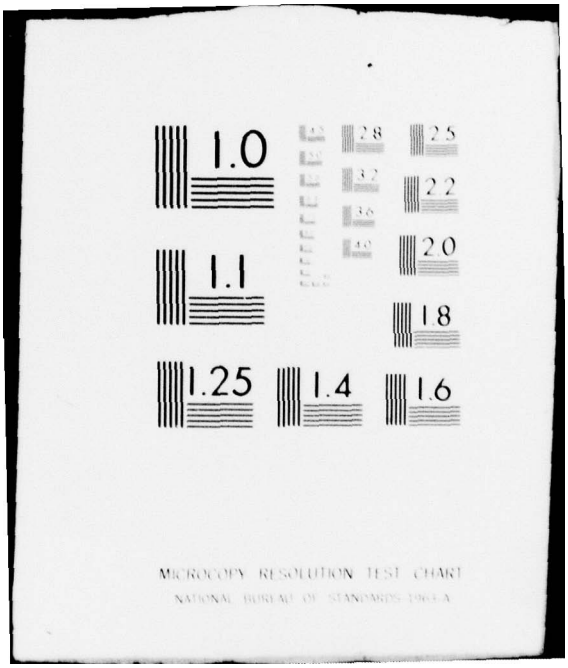
1.0
1.1
1.25
1.4
1.6
2.8
2.5
3.2
2.2
3.6
2.0
4.0
1.8
MICROCOPY RESOLUTION TEST CHART
NATIONAL BUREAU OF STANDARDS-1963-A

```
      IF(NCOUNT.NE.1) GO TO 49
      NFOLD1=0
      NFOLD2=0
      NFOLD3=0
      NFOLD4=0
      NOFOLD1=0
      NOFOLD2=0
      NCHECK1=0
      NCHECK2=0
      NWHAT=0
   49 CONTINUE
      PRINT 65
   65 FORMAT(///,10X,≠FOLD-OVER:FRONT≠,6X,≠FOLD-OVER:BACK≠,5X,
     1≠NO FOLD:FRONT≠,4X,≠NO FOLD:BACK≠)
      PRINT 66
   66 FORMAT(/,9X,≠TYPE:1≠,5X,≠TYPE:2≠,4X,≠TYPE:3≠,4X,≠TYPE:4≠,4X,
     1≠TYPE:5≠,11X,≠TYPE:6≠)
      DO 80 N=2,MM
      IF(V1(N).EQ.1..AND.V1(N-1).EQ.0.) GO TO 50
      GO TO 51
   50 IF(V2(N).EQ.1.) GO TO 52
      NTYPE2=2
      NFOLD2=NFOLD2+1
      NTYPE1=0
      NTYPE3=0
      NTYPE4=0
      NTYPE5=0
      NTYPE6=0
      GO TO 79
   52 IF(V2(N-1).EQ.0.) GO TO 53
      NTYPE5=5
      NOFOLD1=NOFOLD1+1
      NTYPE1=0
      NTYPE2=0
      NTYPE3=0
      NTYPE4=0
      NTYPE6=0
      GO TO 79
   53 NTYPE1=1
      NFOLD1=NFOLD1+1
      NCHECK1=N
      NTYPE2=0
      NTYPE3=0
      NTYPE4=0
      NTYPE5=0
      NTYPE6=0
      GO TO 79
   51 IF(V1(N).EQ.0..AND.V1(N-1).EQ.1.) GO TO 54
      GO TO 80
   54 IF(V2(N).EQ.0.) GO TO 56
      NTYPE6=6
      NOFOLD2=NOFOLD2+1
      NTYPE1=0
      NTYPE2=0
      NTYPE3=0
      NTYPE4=0
      NTYPE5=0
      GO TO 79
   56 IF(V2(N-1).EQ.1.) GO TO 57
      NTYPE4=4
      NFOLD4=NFOLD4+1
      NTYPE1=0
      NTYPE2=0
      NTYPE3=0
```

Figure B-4. Continued.

```
      NTYPE5=0
      NTYPE6=0
      GO TO 79
   57 NTYPE3=3
      NFOLD3=NFOLD3+1
      NCHECK2=N
      NCHECK3=NCHECK2-NCHECK1
      IF(NCHECK3.EQ.1) NUMAT=NUMAT+1
      NTYPE1=0
      NTYPE2=0
      NTYPE4=0
      NTYPE5=0
      NTYPE6=0
   79 CONTINUE
      PRINT 64,NTYPE1,NTYPE2,NTYPE3,NTYPE4,NTYPE5,NTYPE6
   80 CONTINUE
   64 FORMAT(11X,I2,9X,I2,8X,I2,8X,I2,8X,I2,15X,I2)
      IF(NCOUNT.NE.NTIMES) GO TO 77

      NFRONT=NFOLD1+NFOLD2+NOFOLD1
      NBACK=NFOLD3+NFOLD4+NOFOLD2
      PRINT 67,NFOLD1,NFOLD2,NFOLD3,NFOLD4,NOFOLD1,NOFOLD2,
     1NUMAT,NFRONT,NBACK
   67 FORMAT(//,5X,'SUM TYPE:1 =',I3,2X,'SUM TYPE:2 =',I3,2X,
     1'SUM TYPE:3 =',I3,2X,'SUM TYPE:4 =',I3,2X,'SUM NO FOLD:FRONT ='
     2I5,2X,'SUM NO FOLD:BACK =',I5,/,5X,'SUM OF THE STRANGE EVENT ='
     3,I5,2X,'SUM OF FRONT EVENTS =',I5,2X,'SUM OF BACK EVENTS =',I5/)
   77 CONTINUE

      Y1=FLOAT(J1)/FLOAT(NSAMPL)
      Y2=FLOAT(J2)/FLOAT(NSAMPL)
      FY1=F1/T
      FY2=F2/T

      PRINT 35,TH1,TH2,J1,J2,Y1,Y2,F1,F2,FY1,FY2

   35 FORMAT(//,5X,'THRESHOLD-LEVEL:1 =',F15.3,
     35X,'THRESHOLD:2 =',F15.3,/,5X,'TURBULENT SAMPLES:1 =',I10,5X,
     4'TURB SAMPLES:2 =',I10,5X,'INTERMITTENCY FACTOR:1 =',F5.3,5X,
     5'INT FACTOR:2 =',F5.3,/,5X,'LEVEL CHANGES:1 (1-0) =',F10.0,5X,
     6'L-CHANGES:2 (1-0) =',F10.0,/,5X,'CROSSING FREQ.:1 =',F10.2,5X,
     7'CROSSING FREQUENCY:2 =',F10.2////)
      STOP
      END
```

Figure B-4. Continued.

Table B-1. Values for γ and F_γ vs. y/b: Undisturbed Case.

x/D	$P = C/S'^2$	b(in)	y/b	γ	$F_\gamma(sec^{-1})$	$F_{\gamma max}(sec^{-1})$	$F_\gamma/F_{\gamma max}$
35	.25	1.6422	.840	.987	.93	17.4	.053
	.15		.913	.978	1.68		.097
	1.3		1.450	.658	14.90		.856
	.62		1.520	.617	16.01		.920
	2.2		1.750	.353	16.76		.963
	2.4		1.830	.294	14.90		.856
	3.0		2.060	.165	10.80		.621
	3.0		2.130	.136	9.12		.524
	5.4		2.660	.019	2.70		.155
	3.2		2.740	.015	1.77		.102
45	.28	2.1022	.654	.982	1.40	16.0	.088
	.28		.714	.973	2.05		.128
	1.42		1.130	.900	6.80		.425
	.35		1.190	.851	6.70		.419
	1.15		1.610	.502	15.83		.989
	.65		1.660	.446	13.04		.815
	1.34		2.080	.140	9.68		.605
	3.05		2.140	.127	6.15		.384
	6.6		2.560	.025	5.49		.343
	7.0		2.620	.015	4.47		.279
55	.28	2.5622	.930	.947	3.35	18.0	.186
	.18		.980	.933	4.56		.253
	.45		1.120	.916	6.42		.357
	.15		1.170	.850	6.80		.378
	.44		1.320	.796	11.92		.662
	.28		1.370	.763	14.71		.817
	1.70		1.710	.379	17.78		.988
	1.50		1.760	.306	18.08		.843
	3.5		2.150	.098	9.78		.543
	2.9		2.100	.123	12.76		.709

Table B-2. Values for γ and F_γ vs. y/b: Acoustically Excited Jet.

x/D	b(in)	y/b	γ	F_γ (sec^{-1})	$F_{\gamma max}$(sec^{-1})	$F_\gamma/F_{\gamma max}$	$P = C/S'^2$
35	1.8625	1.01	.884	6.80	17.4	0.39	.6
		1.07	.867	7.08		0.41	.4
		1.54	.511	15.83		0.91	.95
		1.61	.465	14.99		0.86	.50
		1.81	.240	13.41		0.77	1.8
		1.88	.235	10.52		0.60	1.1
45	2.3625	1.01	.886	6.33	16.85	0.38	.4
		1.06	.869	6.70		0.40	.15
		1.43	.542	16.85		1.00	1.0
		1.48	.522	13.31		0.79	.4
		1.85	.158	10.89		0.65	2.6
		1.90	.155	7.54		0.45	2.4
55	2.8625	1.0	.849	8.66	18.0	0.48	.5
		1.05	.798	8.94		0.50	.2
		1.18	.765	12.85		0.71	.7
		1.22	.733	9.59		0.53	.25
		1.53	.346	14.90		0.83	1.6
		1.57	.329	13.22		0.73	1.7

Table B-3. Percent Fold-Over: Undisturbed Case.

x/D	y/b	Y	ϕ_i Front	ϕ_i Back	ϕ_i Average
	0.913	0.978	16.67	27.78	22.22
	1.52	0.617	40.35	33.14	36.73
35	1.83	0.294	29.56	39.38	34.48
	2.13	0.136	43.30	39.80	41.54
	2.74	0.015	63.16	78.95	71.05
	0.714	0.973	22.73	36.36	29.55
	1.19	0.851	30.56	16.67	23.61
45	1.66	0.446	28.78	40.71	34.77
	2.14	0.127	64.18	62.12	63.16
	2.62	0.015	80.85	81.25	81.05
	0.98	0.933	30.61	40.82	35.71
	1.37	0.763	45.51	46.84	46.18
55	1.17	0.850	20.83	30.14	25.52
	1.76	0.306	55.83	54.60	55.21
	2.15	0.098	67.62	71.43	69.52

Table B-4. Percent Fold-Over: Acoustically Excited Case: F = 1149 Hz, spl = 105 dB.

x/D	y/b	Y	ϕ_i Front	ϕ_i Back	ϕ_i Average
	1.07	0.867	29.33	30.26	29.80
35	1.61	0.465	38.27	40.99	39.63
	1.88	0.235	43.75	49.56	46.67
	1.06	0.869	39.44	31.94	35.66
45	1.48	0.522	54.93	47.55	51.22
	1.90	0.155	48.15	66.67	57.41
	1.05	0.798	31.58	33.33	32.46
55	1.22	0.733	34.65	36.89	35.78
	1.57	0.329	57.14	55.63	56.38

Table B-5. Fold-Over Frequency: Undisturbed Case.

x/D	T (sec)	$F_{\gamma m}$ (sec^{-1})	$F_{\theta m}$ (sec^{-1})	F_θ Front (sec^{-1})	F_θ Back (sec^{-1})	F_θ Average (sec^{-1})	y/b	γ	$F_\theta/F_{\gamma m}$	$F_\theta/F_{\theta m}$
				0.28	0.47	0.74	0.913	0.978	0.04	0.06
				6.42	5.31	11.73	1.52	0.617	0.67	0.98
35	10.74	17.4	~12.0	4.38	5.87	10.24	1.83	0.294	0.59	0.85
				3.91	3.63	7.54	2.13	0.136	0.43	0.63
				1.12	1.40	2.51	2.74	0.015	0.14	0.21
				0.47	0.74	1.21	0.714	0.973	0.08	0.13
				2.05	1.12	3.17	1.19	0.851	0.20	0.34
45	10.74	16.0	~ 9.2	3.72	5.31	9.03	1.66	0.446	0.56	0.98
				4.00	3.82	7.82	2.14	0.127	0.49	0.85
				3.54	3.63	7.17	2.62	0.015	0.45	0.78
				1.4	1.86	3.26	0.98	0.933	0.18	0.19
				1.4	2.05	3.45	1.17	0.850	0.19	0.20
55	10.74	18.0	~17.6	6.61	6.89	13.50	1.37	0.763	0.75	0.77
				8.47	8.29	16.76	1.76	0.306	0.93	0.95
				6.61	6.98	13.59	2.15	0.098	0.76	0.77

Table B-6. Fold-Over Frequency: Acoustically Excited Case.

x/D	T (sec)	F_θ Front (sec^{-1})	F_θ Back (sec^{-1})	F_θ Average (sec^{-1})	y/b	γ	$F_{\theta m}$ (sec^{-1})	$F_\theta/F_{\theta m}$
35	10.74	2.05	2.14	4.19	1.07	0.867	12.0	0.33
		5.77	6.15	11.92	1.61	0.465		0.95
		4.56	5.21	9.78	1.88	0.235		0.78
45	10.74	2.61	2.14	4.75	1.06	0.869	13.6	0.35
		7.26	6.33	13.59	1.48	0.522		1.0
		3.63	5.03	8.66	1.90	0.155		0.64
55	10.74	2.79	2.98	5.77	1.05	0.798	17.6	0.32
		3.26	3.54	6.80	1.22	0.733		0.38
		7.45	7.36	14.8	1.57	0.329		0.82

APPENDIX C. THE DIFFERENTIATOR CIRCUIT

The differentiator circuit used to differentiate the hot-wire voltages is described here. When the circuit was constructed, a known signal, sine wave, was passed through it to see if a cosine wave was constructed. When a satisfactory combination of resistors and capacitors was found, the values were held constant for the rest of the experiment.

The differentiator circuit used is shown in Figure C-1.

The input impedance, Z_i, is given by the equation:

$$Z_i(\omega) = R_1 + \frac{1}{j\omega c} \qquad \text{(C-1)}$$

Where R_i and c are the resistor and capacitor, ω is frequency, and j is a complex number defined by $j = \sqrt{-1}$. The feedback impedance is

$$Z_f(\omega) = R_2 \qquad \text{(C-2)}$$

Using the Laplace variable, s, equations (C-1) and (C-2) can be written as

$$Z_i(s) = R_1 + \frac{1}{sc} \qquad \text{(C-3)}$$

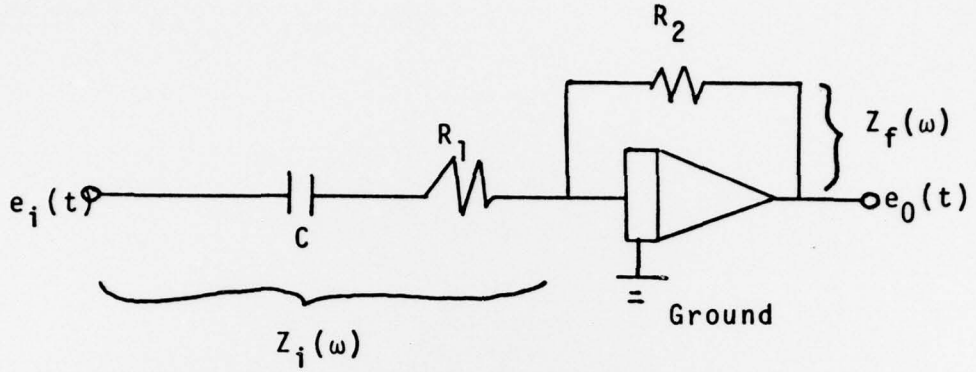

Figure C-1. Schematic of Approximate Differentiator.

and

$$Z_f(s) = R_2 \tag{C-4}$$

Using this notation, the Transfer Function for the circuit is given by

$$TF(s) = \frac{e_o(s)}{e_i(s)} = - \frac{Z_f(s)}{Z_i(s)}$$

$$= - \frac{R_2}{R_1 + \frac{1}{cs}} = - \frac{(R_2c)s}{(R_1c)s + 1} \tag{C-5}$$

Letting $j\omega = s$, equation C-5 becomes

$$TF(\omega) = - \frac{(R_2c)\ (j\omega)}{[(R_1c)\ (j\omega) + 1]} \tag{C-6}$$

The combination R_2c is known as the constant element, j is known as the differentiator element. The break frequency, or cutoff frequency, is defined by:

$$\omega_b = \frac{1}{R_1C} \tag{C-7}$$

Taking the magnitude of TF, we get

$$|TF(\omega)| = \frac{R_2c\ \omega}{\left[\left(\frac{\omega}{\omega_b}\right)^2 + 1\right]^{1/2}} \tag{C-8}$$

for $\omega = \omega_b$, we get

$$|TF(\omega)| = \frac{R_2c\ \omega_b}{\sqrt{2}}$$

For $\omega << \omega_b$, we get

$$|TF(\omega)| = R_2 c \ \omega$$

For $\omega >> \omega_b$:

$$|TF(\omega)| = R_2 c \ \omega_b$$

A sketch of $|TF(\omega)|$, showing the approximate differentiator range of application, can be seen in Figure C-2. It can be seen that for frequencies less than ω_b the circuit will act as a good differentiator circuit. The value of ω_b recommended is:

$$\omega_b \simeq 10 \text{ x highest frequency of interest.}$$

As was previously mentioned, this highest frequency was 2 KHz. Hence, $\omega_b = \frac{1}{R_1 c} = 20$ KHz. The values of R_1, R_2 and c used were: $R_1 = 7.5$ k, $R_2 = 750$ k, and c = 0.001 μf.

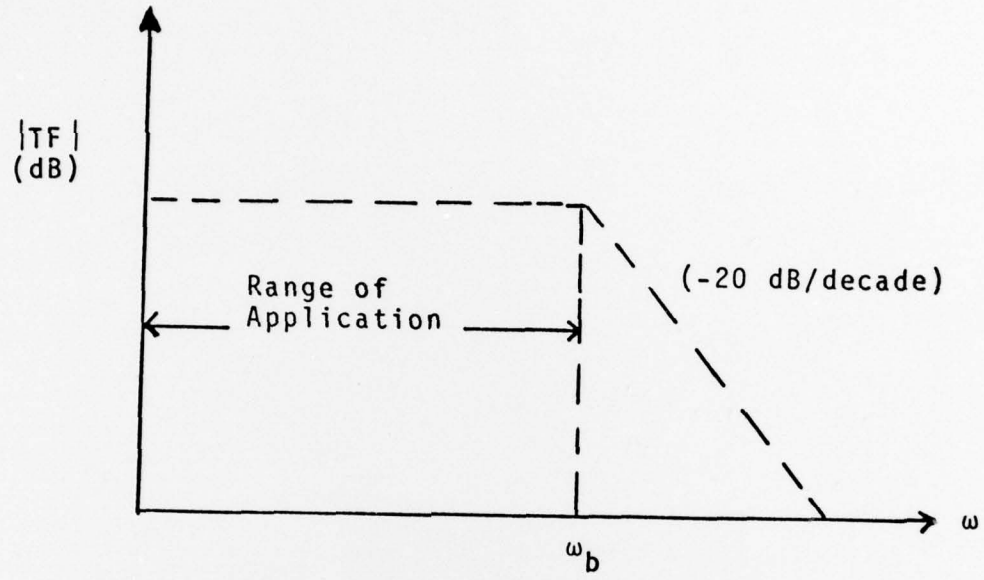

Figure C-2. Sketch of |TF| vs. y/b